**Universität Potsdam**
Mathematisch-Naturwissenschaftliche Fakultät

# Mixtures of Bosonic and Fermionic Atoms

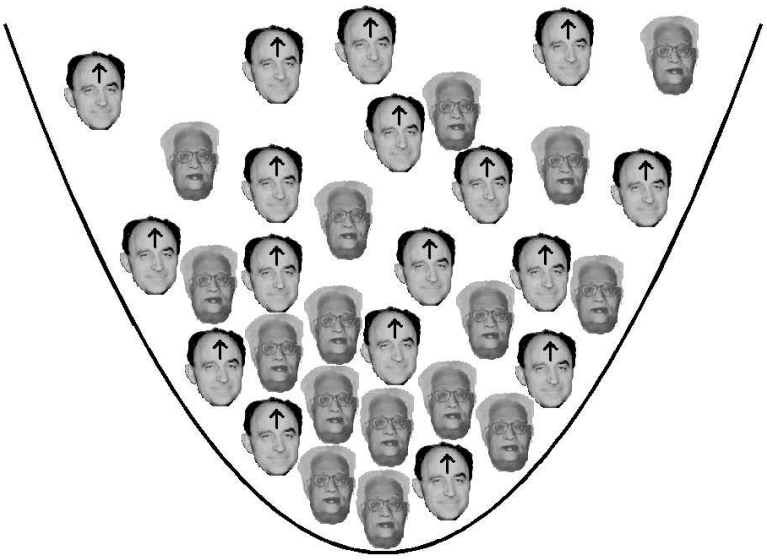

Dissertation zur Erlangung des Doktorgrades
(Dr. rer. nat.)

**Alexander Albus**

Betreuer
Prof. Martin Wilkens

Juni 2003

# Acknowledgments

As we understand today, to completely describe a physical system one needs to specify boundary conditions and propagation rules. Also the work of a theoretical physicist needs the right boundary conditions and propagation. I am grateful that during the three years in Potsdam I received help in both of these. The right boundary conditions were set up by my adviser Martin Wilkens, who lighted the initial spark of the research project, introduced me to a lot of other researchers and gave me the opportunity to work with them. He also created a very warm and inspiring working atmosphere in Potsdam and taught me a lot of things in the context of the "industry of physics". The propagation of the work was also thanks to my colleagues and friends, first of all Fabrizio Illuminati, whose relaxed personality but motivated and productive working attitude I enjoyed very much while he was a visitor in Potsdam and while he hosted me in Salerno for six months. Almost all the novel work presented in this thesis originated from my discussions with him. Also Jens Eisert, who first was a colleague of mine and then became a sort of "colleague and boss", clearly deserves to be thanked here for the stimulating discussions we had, for helping me to get adjusted in the group, and for proof reading this thesis. I also thank Simon Gardiner, Stefano Giorgini, Luciano Viverit and Marcus Cramer for good collaboration, Timo Felbinger for help in all kinds of computer questions and Axel Friedenauer for proof reading.

For the financial boundary conditions of the thesis project I thank the Deutsche Forschungsgemeinschaft and the European Science Foundation for the possibility to stay in Salerno thanks to a fellowship within the BEC2000+ programe.

Special thanks go to some people, that have not contributed to this thesis in a direct way, but whom I want to thank anyway, namely to Olga, Michi, and last but not least to my family.

# Preface

Since the experimental realization of the long–standing theoretical prediction of Bose–Einstein condensation in dilute atomic gases a marriage between two major fields of quantum physics, atomic physics and quantum many-particle physics, took place. In fact, neutral atoms confined in magnetic or optical traps and cooled to temperatures in the some tens nano Kelvin regime provide the most "clean" systems with widely controllable parameters that are known at this time to test the predictions of many-particle quantum theories in a limit that is accessible partly analytically and partly numerically, namely in the dilute limit, where only two-particle interactions are important. In turn, most of the theoretical problems studied in this field are motivated by current experiments. One can talk maybe not about a marriage, but at least of an engagement of theoretical and experimental physics in this new field. The experimental and theoretical attention that was some years ago mainly on Bosons, i.e. atoms with an even number of Fermionic constituents (nuclei and electrons), is shifting now also to Fermions (atoms with an odd number of Fermionic constituents), which can nowadays also be cooled to quantum degeneracy by making use of the experimentalists' experience with cooling Bosons and take a system of ultracold Bosons as a "refrigerator" for the Fermions. In the end, consequently, a mixed system of Bosons and Fermions will result. Maybe the most striking feature one hopes to be able to observe in this way is a Bardeen–Cooper–Schrieffer phase transition of the Fermions. This effect is promoted by means of a Bosonic phonon exchange among the Fermions. Thus a Bose–Fermi mixed system is a promising candidate to observe not "only" Bose–Einstein phase transition of the Bosons but also a Bardeen–Cooper–Schrieffer phase transition of the Fermions. This system is, however, also rich of other phase structures that are only present in mixed systems. Among them are component mixing vs. component separation and stability vs. collapse in continuous systems. In optical lattices one can observe Mott–insulating and superfluid phases and also interesting crystalline structures. This thesis is intended give a complete overview of the theoretical results on atomic Bose–Fermi mixtures to which I contributed during my PhD studies in years 2000–2003. But I will also discuss some results obtained by other authors, sometimes rewriting their derivations in order apply the methods used in this thesis and thus to make the thesis more coherent.

# Deutsche Zusammenfassung

Heutzutage ist es möglich, einen heißen Strahl aus Alkalimetallatomen, die vorher in einem Ofen verdampft wurden, in einer magnetischen Falle einzusperren und anhand von Kühlung mithilfe von Laserstahlen in einen Temperaturbereich von einigen mikro Kelvin, also nahe dem absoluten Nullpunkt, zu kühlen. Man erhält eine Wolke aus ca. einer Million Atomen, die einen Durchmesser von einigen tausendstel Millimetern hat. Verglichen mit "normalen" Umweltbedingungen ist das eine extrem niedrige Teilchendichte — so niedrig, daß die Atome trotz der ultrakalten Temperatur nicht in ihren üblichen metallischen Aggregatzustand zurückfallen, sondern ein meta–stabiles, atomares Gas bilden. Ein solches Gas eignet sich hervorragend zum Studium von Quantenphänomenen. Fundamental verschieden verhalten sich dabei Gase aus Atomen, die einen geradzahligen Spin haben, und solche mit einem ungeraden. Die ersten zählt man deshalb zur Kategorie der Bosonen, die letzteren zu den Fermionen.

Ziel der Arbeit war die systematische theoretische Behandlung von Gemischen aus bosonischen und fermionischen Teilchen in einem Parameterbereich, der sich zur Beschreibung von aktuellen Experimenten mit ultra–kalten atomaren Gasen eignet.

Zuerst wurde der Formalismus der Quantenfeldtheorie auf homogene, atomare Boson–Fermion Gemische verallgemeinert. Mithilfe von Feynman–Diagrammen ließen sich die Terme der zeitabhängigen Störungstheorie darstellen. Werden die Linien der Diagramme als virtuelle Teilchen interpretiert, so laßen sich anhand von Feynman–Diagrammen alle für ein niederdichtes System relevanten störungstheoretischen Terme identifizieren. Auch die Dyson–Reihe mittels Selbstenergien und die Leiterapproximation für die $T$–Matrix sowie deren Renormalisierung konnten auf Boson–Fermion Gemische angewandt werden. Damit konnten alle (unendlich vielen) Feynman–Diagramme, die zur Beschreibung von meta–stabilen Alkaligasen nötig sind, aufsummiert werden. Die $T$–Matrix, die die Boson–Fermion Wechselwirkung beschreibt, ließ sich mittels einer modifizierten Bethe–Salpether–Gleichung bestimmen und mithilfe des Hugenholtz–Pines–Theorems das bosonische chemische Potentials berechnen.
Aus dem bosonischen chemischen Potential und den Ausdrücken für die Dyson–Selbstenergien lassen sich viele physikalisch relevanten Größen über die Molekularfeldnäherung hinaus berechnen. Darunter, die Grundzustandsenergie, der Druck, die modifizierte Boson– bzw. Fermionmasse und die Geschwindigkeit des Phononschalls.

In Experimenten werden die Atomgase mithilfe von Magnetfeldern, die an das magnetische Moment der Atome koppeln, festgehalten. Im Zentrum dieser Falle, wo die Atome sich befinden, können die vom Magnetfeld erzeugten Kräfte durch ein harmonisches Potential beschrieben werden. Unter Zuhilfenahme der Resultate für das entsprechende homogene System wurde ein Boson–Fermion Gemisch in einem Fallenpotential im Rahmen der Dichtefunktionaltheorie beschrieben.

Das Hoheberg–Kohn Theorem, welches besagt, daß bei gegebener Wechselwirkung die Grundzustandsenergie funktional nur von der Dichtverteilung abhängt, wurde auf Boson–Fermion Gemische übertragen. In diesem Fall ist die Grundzustandsenergie $E$ ein Funktional der Bosondichteverteilung $n_B(\mathbf{r})$ und der Fermiondichteverteilung $n_F(\mathbf{r})$. Man schreibt daher $E[n_B, n_F]$.

Zur Bestimmung von $E[n_B, n_F]$ wurde eine Verallgemeinerung des Kohn–Sham–Schemas benutzt. Hierbei wurde ein nichtwechselwirkendes Hilfssystem definiert und es ließ sich zeigen, daß genau ein solches Hilfsystem gefunden werden kann, so daß dessen Dichteverteilungen identisch mit denen des ursprünglichen wechselwirkenden Systems sind. Eine zentrale Größe bei der Konstruktion des Hilfssystems ist die sog. Austausch–Korrelationsenergie.

Für typische Parameterbereiche bei atomaren Gasen läßt sich diese Austausch–Korrelationsenergie mittels lokaler Dichteapproximation ermitteln. Sie besteht aus Termen höherer Ordnung in der Streulänge und ist damit eine Korrektur zur Molekularfeldenergie. Durch numerische Lösung der Kohn–Sham Gleichungen wurden die Dichteprofile in der Falle ermittelt und daraus konnte auf die Phasengrenzen eines gemischten stabilen Regimes geschlossen werden. Im Falle von abstoßender Boson–Fermion Wechselwirkung kommt es an der Phasengrenze zur Entmischung beider Spezies, im Falle von gegenseitiger Anziehung zum Kollaps in das Zentrum der Falle. In beiden Fällen ließen sich untere Schranken für die kritischen Teilchenzahlen an den Phasengrenzen angeben. Im Vergleich zur Molekularfeldnäherung ändert die Austausch-Korrelationsenergie das Phasendiagram bei abstoßender Wechselwirkung wenig. Bei Anziehung hingegen verschieben sich die Phasengrenzen stark. Im Allgemeinen stabilisiert der Beitrag der Austausch–Korrelationsenergie das System gegen Kollaps.

Die kritische Temperatur des Phasenübergangs von einem thermischen Bosonengas zu einem Bose–Einstein–Kondensat (BEK) läßt sich nur für den einfachen Fall eines nicht–wechselwirkenden Gases im thermodynamischen Limes exakt berechnen. Korrekturen, die einerseits der Endlichkeit der Teilchenzahl andererseits der Wechselwirkung der Bosonen untereinander Rechnung tragen, existieren zur jeweils ersten Ordnung. In einem Gemisch aus Bosonen und Fermionen beeinflußt auch die Boson–Fermion Wechselwirkung die kritische Temperatur des Phasenübergans zu einem BEK.
In der semiklassichen Molekularfeldnäherung ließen sich gekoppelte Gleichungen für die Boson– und Fermiondichteverteilungen bei endlicher Temperatur angeben. Durch Expansion in der Boson–Fermion Streulänge zu erster Ordnung wurde die kritische Temperatur durch numerische Integration bestimmt. In den Extremfällen eines thermisch verteilten Fermiongases einerseits bzw. eines voll quantendegenerierten Fermiongases andererseits konnten analytische Ergebnisse angeben werden.

Mittels stehenden Laserlichtwellen kann man periodische Potentiale für atomare Gase erzeugen. Anhand dieser Systeme lassen sich Phänomäne, die ansonsten für die Festkörperphysik typisch sind, mit großer Präzission und in einem vergleichbar breiten Parameterbereich untersuchen. Im Vordergrund steht dabei das Verständnis von Phasenübergängen zwischen Mott–Isolator– und suprafluiden Bereichen. In der Mott–Isolatorphase sitzen die Atome in den Potentialminima fest und es ist kein Teilchentransport möglich während in der suprafluiden Phase die Atome zwischen den Potentialminima "hin– und hertunneln" können.
Eine geeignete Expansion der Feldoperatoren in Anwesenheit eines starken periodischen Potentials existiert mittels Wannier–Funktionen, da in diesem Fall nur das energetisch niedrigste Wannier–Band wesentlich ist. Diese Expansion führt zu einem Hubbard–artigen Hamiltonoperator für Boson–Fermion Gemische, wobei sich alle Parameter dieses

Hamiltonoperators aus den atomaren Parametern wie Massen und Streulängen und der Gitterstärke berechnen ließen.

Eine Molekularfeldnäherung für den Hubbard–Hamiltonoperator erlaubte das Studium der Phasenstabilitäten. Mittels Störungstheorie konnten approximativ die jeweiligen Bereiche des Phasendiagramms gefunden werden, in denen die Bosonen in einem Mott–Isolator bzw. in einen suprafluiden Zustand sind. Anhand eines Gutzwilleransatzes ließen sich weiterhin Besetzungszahlen der Gitterplätze und lokale Suprafluidparameter durch numerische Minimierung mittels einer "simulated annealing"–Methode berechnen und auf kritische Werte der Gitterstärke für einen Phasenübergang schließen. Im Falle eines sehr starken Gitterpotentials wurden hochgradig degenerierte Grundzustände gefunden. In diesem Fall ist das Ensemble der Grundzustände symmetrisch bei Austausch von Bosonen und Fermionen und die räumliche Spiegelsymmetrie des Systems wird gebrochen.

# Contents

# List of Figures

# Part I

# Introduction to the thesis

As almost any publication in the field of cold trapped atoms this thesis also starts with a brief discussion of Bose-Einstein condensation. The first experimental realizations of a Bose–Einstein Condensate (BEC) were achieved in 1995 by the groups of E. Cornell, C. E. Wieman [1] and W. Ketterle [2] and lead to the Nobel price. The striking feature of a BEC is that on can literally take photographs of the signatures of Quantum mechanics. In a BEC, which was theoretically predicted already in 1924 by Bose [3] for photons and extended to conserved particles and brought to a wide attention by Einstein [4, 5, 6], the remarkable feature is that a single wave function is occupied by a macroscopic number (up to $10^7$) of particles. This is due to the peculiar statistics of Bosonic particles, which allows many particles to occupy one single quantum mechanical wavefunction. The reason, why it took so long to experimentally verify this effect is that usually thermal fluctuations are so large that a single wavefunction cannot be populated by a macroscopic number of particles. Only when the system is cooled to very low temperatures, the thermal fluctuations are small enough such that the occupation number of a certain state (usually the ground state) $N_0$ can be of the order of the total number of particles $N$. According to a simple argument by Noziéres (in Ref. [7]), one knows that for energetic reasons only one (not two or more) wave-function can be occupied macroscopically. The change from a microscopic to a macroscopic occupation of this wavefunction takes place at a certain critical temperature $T_c$. Above this temperature (if we extrapolate to the case $N \to \infty$) the relative population of the BEC is zero ($N_0/N = 0$). For the ideal case of non-interacting Bosons, this changes suddenly at $T_c$ and the order parameter $N_0/N$ becomes finite with a kink at $T_c$. Clearly, in this idealized case a first order quantum phase transition[1] takes place with the order parameter being $N_0/N$. As the temperature is decreased even farther the number of particles not in the BEC, the so-called thermal particles $N - N_0$, decreases as $(T/T_c)^{3/2}$. This means that for temperatures that are much lower than $T_c$ almost all particles are in the BEC or, put in another way, a large number of particles occupies one single–particle wavefunction. Thus, the wavefunction must be visible in principle. With the proper technical equipment this is indeed the case (for reviews of experimental techniques, see Ref. [9]). The results are shown in Fig. 1. These pictures are taken for temperatures above, at and below the critical temperature. We can observe, how the sharply peaked ground state wave function emerges from widely distributed thermal particles.

Since Bosons are that interesting one might ask what happens for Fermions. Clearly, several identical Fermions (named after E. Fermi who discovered their statistics [10, 11]; and rediscovered by P. Dirac [12]) cannot occupy a single wavefunction which is explicitly forbidden by the Pauli principle [13]. Thus, the "most quantum" many–particle state one can think of for Fermions is a state in which each single–particle wavefunction starting from the lowest energetic wavefunction to one with energy $E_F = k_B T_F$ is occupied by exactly one particle. Here, the Fermi energy $E_F$ is determined by the total number for Fermions. Single–particle wavefunctions with higher energies than $E_F$ should not be occupied at all in this ideal scenario. Certainly, thermal fluctuations also play a role for Fermions and this ideal case can only be reached approximately. In contrast to the case of Bosons, the transition is continuous (no kink), meaning that there is no phase transition. In any case, the passing to a quantum degenerate regime has been observed in the experiment. Most clearly, this can be understood by looking at the momentum distributions of the particles which are shown in the pictures of Fig. 2. The plots can obtained by a "time-of-flight" measuring technique, where roughly speaking the trap is

[1] When using the term phase transition in this context we skip to discuss the question how a phase transition can be defined for finite systems. In the case of a BEC phase transition there are finite system analogies to a real phase transition [8].

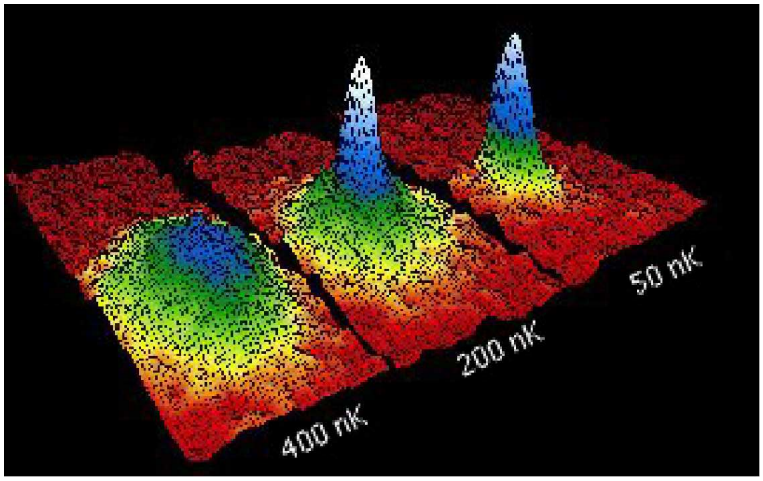


Figure 1: Momentum density distribution of a BEC, taken from the homepage of the group of E. Cornell at JILA

suddenly turned off and the particles with a higher momentum escape faster than the particles with a lower momentum. By measuring the time the particles need to reach a detector one can deduce the initial momentum distribution. The picture on the right which was taken at a temperature below the Fermi temperature shows that a lot of particles have energies below the Fermi energy and only few have energies above. So to say, the Fermions stack up to the Fermi energy. For this reason, one does not speak of a Fermi-Dirac condensate in analogy to a BEC but of a Fermi-Dirac stack (FDS). A possible phase transition that is expected for the Fermions to take place is a Bardeen–Cooper–Schrieffer (BCS) transition which is known from the theory of superconductivity [14]. In order to lower the total energy, the Fermions can form pairs (e.g. Cooper pairs) and the pairs being Bosons can condense and thus lower the total energy. Usually, the pairing mechanism and condensation takes place at the same temperature, but this is not necessarily so. These issues are investigated in the theory of the BEC–BCS crossover [15, 16, 17], but are not topic of this thesis. One should mention that no experiment has been carried out so far in which the existence of a BCS transition was proved (see however [18]). The reason is that one needs even lower temperatures than for BEC and Fermi degeneracy.

The main problem is that it is much harder to cool Fermions than Bosons. Atoms are usually trapped by a magnetic "potential" $V_T(\mathbf{r}) = -\mu B(\mathbf{r})$, where $\mu$ is the magnetic dipole moment of the atoms. Strong magnetic fields are required and thus the spins of the atoms are aligned either all parallel or all anti–parallel (depending on the sign of the coupling constant between the spin and the magnetic field). In other words, the spins are polarized. But Fermions do not $s$-wave scatter since this would be only allowed by the Pauli principle in the case of anti–parallel spin alignments between two atoms. Since $s$-wave scattering is the dominant interaction in the low momentum regime (cf. chapter 1) the Fermions can be approximated as non-interacting with each other. Interactions are, on the other hand, needed in the final stage of the cooling process which is the process of evaporative cooling. Roughly, this cooling procedure can be summarized in the following way: In the beginning, the particles in the trap are already rather cool

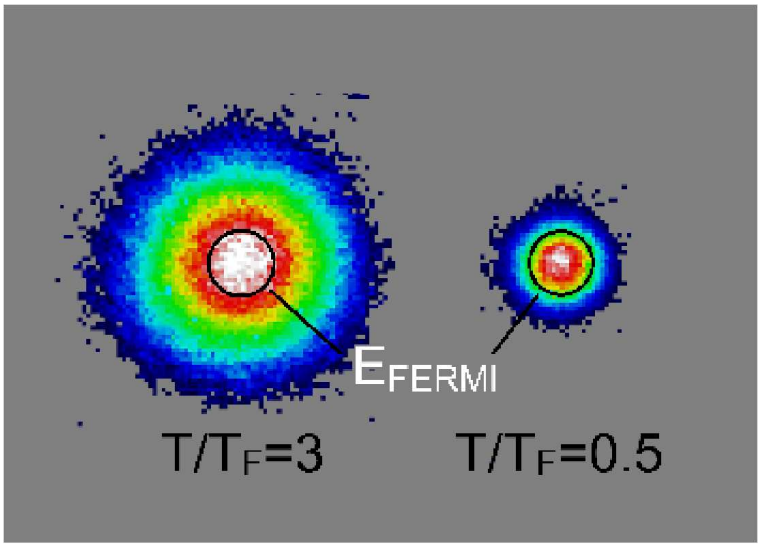


Figure 2: Momentum density distribution of a FDS ($T_F \approx 100nK$) taken from the homepage of D. Jin at JILA

due to other cooling procedures applied before. Now, the potential ramp at the edges of the trap are decreased slightly, and consequently some particles are lost from the trap. But just the most energetic particles are lost because only they "can climb the potential ramp up to the edge". After re–thermalization the remaining particles have less average energy and are thus cooler. Interactions among the particles, however, are required for re–thermalization process and the number of particles that are left in the trap after many iterations of this step strongly depends on the quality of the re–thermalization. Thus, this procedure cannot work for pure Fermions unless some tricks are applied as done in the group of D. Jin [19], where the previous figure was taken from. Perhaps a simpler trick is to put other particles (e.g Bosons) into the same trap and let the Fermions re–thermalize via interactions with them. Because of this idea many experimental groups have produced Bose–Fermi mixtures rather than pure Fermion systems [20, 21, 22, 23]. This cooling technique is termed sympathetic cooling. For a theoretical description of this process the reader is referred to Refs. [24, 25]. Fig 3 shows the density distributions measured in the Florence group for such a system of ultracold mixtures of Bosons and Fermions.

Among other things, this experiment led to the observation of a phenomenon that is not present in pure systems, namely the mutual collapse of the system. In this experiment, the Bosonic component was formed by $^{87}$Rb atoms while the Fermionic component consisted of $^{40}$K atoms. For those isotopes, the Boson–Boson interaction is repulsive, but the Boson–Fermion interaction is attractive. Although Bose systems with a repulsive interaction are stable a collapse of this system was be observed if the number of both the Bosonic and the Fermionic atoms were large. The reason why a collapse occurs is the following: Due to the Boson–Fermion attraction, the Bosons that are located close to the center of the trap pull the Fermions to the center of the trap. In turn, the Fermions at the center also pull even more Bosons inside and vice versa. If the number of particles is large enough such that this mutual attraction cannot be balanced by the Boson–Boson

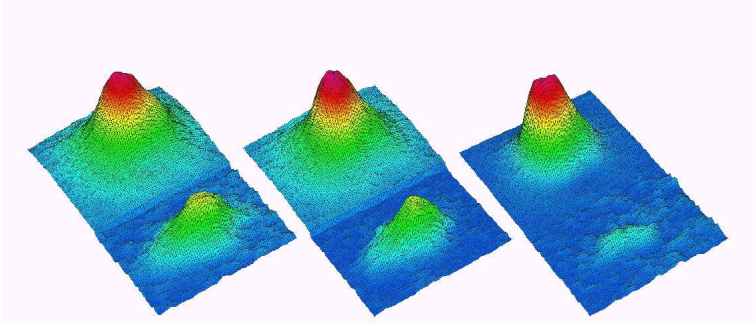

Figure 3: Density distributions of a Bose-Fermi mixture, taken from Science 297, 2240 (2002), top: Boson density, bottom: Fermion density. For better visibility, the two density distributions are displayed separately, in the system they are on top of each other.

repulsion or the Fermion Pauli pressure the system eventually implodes. Finally, the implosion stopes when a 'high density configuration' in the center is reached. In this 'high density configuration', formation of molecules and solid structures may occur in contrast to the dilute regime (which is said to be meta–stable against formation of molecules or solid structures). The crucial difference is that in the dilute regime three or more particle processes are very unlikely whereas for high densities they are not. In two particle processes, energy and momentum conservation does not allow for molecule formation whereas three or more particle processes can result in molecules. Unfortunately, these molecules are lost from the trap and as in the above figure we can only see a strong particle loss of $^{40}$K atoms. On might ask the question why nothing similar can be seen for the $^{87}$Rb atoms. The reason is simply that initially there are many more $^{87}$Rb in the trap and the mutual collapse is halted when almost all the $^{40}$K are lost from the trap by molecule formation, but still a large number of $^{87}$Rb atoms remains in the trap.

As the previous pictures have shown the density of the particles (either in real or momentum space) are directly observable in the experiment. A theory which uses the density of particles as a basic variable is thus ab initio closely related to the experiment since the basic variable is observable. Maybe this was the original idea of density functional theory invented by Hohenberg and Kohn in 1964 [26] for electron systems. As shown in this thesis, one can adapt this theory also for Bosons and for mixtures of Bosons and Fermions. The shift from wave-functions to densities as basic variables has also a pragmatic advantage. As mentioned before, we deal with particle numbers of the order of $10^7$. The particle density is only a function of the three spacial coordinates, whereas the many-particle wave-functions are functions of three spacial coordinates *times* the number of particles present in the system. To simulate a many–particle ground–state wavefunction numerically would be an impossible task due to the large number of its arguments. The number of arguments of the densities, however, is always three — independently of the number of particles. This drastic advantage, of course, comes with a price, since one has to express other observables in terms of densities, or say, as functionals of the density distributions. These are not a priori known. For example, to obtain the ground state properties one has to minimize the energy functional with respect to the densities. The first task is thus to calculate the ground state energy functionals. The first part of

this thesis was motivated by this task for the most simple case of a homogeneous system. The condition of diluteness that was already mentioned several times can be formalized in terms of densities in a very intuitive way. One simply requires the average radius occupied by a single particle in the systems to be small compared to the characteristic length scales of the particle–particle interactions. The average radius is roughly the third root of the inverse of the particle density and the length scale of the interaction is given by the $s$–wave scattering length. Thus, the diluteness condition is that the product of the third square root of the density times the $s$-wave scattering length has to be small. A closer look in the following shows that more precisely these conditions read: $\sqrt{n_B a_{BB}^3} << 1$ and $k_F a_{BF} << 1$, where $n_B$ is the Boson density, the Fermi wave vector is related to the Fermion density by $k_F = (6\pi^2 n_F)^{1/3}$ for spin–aligned systems, and the Bose–Bose and Bose–Fermi $s$–wave scattering lengths are $a_{BB}$ and $a_{BF}$, respectively.

The parameters $a_{BB}$ and $a_{BF}$ are hard to determine theoretically, since for neutral atoms they reflect a net interaction of the entire electronic clouds of the scattering atoms. Furthermore, the interactions also depend on the internal state of the atoms and even on the external magnetic field. This latter effect experimentalists can use to tune the values over a wide range by simply applying an additional magnetic field. What then happens is that by tuning the magnetic field one can bring a virtual bound state (with different magnetic properties than the two atom scattering state) into resonance with the two atom scattering state. The particles cannot bind because of energy and momentum conservation, but this resonant molecular state has a strong influence on the scattering process. By this means, the scattering lengths depends on the magnetic field in the following way $a(B) = a - \frac{A}{B-B_0}$ [27], where $A$ is independent of $B$ and $B_0$ is the magnetic field strength where the Feshbach resonance occurs. From this dependence, one can see that close to $B_0$ on can in principle adjust any (positive and negative!) values of the scattering length. In this thesis, the scattering length is regarded as a basic input variable to be determined by methods not considered here (or practically, mostly experimentally).

## Thesis outline

Before the work on this thesis was started, the situation on the theoretical description of dilute Bose–Fermi mixtures can briefly be summarized in the following way: For trapped systems the theory has been developed in the mean–field approximation to determine the Boson and Fermion density profiles at zero temperature [28, 29, 30], and the related properties of stability against phase separation and collapse, numerically in Refs. [31, 32, 33, 34] and by a Gaussian variational Ansatz in Ref. [35]. Speculations about a possible BCS phase transition were drawn in Refs. [36, 37, 38]. Recent work was performed on the strongly interacting mixture of $^4$He-$^3$He was mainly on the calculation of the structure factors. (within a linear response theory [39] or using a correlated basis Ansatz [40]).

The work for alkali–metal atoms was mostly done with the help of the mean–field approximation while variational approaches were used for srongly–interacting helium. Beyond mean–field studies on Bose–Fermi mixtures were mostly done within the so–called Boson–Fermion model (BFM) of superconductivity [41, 42]. The results obtained for this model, however, can not be carried over to the description of atomic Bose–Fermi mixtures, since the Hamiltonian and the particle conservation laws are different in the two cases.

In the mean–field approximation, the interaction energy functionals are $4\pi\hbar^2 a_{BB} n_B n_F / m_B$ for the Boson–Boson interaction, and $2\pi\hbar^2 a_{BF} m_B^2 / m$ for the Boson–Fermion interaction. Here, $m_B$ is the Boson mass and $m = m_B m_F/(m_B + m_F)$ is the reduced mass, $m_F$ being the Fermion mass. By using the methods of quantum field theory and density functional theory, beyond mean–field studies are possible. They are

relevant when the interaction parameters are large or to gain a very precise knowledge of the density profiles and the related properties of stability. One might also be interested in checking under what circumstances mean–field leads to reliable results.

The theory of atomic Bose–Fermi mixtures beyond mean–field is considered in this thesis. We will show that the mean–field is the zeroth order expansion of the interaction energies in terms of the above gas parameters and ignores quantum fluctuations. Corrections to the mean–field are of first or higher order in the gas parameters. Important are these corrections in a regime at the onset collapse. In optical lattices, exchange–correlation effects essential to describe to Mott-insulation regime.

In chapter 1 the theory of two–particle scattering processes is reviewed. The results of this chapter will be fundamental for the later development of the theory of dilute systems, since the interaction properties of those systems are described by two–particle interactions. This reader is probably familiar with this subject from a Quantum mechanics course. Yet, attention is paid to the modification due to particle statistics already on this level.

Chapter 2 summarizes the methods needed from many–particle Quantum mechanics. The main ideas were developed already in 1958 by Galitskii for Fermion and Beliaev for Bosons. This chapter is intended to show that most of the results can be adapted to Bose–Fermi mixtures. The content is published in less detail in the first part of Ref. [A].

The application of the methods presented in chapter 2 to dilute systems comprises the content of chapter 3. The results of this chapter are published in the second part of Ref. [A]. Results published by other authors are also presented making use of the methods of chapter 2 (mostly in contrast to the original work).

While the previous development was on the ideal case of homogeneous systems, chapter 4 shows how some results can be taken over to actual experimental systems that are confined by a trapping potential. The method of density functional theory applied here is briefly (i.e. omitting the mathematical details) formulated for Bose–Fermi mixtures. This chapter was published with some modifications in Ref. [B].

Chapter 5 addresses the problem of the critical temperature of Bose-Einstein condensation in trapped Bose–Fermi mixtures and was published in Ref. [C]. There, we make use of finite temperature theory which is briefly described in the beginning of the chapter.

The topic of Bose–Fermi mixtures in optical lattices is introduced in chapter 6 and some basics results that can be obtained by rather simple methods are given. Chapter 6 was published in Ref. [D] with slight changes.

The appendices consist of some lengthy calculations and an alternative derivation of a result in the main text.

While the studies for this thesis a tremendous work on Bose–Fermi mixtures was done by other authors. In brief, some of their work is listed paying attention to topics that are not or only briefly addressed in this thesis:

Various excitations of the system have been studied. Among them are the zero–sound density oscillations within a random phase approximation [43] and other collective oscillations within a sum–rule approach [44]. The dynamical behavior during an expansion [45], close to a Feshbach resonance [46], and in a monopole oscillation [47] has been stud-

ied. Hydrodynamic excitation have been calculated in local density approximation [48] and beyond local density approximation by using a Weizsäcker kinetic energy functional for the Fermions [49]. Other collective modes were considered within a linear response theory [50] and in the random phase approximation [51]. The system behavior in presence of BCS pairing for the Fermions has been considered in Refs. [52, 53, 54, 55], and the transition temperature of BCS was calculated in Ref. [56] for spin unpolarized systems and in Ref. [57] for spin polarized systems.

# List of publications

[A] A. P. Albus, S. A. Gardiner, F. Illuminati, and M. Wilkens, *Quantum field theory of dilute homogeneous Bose-Fermi mixtures at zero temperature: General formalism and beyond mean-field corrections*, Phys. Rev. A **65**, 053607 (2002).

[B] A. P. Albus, F. Illuminati, and M. Wilkens, *Density functional theory and ground-state properties of trapped Bose-Fermi mixtures*, Phys. Rev. A **67**, 063606 (2003).

[C] A. P. Albus, S. Giorgini, F. Illuminati, and L. Viverit, *Critical temperature of Bose-Einstein condensation in trapped atomic Bose-Fermi mixtures*, J. Phys. B **35**, L511 (2002).

[D] A. P. Albus, F. Illuminati, and J. Eisert, *Mixtures of Bosonic and Fermionic Atoms in Optical Lattices*, accepted for publication in Phys. Rev. A **68**, 023606 (2003).

| | |
|---|---|
| $\hbar$ | Planck constant $1.055 \times 10^{-34} Js$ |
| $k_B$ | Boltzmann constant $1.381 \times 10^{-23} J/K$ |
| $a_0$ | Bohr radius $5.292 \times 10^{-11} m$ |
| $m_0$ | atomic mass unit $1.661 \times 10^{-27} kg$ |
| $m_B$ | mass of the Bosonic atoms |
| $m_F$ | mass of the Fermionic atoms |
| $m$ | reduced mass $m_B m_F/(m_B + m_F)$ |
| $\delta$ | relative mass difference $(m_B - m_F)/(m_B + m_F)$ |
| $a_{BB}$ | Boson-Boson scattering length |
| $a_{BF}$ | Boson-Fermion scattering length |
| $n_B$ | density of the Bosonic atoms |
| $n_F$ | density of the Fermionic atoms |
| $t$ | time variable |
| $\mathbf{x}, \mathbf{y}, \mathbf{r}$ | position vectors |
| $\omega$ | frequency variable |
| $\mathbf{k}, \mathbf{p}, \mathbf{q}$ | wave vectors |
| $x, y, r, k, \ldots$ | the magnitudes of $\mathbf{x}$, $\mathbf{y}$, etc. |
| $x_i, y_i, r_i, k_i, \ldots$ | the $i$-th component of $\mathbf{x}$, $\mathbf{y}$, etc. |
| $x^\mu, y^\mu$ | four vectors $x^\mu = (t, \mathbf{x})$ etc. |
| $k^\mu, q^\mu, p^\mu$ | four wave vectors $k^\mu = (\omega, \mathbf{k})$ etc. |
| $\hat{O}$ | an operator |
| $\|\psi\rangle$ | a ket vector |
| $\langle\psi\|$ | a bra vector |
| $\delta(\mathbf{x})$ | the Dirac delta function |

Table 1: Some commonly used symbols

# Part II

# Homogeneous Boson-Fermion systems

# Chapter 1

# Two–particle scattering in various dimensions

In this introductory chapter, we mostly follow the textbook Ref. [58] and the paper by Lee, Morgan and Burnett [59]. In the latter, calculations are done not only in three, but also in one and two spacial dimensions. Even though in the following chapters of this thesis reduced dimensions are not considered, it is maybe useful to have a parallel treatment for one, two and three dimensions. At the end of this section we briefly motivate to consider also Bose–Fermi mixtures in low dimensions.

## 1.1 Reduction to an effective one-particle problem

The Hamiltonian for a system of two particles in homogeneous and isotropic space interacting via a potential $U$ is:

$$\hat{H} = -\frac{\hbar^2 \nabla_B^2}{2m_B} - \frac{\hbar^2 \nabla_F^2}{2m_F} + U(|\mathbf{r}_B - \mathbf{r}_F|) \tag{1.1}$$

For the purpose of this thesis, we mostly assume that one of the particles is a Boson and the other one a Fermion, so we label the parameters of one particle by a subscript $B$ and the parameters of the other particle by $F$, e.g. $\mathbf{r}_B$ is the Boson coordinate and $\mathbf{r}_F$ is the Fermion coordinate. From the very beginning it is assumed that $U(r)$ decays faster that $\frac{1}{r}$ for large r.
The Laplacian is defined as

$$\nabla_i^2 = \sum_{j=1}^{D} \frac{\partial^2}{\partial r_{i,j}^2}, \tag{1.2}$$

where the index $i$ is either $B$ or $F$ and $D$ is the spatial dimension. As indicated above the three cases $D = 1, 2, 3$ are treated here.
An eigenstate $\Phi(\mathbf{r}_B, \mathbf{r}_F)$ of the above Hamilton operator with energy $E_{total}$ satisfies the Eigenvalue equation:

$$\hat{H}\Phi(\mathbf{r}_B, \mathbf{r}_F) = E_{total}\Phi(\mathbf{r}_B, \mathbf{r}_F). \tag{1.3}$$

If the center–of–mass coordinates (as e.g. in [60]) are defined as

$$\begin{aligned} \mathbf{R} &= \frac{m_B \mathbf{r}_B + m_F \mathbf{r}_F}{m_B + m_F} \\ \mathbf{r} &= \mathbf{r}_B - \mathbf{r}_F, \end{aligned} \tag{1.4}$$

we immediately see that

$$\begin{aligned} \hat{H} &= \hat{H}_{CM} + \hat{H}_{rel}, \\ \hat{H}_{CM} &= -\frac{\hbar^2}{2(m_B+m_F)} \sum_{j=1}^{D} \frac{\partial^2}{\partial R_j^2}, \\ \hat{H}_{rel} &= -\frac{\hbar^2}{2m} \sum_{j=1}^{D} \frac{\partial^2}{\partial r_j^2} + U(r), \end{aligned} \tag{1.5}$$

where $m = \frac{m_B m_F}{m_B+m_F}$ is the relative mass. This means that the Hamiltonian separates into a center–of–mass part and a part which describes the relative motion. Thus, for the wave function it is useful to choose a product Ansatz:

$$\Phi(\mathbf{r}_B, \mathbf{r}_F) = \Psi(\mathbf{R})\psi(\mathbf{r}) \tag{1.6}$$

The center–of–mass part can be easily solved by a plane–wave:

$$\Psi(\mathbf{R}) = e^{i\mathbf{K}\mathbf{R}}. \tag{1.7}$$

We now define $\frac{\hbar^2 k^2}{2m} = E_{total} - \frac{\hbar^2 K^2}{2(m_B+m_F)}$. Assuming that the particles do not bind and form a molecule (i.e $\psi(\mathbf{r})$ does not decay exponentially for large $r$), we can infer that $k$ is real. Redefining the potential $u(r) = \frac{2m}{\hbar^2}U(r)$, we arrive at the following effective Schrödinger equation for the relative motion:

$$\left( -\sum_{j=1}^{D} \frac{\partial^2}{\partial r_j^2} + u(r) \right) \psi_{\mathbf{k}}^{(D)}(\mathbf{r}) = k^2 \psi_{\mathbf{k}}^{(D)}(\mathbf{r}). \tag{1.8}$$

Consider only for a moment that the two particles are identical (this of course then implies that either both of them are Bosons or both of them are Fermions, and also $m_B = m_F$). Then, because of the symmetry postulate of Quantum Mechanics, the wave function has to be (anti-)symmetric if we exchange the arguments $\mathbf{r}_B$ and $\mathbf{r}_F$ of $\Phi$. This parity operation is equivalent to the replacement (see Eqns. 1.4): $\mathbf{R} \to \mathbf{R}$ and $\mathbf{r} \to -\mathbf{r}$. Looking at Eqn. (1.8), we can see that because of the symmetry of $u(r)$ (and also of the Laplacian), $\psi_{\mathbf{k}}^{D}(-\mathbf{r})$ is a also solution if $\psi_{\mathbf{k}}^{D}(\mathbf{r})$ is a solution (of no definite symmetry). Thus, if the two particles are Bosons then we can construct the solution with the correct symmetry by setting:

$$\psi_{\mathbf{k}}^{B(D)}(\mathbf{r}) = \tfrac{1}{2}\left( \psi_{\mathbf{k}}^{(D)}(\mathbf{r}) + \psi_{\mathbf{k}}^{(D)}(-\mathbf{r}) \right). \tag{1.9}$$

And likewise if the two particles are Fermions the solution with the correct symmetry is:

$$\psi_{\mathbf{k}}^{F(D)}(\mathbf{r}) = \tfrac{1}{2}\left( \psi_{\mathbf{k}}^{(D)}(\mathbf{r}) - \psi_{\mathbf{k}}^{(D)}(-\mathbf{r}) \right). \tag{1.10}$$

We come back to this argument below.

## 1.2 The scattering amplitude

The usual way to analyze a scattering process like the one given in Eqn. (1.8) is by means of the Lippmann-Schwinger equation for the outgoing wave:

$$\psi_{\mathbf{k}}^{(D)}(\mathbf{r}) = e^{i\mathbf{k}\mathbf{r}} + \int d^D\mathbf{r}' G_{\mathbf{k}}^{(D)}(\mathbf{r}, \mathbf{r}') u(\mathbf{r}') \psi_{\mathbf{k}}^{(D)}(\mathbf{r}'), \tag{1.11}$$

This equation is equivalent to Eqn. (1.8), if the Green's functions $G_{\mathbf{k}}^{(D)}(\mathbf{r},\mathbf{r}')$ satisfy:

$$\left(\nabla^2 + k^2\right) G_{\mathbf{k}}^{(D)}(\mathbf{r},\mathbf{r}') = \delta^{(D)}(\mathbf{r}-\mathbf{r}'), \tag{1.12}$$

where $\delta^{(D)}(\mathbf{r}-\mathbf{r}')$ is the $D$-dimensional delta function. By the requirement that the Green's functions behave for large $r$ as outgoing spherical waves with origin $\mathbf{r}'$, they are uniquely fixed:

$$G_{\mathbf{k}}^{(D)}(\mathbf{r},\mathbf{r}') = \lim_{\eta\to 0} \left\langle \mathbf{r} \left| \frac{1}{k^2 + \sum_{j=1}^{D} \frac{\partial^2}{\partial r_j^2} + i\eta} \right| \mathbf{r}' \right\rangle. \tag{1.13}$$

As usual, $|\mathbf{r}\rangle$ is the (improper) bra position eigenvector and $\langle\mathbf{r}|$ the corresponding ket vector. Since the Laplacian looks particularly simple in momentum space, it is not hard to see that

$$G_{\mathbf{k}}^{(D)}(\mathbf{r},\mathbf{r}') = \lim_{\eta\to 0} \frac{1}{(2\pi)^D} \int d^D\mathbf{p} \frac{e^{i\mathbf{p}(\mathbf{r}-\mathbf{r}')}}{k^2 - p^2 + i\eta}, \tag{1.14}$$

which is simply the Fourier transform (with respect to $\mathbf{r}-\mathbf{r}'$) of

$$G_{\mathbf{k}}^{(D)}(\mathbf{p}) = \frac{1}{k^2 - p^2 + i\eta}, \tag{1.15}$$

where the limit $\eta \to 0$ is now implicit.

We now study the behavior of the wave function given by Eqn. (1.11) at large distances from the scattering center. Large means $r$ is a lot larger than the range of the potential $u(r')$ and also a lot larger that $\frac{1}{k}$. After making use of the approximation $k|\mathbf{r}-\mathbf{r}'| \approx kr - \mathbf{k}'\mathbf{r}'$ with $\mathbf{k}' = k\frac{\mathbf{r}}{r}$ which is valid for large $r$ and some algebra, the resulting expressions for the Green's functions at large $r$ can be inserted into the Lippmann-Schwinger equations (1.11). This leads to expressions for the wavefunctions at large distances from the scattering center:

$$\psi_{\mathbf{k}}^{(1)}(\mathbf{r}) \approx e^{i\mathbf{k}\mathbf{r}} - \frac{i}{2k} e^{ikr} f^{(1)}(\mathbf{k}',\mathbf{k}), \tag{1.16}$$

$$\psi_{\mathbf{k}}^{(2)}(\mathbf{r}) \approx e^{i\mathbf{k}\mathbf{r}} - \frac{e^{i\pi/4}}{4}\sqrt{\frac{2}{\pi kr}} e^{ikr} f^{(2)}(\mathbf{k}',\mathbf{k}), \tag{1.17}$$

$$\psi_{\mathbf{k}}^{(3)}(\mathbf{r}) \approx e^{i\mathbf{k}\mathbf{r}} - \frac{1}{4\pi}\frac{e^{ikr}}{r} f^{(3)}(\mathbf{k}',\mathbf{k}), \tag{1.18}$$

where the scattering amplitudes are defined as:

$$f^{(D)}(\mathbf{k}',\mathbf{k}) = \int d^D\mathbf{r}' e^{-i\mathbf{k}'\mathbf{r}'} u(r') \psi_{\mathbf{k}}^{(D)}(\mathbf{r}'). \tag{1.19}$$

All this reads in momentum space:

$$u(\mathbf{q}) = \int d^D\mathbf{r}\; e^{-i\mathbf{q}\mathbf{r}} u(\mathbf{r}), \tag{1.20}$$

$$\psi_{\mathbf{k}}^{(D)}(\mathbf{q}) = \int d^D\mathbf{r}\; e^{-i\mathbf{q}\mathbf{r}} \psi_{\mathbf{k}}^{(D)}(\mathbf{r}), \tag{1.21}$$

$$f^{(D)}(\mathbf{k}',\mathbf{k}) = \frac{1}{(2\pi)^D} \int d^D\mathbf{q}\; u(\mathbf{q}) \psi_{\mathbf{k}}^{(D)}(\mathbf{k}'-\mathbf{q}). \tag{1.22}$$

The last equation can be also be written $\big($upon using the completeness relation $\frac{1}{(2\pi)^D}\int d^D\mathbf{k}\;\psi^{(D)}_{\mathbf{k}}(\mathbf{p})\psi^{(D)}_{\mathbf{k}}(\mathbf{p}')^* = (2\pi)^D\delta^{(D)}(\mathbf{p}-\mathbf{p}')\big)$:

$$\frac{1}{(2\pi)^D}\int d^D\mathbf{k}\; f^{(D)}(\mathbf{k}',\mathbf{k})\psi^{(D)}_{\mathbf{k}}(\mathbf{p})^* = u(\mathbf{k}'-\mathbf{p}). \tag{1.23}$$

The Fourier transform of the Lippmann-Schwinger equation is:

$$\psi^{(D)}_{\mathbf{k}}(\mathbf{p}) = (2\pi)^D\delta^{(D)}(\mathbf{p}-\mathbf{k}) + G^{(D)}_{\mathbf{k}}(\mathbf{p})\int d^D\mathbf{q}\; u(\mathbf{q})\psi^{(D)}_{\mathbf{k}}(\mathbf{p}-\mathbf{q}). \tag{1.24}$$

Inserting Eqns. (1.22) and (1.15) the Lippmann-Schwinger equation in momentum space can also be written as

$$\psi^{(D)}_{\mathbf{k}}(\mathbf{p}) = (2\pi)^D\delta^{(D)}(\mathbf{p}-\mathbf{k}) + \frac{f^{(D)}(\mathbf{p},\mathbf{k})}{k^2-p^2+i\eta}, \tag{1.25}$$

which, in turn, we can insert into Eqn. (1.22) in order to get an integral relation for the scattering amplitudes:

$$f^{(D)}(\mathbf{k}',\mathbf{k}) = u(\mathbf{k}'-\mathbf{k}) + \frac{1}{(2\pi)^D}\int d^D\mathbf{q}\; u(\mathbf{k}'-\mathbf{q})\frac{f^{(D)}(\mathbf{q},\mathbf{k})}{k^2-q^2+i\eta} \tag{1.26}$$

Finally, we can insert Eqn. (1.25) into Eqn. (1.23) to get:

$$u(\mathbf{k}'-\mathbf{p}) = f^{(D)}(\mathbf{k}',\mathbf{p}) + \frac{1}{(2\pi)^D}\int d^D\mathbf{k}\frac{f^{(D)}(\mathbf{k}',\mathbf{k})f^{(D)}(\mathbf{p},\mathbf{k})^*}{k^2-p^2-i\eta} \tag{1.27}$$

In this way, the potential is completely expressed in terms of the scattering amplitude, but the values of the amplitude are not only required *on* the energy shell (i.e. for $(\mathbf{k}')^2 = \mathbf{k}^2$), but also *off* the energy shell.

For $D = 1, 2, 3$ the off shell scattering amplitude was determined in Ref. [59] for a hard-sphere scattering potential using an approach based on solving an inhomogeneous Schrödinger equation. The authors call the scattering amplitude "half on the energy shell $T$–matrix". But we do not use this terminology here in order to avoid confusion with the many–body $T$–matrix, which is introduced below. Also, the definition used here deviates from theirs by a factor of $\frac{\hbar^2}{2m}$. With the definitions used here the results are:

$$f^{(1)}(\mathbf{k}',\mathbf{k}) = -2ik\exp\left(-i(k+k'\cos\theta)a^{(1)}\right), \tag{1.28}$$

$$f^{(2)}(\mathbf{k}',\mathbf{k}) = 4\sum_{m=0}^{\infty}\epsilon_m\frac{J_m(k'a^{(2)})}{iH_m(ka^{(2)})}\cos(m\theta), \tag{1.29}$$

$$f^{(3)}(\mathbf{k}',\mathbf{k}) = -4ia^{(3)}\sum_{l=0}^{\infty}(2l+1)\frac{j_l(k'a^{(3)})}{(ka^{(3)})h_l(ka^{(3)})}P_l(\cos\theta), \tag{1.30}$$

where $\theta$ is the angle between $\mathbf{k}$ and $\mathbf{k}'$ (in $1D$ $\theta$ is either 0 or $\pi$), $J_m$ ($j_l$) is the (spherical) Bessel function of the first kind and order $m$ ($l$), $H_m$ ($h_l$) is the first (spherical) Hankel function of order $m$ ($l$), $\epsilon_m = 1$ for $m = 0$ and $\epsilon_m = 2$ otherwise, and $P_l$ is the Legendre polynomial of oder $l$. The parameters $a^{(i)}$ can be identified with the radii of the atoms if the interaction potential is modeled by hard sphere potentials. For more general potentials, they are identified with the ($s$–wave) scattering lengths. In the limit of low momenta ($k'a^{(i)} \ll 1$ and $ka^{(i)} \ll 1$) the appropriate limits of the Bessel (Hankel)

functions (see e.g. [61]) show that only the first terms of the series expansions are important to first order in $k'a^{(i)}$ and $ka^{(i)}$. In this limit, the expressions for the scattering amplitudes simplify considerably:

$$f^{(1)}(\mathbf{k}',\mathbf{k}) = -2ik\left(1 - ika^{(1)} - ik'a^{(1)}\cos\theta\right), \tag{1.31}$$

$$f^{(2)}(\mathbf{k}',\mathbf{k}) = -4\pi/\left(2\ln(ka^{(2)}/2) + 2\gamma - i\pi\right), \tag{1.32}$$

$$f^{(3)}(\mathbf{k}',\mathbf{k}) = 4\pi a^{(3)}\left(1 - ika^{(3)}\right), \tag{1.33}$$

where $\gamma \approx 0.577$ is the Euler-Mascheroti constant. We observe that in two and three dimensions in the low momentum limit the scattering amplitudes do not depend on $k'$ and $\theta$. These are the main results of this section.

Going back to Eqns. (1.9) and (1.10) we can conclude that for two identical Bosons (we assume Spin 0) the scattering amplitude is:

$$\tfrac{1}{2}\left(f^{(D)}(\mathbf{k}',\mathbf{k}) + f^{(D)}(-\mathbf{k}',\mathbf{k})\right). \tag{1.34}$$

Fermions have at least spin $\frac{1}{2}$. If the spin wavefunction is antisymmetric then the spatial wave function has to be symmetric and the scattering amplitude in this case is the same as for Bosons. In the following, however, we consider spin-polarized Fermions. Since in this case all spins point into the same direction, the spin wavefunction is symmetric and thus the spacial wavefunction has to be antisymmetric. We then get:

$$\tfrac{1}{2}\left(f^{(D)}(\mathbf{k}',\mathbf{k}) - f^{(D)}(-\mathbf{k}',\mathbf{k})\right). \tag{1.35}$$

Since we know from the preceding discussion that in two and three dimensions the low momentum scattering amplitude does not depend on the scattering angle, we have $f^{(D)}(\mathbf{k}',\mathbf{k}) = f^{(D)}(-\mathbf{k}',\mathbf{k})$ in this case. We conclude: *In two and three dimensions the low momentum scattering amplitude for identical Bosons is the same as for distinguishable particles. The scattering amplitude for spin-polarized identical Fermions is zero.*

## 1.3 Replacing the interaction potential by the scattering length

In this section, we derive expressions for the interaction potential in terms of the scattering lengths. There are basically three reasons for doing this.

The first pragmatic reason is that when we deal with atomic interactions it is very hard to determine the interaction potential precisely, since atom–atom interactions are a net result of the interactions between the their electron clouds. But, to completely describe interactions of two electronic clouds is a really complicated many–body problem. Also experimentally, it is hard to measure the shape of the interaction potentials. On the other hand, there are some measurements available for the scattering lengths.

A more mathematical argument in favor the notion of the scattering length is that even if the Fourier transform of the interaction potential is not defined (as e.g. for the Coulomb potential or the hard-sphere potential) or the potential has bound states, it is still possible to apply the concept of a scattering length. We then automatically describe the system in a state that is meta–stable against binding. This is exactly the situation we aim to describe in atomic gases.

The third point is that as we have seen in the last section, the scattering amplitude depends only on the scattering length and the relative momentum of the particles in the

low momentum limit (a limit which is approriate for atomic gases as we will see in the following). In this limit, the only parameter we need to specify the scattering amplitude is the scattering length. The same is also true for the interaction potential as we will see now.

Starting from Eqn. (1.27) along with Eqns. (1.31)–(1.33), we find:

$$\begin{aligned} u(\mathbf{k}'-\mathbf{p}) &= -2ip\left(1-ipa^{(1)}-ik'a^{(1)}\cos\theta\right) \\ &\quad +\frac{4}{\pi}\int_0^\infty dk\frac{k^2(1-2ika^{(1)})}{k^2-p^2-i\eta} \qquad (1.36) \\ u(\mathbf{k}'-\mathbf{p}) &= -2\pi/\ln(pa^{(2)})+\pi(2\gamma-2\ln 2-i\pi)/\ln^2(pa^{(2)}) \\ &\quad +2\pi\int_0^\infty dk\frac{k}{\ln^2(ka^{(2)})}\frac{1}{k^2-p^2-i\eta} \qquad (1.37) \\ u(\mathbf{k}'-\mathbf{p}) &= 4\pi a^{(3)}\left(1-ipa^{(3)}\right) \\ &\quad +8(a^{(3)})^2\int_0^\infty dkk^2\frac{1}{k^2-p^2-i\eta}, \qquad (1.38) \end{aligned}$$

where we integrated (summed) over the angels and kept only terms to maximally second order in the small parameters $k'a^{(i)}$ and $pa^{(i)}$ or $1/\ln(k'a^{(2)})$ and $1/\ln(pa^{(i)})$, respectively. We also assumed that the main contribution to the non divergent parts of the integrals come from regions with $k\approx p$. To the issue of divergences we come later in the context of the many–body $T$–Matrices.

## 1.4 Comments on reduced dimensions

Up to this point, it was not motivated why other than three dimensional scattering processes might be interesting. The reason is that in experiments with atomic gases in magnetic traps one can (almost arbitrarily) choose the shape of the trap by varying the strengths of the magnetic fields in each spacial direction [62, 63, 64]. In the center of a magnetic trap, the confining potential is nearly harmonic in all directions. To be specific let us consider the following one-particle Hamiltonian:

$$\begin{aligned} \hat{H}_{xy} &= -\frac{\hbar^2}{2m}\left(\frac{\partial^2}{\partial x^2}+\frac{\partial^2}{\partial y^2}\right)+\tfrac{1}{2}m\omega_{xy}^2\left(x^2+y^2\right), \qquad (1.39) \\ \hat{H}_z &= -\frac{\hbar^2}{2m}\frac{\partial^2}{\partial z^2}+\tfrac{1}{2}m\omega_z^2z^2. \qquad (1.40) \end{aligned}$$

There, we have an isotropic part within the $xy$-plane (the radial part) and an axial part with a different trapping frequency $\omega_z\neq\omega_{xy}$. The trapping frequencies are determined by the masses, the magnetic moments, and the magnetic fields in the radial and axial directions. Experimentalists can increase the trapping frequency in either the radial $\omega_{xy}\gg\omega_z$ or the axial direction $\omega_z\gg\omega_{xy}$ considerably. Correspondingly, the energy quantum in these direction(s) ($\hbar\omega_{xy}$ or $\hbar\omega_z$, respectively) also increases and if it is larger than all other energy scales of the system only the ground state wavefunction(s) in this (these) direction(s) is (are) populated for energetic reasons. Straightforwardly, one writes the 3D wavefunction as a product of this ground state (a Gaussian state) and another wavefunction in the direction with the weak confinement. The problem is then solved in the direction(s) of the strong confinement and only the wavefunction in the other directions(s) is yet unknown. Then we have a so–called confinement dominated system that behaves in some aspects effectively one or two dimensionally. Some consequences

for Bose–Fermi mixtures have been explored in Ref. [65]. But this is not yet exhaustive, because as the trapping frequency in a certain direction raises the harmonic oscillator length ($l_{xy} = \sqrt{\hbar/m\omega_{xy}}$ or $l_z = \sqrt{\hbar/m\omega_z}$, respectively) in this direction decreases. At some point, it will be comparable and even smaller than the magnitude of the inter–particle scattering length. This has a dramatic impact on the scattering process because then some intermediate states of the scattering process are suppressed in the direction(s) with the strong confinement. In this regime, the results of the low dimensional scattering amplitudes of the previous sections have to be applied. The system is then said to be quasi one dimensional or quasi two dimensional, respectively (in contrast to confinement dominated), because in every respect it behaves as if its world had only one or two spacial dimension(s). In the case of pure quantum gases, interesting properties of quasi low dimensional system were found that are very different from the 3D–case, e.g. quasi–1D or quasi–2D Fermi gases were studied in Refs. [66, 67] while quasi–1D gases were considered in Refs. [68, 69, 70] for quasi–1D Bosons and and quasi–2D Bose gases in Refs. [71, 72, 73, 74]. It was also possible to derive expressions for the scattering lengths in quasi low dimensional systems, only in terms of the three dimensional scattering length and the harmonic oscillator length of the strong confinement:

$$a^{(1)} = -\frac{l_{xy}}{2a^{(3)}}\left(1 - C\frac{a^{(3)}}{l_{xy}}\right), \tag{1.41}$$

where $C \approx 1.4603\ldots$. This was derived in Ref. [75]. And in Ref. [76] it was shown that:

$$a^{(2)} = 2\sqrt{\frac{\pi}{B}}l_z e^{-\sqrt{\pi}l_z/a^{(3)}-\gamma}, \tag{1.42}$$

where $B \approx 0.915\ldots$.

To our best knowledge nobody has investigated Bose–Fermi mixtures in this regime. Thus interesting new projects are possible and the results for the low dimension scattering amplitudes could be a starting point. The following methods applied in this thesis might also be useful as a guideline, even though only three dimensional systems are treated. If one, however, wants to apply Eqn. (1.31) special attention has been drawn to the validity of perturbation theory. In fact, for $a^{(1)} \to 0$, the scattering amplitude does not vanish and thus not correspond to the non-interacting limit. Useful remarks about this observation can be found in Ref. [69].

# Chapter 2

# Many–particle Bose–Fermi systems

## 2.1 Formulation of second quantization for many–particle Systems

A pure state of a single quantum mechanical particle can be described by a vector from a Hilbert space $\mathcal{H}$. In the last chapter, we have worked with elements in the two–particle space $\mathcal{H}\otimes\mathcal{H}$. As the number of particles increases the so called "first quantized" notation we used there becomes more and more cumbersome. In this section, we briefly review the formulation of "second quantization" which is suitable for the description of many–particle systems.

A pure state of $N$ distinguishable particles is represented by a vector out of the tensor product $\mathcal{H}^{\otimes N} := \mathcal{H}_1\otimes\ldots\otimes\mathcal{H}_N$. For completeness we also define $\mathcal{H}^{\otimes 0} := \mathrm{Span}\{|\rangle\}$, where $|\rangle$ is the so–called vacuum state. If the particles are indistinguishable (i.e. no quantum measurement can be designed to distinguish a certain particle from all the $N-1$ others), then $\mathcal{H}_1 = \mathcal{H}_i = \mathcal{H}_N = \mathcal{H}$ and the state is necessarily contained in a subspace of the full tensor product space, namely either an element of $\mathcal{H}_B^{\otimes N} := \mathcal{S}\mathcal{H}^{\otimes N}$ or $\mathcal{H}_F^{\otimes N} := \mathcal{A}\mathcal{H}^{\otimes N}$, where the operators $\mathcal{S}$ and $\mathcal{A}$ are the complete symmetrization and anti-symmetrization operators, respectively:

$$\mathcal{S}\psi_1\otimes\ldots\otimes\psi_N \quad := \quad \frac{1}{N!}\sum_P \psi_{P(1)}\otimes\ldots\otimes\psi_{P(N)}, \tag{2.1}$$

$$\mathcal{A}\psi_1\otimes\ldots\otimes\psi_N \quad := \quad \frac{1}{N!}\sum_P (-1)^{|P|}\psi_{P(1)}\otimes\ldots\otimes\psi_{P(N)}. \tag{2.2}$$

The sums run over all permutations $P$ and $|P|$ denotes the number of transpositions in $P$. The extension of the above definitions to arbitrary states is done by linearity. We note that these operators are projectors. Bosonic particles are described by the elements in $\mathcal{H}_B^{\otimes N}$ and Fermionic ones by the elements in $\mathcal{H}_F^{\otimes N}$. A more complete space for the Bosons, which also allows a superposition of arbitrary numbers of particles is the Bosonic Fock[1] space:

$$\mathcal{F}_B = \bigoplus_{N=0}^{\infty} \mathcal{H}_B^{\otimes N} \tag{2.3}$$

[1]Sometimes the term "Fock state" is used to denote a state with a sharp number of particles. We adopt a more general definition here.

and likewise for the Fermions the Fermionic Fock space:

$$\mathcal{F}_F = \bigoplus_{N=0}^{\infty} \mathcal{H}_F^{\otimes N}. \tag{2.4}$$

Creation and destruction operators on the respective Fock spaces can be defined with help of the auxiliary operators:

$$\begin{aligned} \hat{c}^\dagger(\psi)|\rangle &:= \psi, \\ \hat{c}^\dagger(\psi)\psi_1 \otimes \ldots \otimes \psi_N &:= \sqrt{N+1}\psi \otimes \psi_1 \otimes \ldots \psi_N, \qquad (2.5) \\ \hat{c}(\psi)|\rangle &:= 0, \\ \hat{c}(\psi)\psi_1 \otimes \ldots \otimes \psi_N &:= \sqrt{N}\langle\psi|\psi_1\rangle\psi_2 \otimes \ldots \psi_N. \qquad (2.6) \end{aligned}$$

Again, the extension to arbitrary states is done by linearity. After a little algebra one can see that indeed $\hat{c}^\dagger(\psi)$ is the adjoint of $\hat{c}(\psi)$. Also we note that the operators $\hat{c}^\dagger(\psi)$ depend linearly on $\psi$ and the operators $\hat{c}(\psi)$ are anti-linear in $\psi$. Thus, a basis in $\mathcal{H}$ induces a corresponding basis for the Fock space operators. The Bosonic creation and destruction operators are

$$\hat{a}^\dagger(\psi) := \mathcal{S}\hat{c}^\dagger(\psi)\mathcal{S}, \quad \hat{a}(\psi) := \mathcal{S}\hat{c}(\psi)\mathcal{S}, \tag{2.7}$$

and likewise the Fermionic creation and destruction operators are

$$\hat{b}^\dagger(\psi) := \mathcal{A}\hat{c}^\dagger(\psi)\mathcal{A}, \quad \hat{b}(\psi) := \mathcal{A}\hat{c}(\psi)\mathcal{A}. \tag{2.8}$$

Because $\mathcal{S}$ and $\mathcal{A}$ are projectors $\hat{a}^\dagger(\psi)$ is still the adjoint of $\hat{a}(\psi)$ and $\hat{b}^\dagger(\psi)$ is still the adjoint of $\hat{b}(\psi)$. The physical interpretation is that $\hat{a}^\dagger(\psi)$ creates a Boson in the state $\psi$ and $\hat{a}(\psi)$ destroys a Boson in the state $\psi$. The interpretation of the Fermion operators is analogous. After some algebra, it follows:

$$\begin{aligned} &[\hat{a}^\dagger(\psi_1), \hat{a}^\dagger(\psi_2)] = 0, \quad [\hat{a}(\psi_1), \hat{a}(\psi_2)] = 0, \\ &[\hat{a}(\psi_1), \hat{a}^\dagger(\psi_2)] = \langle\psi_1|\psi_2\rangle \end{aligned} \tag{2.9}$$

and

$$\begin{aligned} &\{\hat{b}^\dagger(\psi_1), \hat{b}^\dagger(\psi_2)\} = 0, \quad \{\hat{b}(\psi_1), \hat{b}(\psi_2)\} = 0, \\ &\{\hat{b}(\psi_1), \hat{b}^\dagger(\psi_2)\} = \langle\psi_1|\psi_2\rangle \end{aligned} \tag{2.10}$$

where $[\cdot,\cdot]$ denotes the commutator and $\{\cdot,\cdot\}$ denotes the anti-commutator. The creation and destruction operators are not Hermitian and thus not observables. The operators $\hat{N}_B(\psi) = \hat{a}^\dagger(\psi)\hat{a}(\psi)$ and $\hat{N}_F(\psi) = \hat{b}^\dagger(\psi)\hat{b}(\psi)$, however, are observables. If $N_B(\psi)$ denotes an eigenvalue of $\hat{N}_B(\psi)$, $N_F(\psi)$ denotes an eigenvalue of $\hat{N}_F(\psi)$ and $|\ldots, N_B(\psi), \ldots\rangle$ or $|\ldots, N_F(\psi), \ldots\rangle$ denote the corresponding eigenvectors, then it can be shown from the (anti-)commutator relations that

$$\begin{aligned} &\hat{N}_B(\psi)\hat{a}^\dagger(\psi)|\ldots, N_B(\psi), \ldots\rangle \\ &\quad = (N_B(\psi)+1)\ \hat{a}^\dagger(\psi)|\ldots, N_B(\psi), \ldots\rangle, \qquad (2.11) \\ &\hat{N}_B(\psi)\hat{a}(\phi)|\ldots, N_B(\psi), \ldots\rangle \\ &\quad = (N_B(\psi)-1)\ \hat{a}(\psi)|\ldots, N_B(\psi), \ldots\rangle, \qquad (2.12) \\ &\hat{N}_F(\psi)\hat{b}^\dagger(\psi)|\ldots, N_F(\psi), \ldots\rangle \qquad (2.13) \\ &\quad = (N_F(\psi)+1)\ \hat{b}^\dagger(\psi)|\ldots, N_F(\psi), \ldots\rangle, \qquad (2.14) \\ &\hat{N}_F(\psi)\hat{b}(\psi)|\ldots, N_F(\psi), \ldots\rangle \\ &\quad = (N_F(\psi)-1)\ \hat{b}(\psi)|\ldots, N_F(\psi), \ldots\rangle, \qquad (2.15) \end{aligned}$$

such that the operator $\hat{N}_B(\psi)$ counts the number of Bosons in the state $\psi$ and the operator $\hat{N}_F(\psi)$ counts the number of Fermions in the state $\psi$. We can use this interpretation to promote a single–particle operator $\hat{O}_{\mathcal{H}}$ on $\mathcal{H}$ to an operator on the Fock space:

$$\hat{O}_{\mathcal{F}_B} = \sum_i \langle\psi_i|\hat{O}_{\mathcal{H}}|\psi_i\rangle \hat{N}_B(\psi_i), \tag{2.16}$$

$$\hat{O}_{\mathcal{F}_F} = \sum_i \langle\psi_i|\hat{O}_{\mathcal{H}}|\psi_i\rangle \hat{N}_F(\psi_i), \tag{2.17}$$

with $\{\psi_i\}$ being an orthonormal basis of $\mathcal{H}$, where $\hat{O}_{\mathcal{H}}$ is diagonal[2]. Since $i$ can also be a continuous index, the sum may be changed into an integral in this case. The above definition is independent of the choice of this orthonormal basis and thus well–defined and a Hermitian single-particle operator goes into a Hermitian operator on Fock space. Similarly, one can extend all two–particle operators $\hat{O}_{\mathcal{H}\otimes\mathcal{H}}$ to the Fock space by defining:

$$\hat{O}_{\mathcal{F}_B} = \sum_{i,j} \langle\psi_i\otimes\psi_j|\hat{O}_{\mathcal{H}\otimes\mathcal{H}}|\psi_i\otimes\psi_j\rangle \hat{a}^\dagger(\psi_j)\hat{a}^\dagger(\psi_i)\hat{a}(\psi_i)\hat{a}(\psi_j) \tag{2.18}$$

$$\hat{O}_{\mathcal{F}_F} = \sum_{i,j} \langle\psi_i\otimes\psi_j|\hat{O}_{\mathcal{H}\otimes\mathcal{H}}|\psi_i\otimes\psi_j\rangle \hat{b}^\dagger(\psi_j)\hat{b}^\dagger(\psi_i)\hat{b}(\psi_i)\hat{b}(\psi_j). \tag{2.19}$$

Again, $\hat{O}_{\mathcal{H}\otimes\mathcal{H}}$ has to be diagonal in the basis $\{\psi_i\otimes\psi_j\}$. It has to be noted that the Fock space operators appearing in Eqns. (2.18) and (2.19) are not simply $\hat{N}_B(\psi_i)\hat{N}_B(\psi_j)$ or $\hat{N}_F(\psi_i)\hat{N}_F(\psi_j)$, because the latter are not Hermitian.

From the anti-commutators for the Fermions is follows that $\hat{b}^\dagger(\psi)\hat{b}^\dagger(\psi) = 0$, i.e. no two Fermions can be created in the same state. This is the mathematical statement of the Pauli principle. There is no such relation for the Bosons which opens the possibility of Bose-Einstein-condensation (BEC).

It is very common to work with creation and destruction operators for certain $\psi$'s namely the (improper) eigenstates of the position ($\sqrt{V}\delta(\cdot - \mathbf{x})$) or momentum operators ($e^{i\mathbf{k}\cdot}/\sqrt{V}$) respectively, where $V$ is the volume of the system ($f(\cdot)$ is a short hand notation for an entire function $x \mapsto f(x)$). Therefore, we make the following identifications:

$$\hat{a}^\dagger_{\mathbf{k}} := \hat{a}^\dagger\left(e^{i\mathbf{k}\cdot}/\sqrt{V}\right), \qquad \hat{a}_{\mathbf{k}} := \hat{a}\left(e^{i\mathbf{k}\cdot}/\sqrt{V}\right), \tag{2.20}$$

$$\hat{\Phi}^\dagger(\mathbf{x}) := \hat{a}^\dagger\left(\sqrt{V}\delta(\cdot - \mathbf{x})\right), \qquad \hat{\Phi}(\mathbf{x}) := \hat{a}\left(\sqrt{V}\delta(\cdot - \mathbf{x})\right), \tag{2.21}$$

and

$$\hat{b}^\dagger_{\mathbf{k}} := \hat{b}^\dagger(e^{i\mathbf{k}\cdot}/\sqrt{V}), \qquad \hat{b}_{\mathbf{k}} := \hat{b}(e^{i\mathbf{k}\cdot}/\sqrt{V}), \tag{2.22}$$

$$\hat{\Psi}^\dagger(\mathbf{x}) := \hat{b}^\dagger\left(\sqrt{V}\delta(\cdot - \mathbf{x})\right), \qquad \hat{\Psi}(\mathbf{x}) := \hat{b}\left(\sqrt{V}\delta(\cdot - \mathbf{x})\right). \tag{2.23}$$

The operators $\hat{\Phi}^\dagger(\mathbf{x}), \hat{\Phi}(\mathbf{x}), \hat{\Psi}^\dagger(\mathbf{x}), \hat{\Psi}(\mathbf{x})$ are the field operators. Using the (anti–) linearity of the operators in $\phi$ and

$$\sqrt{V}\delta(\cdot - \mathbf{x}) = \frac{1}{\sqrt{V}} \sum_{\mathbf{k}} e^{i\mathbf{k}\cdot} e^{-i\mathbf{k}\mathbf{x}} \tag{2.24}$$

[2]If one wants to relax the condition that $\hat{O}_{\mathcal{H}}$ has to be diagonal, the definition looks $\hat{O}_{\mathcal{F}_B} = \sum_{i,j}\langle\psi_j|\hat{O}_{\mathcal{H}}|\psi_i\rangle\hat{a}^\dagger(\psi_i)\hat{a}(\psi_j)$, but then the interpretation is only obvious, if we diagonalize $\hat{O}_{\mathcal{H}}$, and thus we are back at the original definition.

we can express the field operators in terms of the $\hat{a}^\dagger_{\mathbf{k}}, \hat{a}_{\mathbf{k}}, \hat{b}^\dagger_{\mathbf{k}}, \hat{b}_{\mathbf{k}}$:

$$\hat{\Phi}^\dagger(\mathbf{x}) = \hat{a}^\dagger \left( \frac{1}{\sqrt{V}} \sum_{\mathbf{k}} e^{i\mathbf{k}\cdot} e^{-i\mathbf{k}\mathbf{x}} \right) = \sum_{\mathbf{k}} e^{i\mathbf{k}\mathbf{x}} \hat{a}^\dagger_{\mathbf{k}}, \tag{2.25}$$

$$\hat{\Phi}(\mathbf{x}) = \hat{a} \left( \frac{1}{\sqrt{V}} \sum_{\mathbf{k}} e^{i\mathbf{k}\cdot} e^{-i\mathbf{k}\mathbf{x}} \right) = \sum_{\mathbf{k}} e^{-i\mathbf{k}\mathbf{x}} \hat{a}_{\mathbf{k}}, \tag{2.26}$$

$$\hat{\Psi}^\dagger(\mathbf{x}) = \hat{b}^\dagger \left( \frac{1}{\sqrt{V}} \sum_{\mathbf{k}} e^{i\mathbf{k}\cdot} e^{-i\mathbf{k}\mathbf{x}} \right) = \sum_{\mathbf{k}} e^{i\mathbf{k}\mathbf{x}} \hat{b}^\dagger_{\mathbf{k}}, \tag{2.27}$$

$$\hat{\Psi}(\mathbf{x}) = \hat{b} \left( \frac{1}{\sqrt{V}} \sum_{\mathbf{k}} e^{i\mathbf{k}\cdot} e^{-i\mathbf{k}\mathbf{x}} \right) = \sum_{\mathbf{k}} e^{-i\mathbf{k}\mathbf{x}} \hat{b}_{\mathbf{k}}. \tag{2.28}$$

The following (anti–)commutators are merely special cases of the above Eqns. (2.9) and (2.10):

$$[\hat{a}_{\mathbf{k}}, \hat{a}^\dagger_{\mathbf{k}'}] = \delta_{\mathbf{k},\mathbf{k}'}, \quad [\hat{a}^\dagger_{\mathbf{k}}, \hat{a}^\dagger_{\mathbf{k}'}] = 0, \quad [\hat{a}_{\mathbf{k}}, \hat{a}_{\mathbf{k}'}] = 0, \tag{2.29}$$

$$[\hat{\Phi}(\mathbf{x}), \hat{\Phi}^\dagger(\mathbf{x}')] = \delta(\mathbf{x} - \mathbf{x}'), \quad [\hat{\Phi}^\dagger(\mathbf{x}), \hat{\Phi}^\dagger(\mathbf{x}')] = 0, \tag{2.30}$$

$$[\hat{\Phi}(\mathbf{x}), \hat{\Phi}(\mathbf{x}')] = 0, \tag{2.31}$$

$$\{\hat{b}_{\mathbf{k}}, \hat{b}^\dagger_{\mathbf{k}'}\} = \delta_{\mathbf{k},\mathbf{k}'}, \quad \{\hat{b}^\dagger_{\mathbf{k}}, \hat{a}^\dagger_{\mathbf{k}'}\} = 0, \quad \{\hat{b}_{\mathbf{k}}, \hat{b}_{\mathbf{k}'}\} = 0, \tag{2.32}$$

$$\{\hat{\Psi}(\mathbf{x}), \hat{\Psi}^\dagger(\mathbf{x}')\} = \delta(\mathbf{x} - \mathbf{x}'), \quad \{\hat{\Psi}^\dagger(\mathbf{x}), \hat{\Psi}^\dagger(\mathbf{x}')\} = 0, \tag{2.33}$$

$$\{\hat{\Psi}(\mathbf{x}), \hat{\Psi}(\mathbf{x}')\} = 0. \tag{2.34}$$

We now look at some examples of how to extend single–particle and two–particle operators on Fock–space. We start with the single–particle operator which gives the density at position $\mathbf{x}$ and reads $\int d^3\mathbf{x}' \delta(\mathbf{x}' - \mathbf{x}) |\mathbf{x}'\rangle\langle\mathbf{x}'|$, where $|\mathbf{x}'\rangle\langle\mathbf{x}'|$, is the projection operator onto the the position eigenvector at $\mathbf{x}'$. This operator is as it stands diagonal in space representation and its diagonal elements are $\delta(\mathbf{x}' - \mathbf{x})$. So we can apply the above Defs. (2.16) and (2.17) to see that the density operator in Fock space reads

$$\hat{n}_B(\mathbf{x}) = \int d^3\mathbf{x}' \delta(\mathbf{x}' - \mathbf{x}) \hat{\Phi}^\dagger(\mathbf{x}') \hat{\Phi}(\mathbf{x}') = \hat{\Phi}^\dagger(\mathbf{x}) \hat{\Phi}(\mathbf{x}). \tag{2.35}$$

The same reasoning leads to

$$\hat{n}_F(\mathbf{x}) = \hat{\Psi}^\dagger(\mathbf{x}) \hat{\Psi}(\mathbf{x}). \tag{2.36}$$

Similarly, the operator of potential energy $\int d^3\mathbf{x}' V_B(\mathbf{x}') |\mathbf{x}'\rangle\langle\mathbf{x}'|$ extended to Fock space reads

$$\hat{V}_B = \int d^3\mathbf{x}' V_B(\mathbf{x}') \hat{\Phi}^\dagger(\mathbf{x}') \hat{\Phi}(\mathbf{x}') \tag{2.37}$$

On the other hand, the single-particle kinetic energy operator is diagonal in momentum representation: $\sum_{\mathbf{k}} \frac{\hbar^2 k^2}{2m} |\mathbf{k}\rangle\langle\mathbf{k}|$. The corresponding Fock space operator is then:

$$\hat{T}_B = \sum_{\mathbf{k}} \frac{\hbar^2 \mathbf{k}^2}{2m_B} \hat{a}^\dagger_{\mathbf{k}} \hat{a}_{\mathbf{k}}$$

$$
\begin{aligned}
&= \sum_{\mathbf{k}} \frac{\hbar^2\mathbf{k}^2}{2m_B} \int d^3\mathbf{x}\, e^{-i\mathbf{k}\mathbf{x}} \hat{\Phi}^\dagger(\mathbf{x}) \int d^3\mathbf{x}' e^{i\mathbf{k}\mathbf{x}'} \hat{\Phi}(\mathbf{x}') \\
&= -\int d^3\mathbf{x} \hat{\Phi}^\dagger(\mathbf{x}) \frac{\hbar^2\nabla^2}{2m_B} \int d^3\mathbf{x}' \sum_{\mathbf{k}} e^{i\mathbf{k}(\mathbf{x}'-\mathbf{x})} \hat{\Phi}(\mathbf{x}') \\
&= -\int d^3\mathbf{x}\, \hat{\Phi}^\dagger(\mathbf{x}) \frac{\hbar^2\nabla^2}{2m_B} \hat{\Phi}(\mathbf{x}), \qquad (2.38)
\end{aligned}
$$

where the inversions Eqns. (2.25) and (2.26) were inserted and $\sum_{\mathbf{k}} e^{i\mathbf{k}(\mathbf{x}'-\mathbf{x})} = \delta(\mathbf{x}'-\mathbf{x})$ was used. $\nabla^2$ is supposed to act on the unprimed $\mathbf{x}$.

An important two–particle operator is that of interaction energy. It reads in two–particle space $\frac{1}{2}\int\int d^3\mathbf{x} d^3\mathbf{x}' U(\mathbf{x}-\mathbf{x}')|\mathbf{x}\rangle\otimes|\mathbf{x}'\rangle\langle\mathbf{x}|\otimes\langle\mathbf{x}'|$ (i.e diagonal in the basis $|\mathbf{x}\rangle\otimes|\mathbf{x}'\rangle$) and in Fock space:

$$
\hat{U} = \tfrac{1}{2}\int\int d^3\mathbf{x}\, d^3\mathbf{x}' U(\mathbf{x}-\mathbf{x}')\hat{\Phi}^\dagger(\mathbf{x}')\hat{\Phi}^\dagger(\mathbf{x})\hat{\Phi}(\mathbf{x})\hat{\Phi}(\mathbf{x}'). \qquad (2.39)
$$

All the corresponding Fermionic operators are very similar only with Bosonic field operators replaced by Fermion field ones.

For a mixed system of identical Bosons and identical Fermions we work in the space $\mathcal{F}_B \otimes \mathcal{F}_F$. Of course, then all operators which act only on the Boson part of this space commute with all operators that act only on the Fermion part. The Boson-Fermion interaction energy operator in Fock–space is derived from the two–particle interaction energy operator just in the same way as before. Its expression is:

$$
\hat{V} = \int\int d^3\mathbf{x}\, d^3\mathbf{x}' V(\mathbf{x}-\mathbf{x}')\hat{\Phi}^\dagger(\mathbf{x}')\hat{\Psi}^\dagger(\mathbf{x})\hat{\Psi}(\mathbf{x})\hat{\Phi}(\mathbf{x}'). \qquad (2.40)
$$

## 2.2 Particle-hole transformation and Bogoliubov replacement

In this section, we consider the simplest case of a many–particle Boson-Fermion system, namely a system with no external potential, neither for the Bosons nor for the Fermions, and no particle–particle interactions at all. Then the Hamiltonian reads:

$$
\hat{H}_0 = \hat{T}_B + \hat{T}_F, \qquad (2.41)
$$

with $\hat{T}_B$ and $\hat{T}_F$ as defined in the previous section. In the absence of Boson-Fermion interactions, the Boson and the Fermion sector completely decouple. To label the states, we use the eigenvalues of the number operators as defined in the previous section. If the boundaries of the system is the surface of a large cube with volume $V$ and we choose periodic boundary conditions, the single particle states are simply $\frac{1}{\sqrt{V}} e^{-i\mathbf{k}\mathbf{x}}$, where

$$
\mathbf{k} = \frac{2\pi}{V^{1/3}}(n_x, n_y, n_z), \qquad (2.42)
$$

and where all natural numbers $n_i$ are allowed. As seen in the last section, the number of particles in each state is determined as the eigenvalue of the operators $N_{B/F}(\mathbf{k})$. The operators of total numbers of Bosons and Fermions respectively,

$$
\begin{aligned}
\hat{N}_B &= \sum_{\mathbf{k}} \hat{a}^\dagger_{\mathbf{k}} \hat{a}_{\mathbf{k}}, \qquad (2.43) \\
\hat{N}_F &= \sum_{\mathbf{k}} \hat{b}^\dagger_{\mathbf{k}} \hat{b}_{\mathbf{k}}, \qquad (2.44)
\end{aligned}
$$

are constants. The ground state of the systems is then simply:

$$|\mathbf{G}\rangle = |N_B, 0, 0, \ldots\rangle \otimes |1, 1, \ldots, 1, 0, 0, \ldots\rangle = \frac{1}{\sqrt{N_B!}} \left(\hat{a}_{\mathbf{0}}^\dagger\right)^{N_B} \hat{b}_{\mathbf{0}}^\dagger \ldots \hat{b}_{\mathbf{k}_F}^\dagger |\rangle, \tag{2.45}$$

where $\mathbf{k}_F$ is the highest occupied Fermion momentum. As seen in the previous section, all Fermion momenta in Eqn. (2.45) have to be different, otherwise the result would be zero. $|\mathbf{G}\rangle$ can also be characterized as:

$$\hat{a}_{\mathbf{k}}|\mathbf{G}\rangle = 0 \quad \text{for} \quad |\mathbf{k}| > 0, \tag{2.46}$$

$$\hat{b}_{\mathbf{k}}^\dagger|\mathbf{G}\rangle = 0 \quad \text{for} \quad |\mathbf{k}| \leq k_F, \tag{2.47}$$

$$\hat{b}_{\mathbf{k}}|\mathbf{G}\rangle = 0 \quad \text{for} \quad |\mathbf{k}| > k_F. \tag{2.48}$$

This suggests to re–define the Fermion operators:

$$\hat{c}_{\mathbf{k}} = \hat{b}_{-\mathbf{k}}^\dagger \quad \text{for} \quad |\mathbf{k}| \leq k_F, \quad \hat{c}_{\mathbf{k}} = \hat{b}_{\mathbf{k}} \quad \text{for} \quad |\mathbf{k}| > k_F. \tag{2.49}$$

This transformation does not alter the anti–commutation relations. The interpretation is that $\hat{c}_{\mathbf{k}}$ destroys a Fermion hole if $\mathbf{k}$ is below the Fermi momentum and destroys a Fermion particle if $\mathbf{k}$ is above the Fermi momentum. Unfortunately, it is not possible to define a complete set of annihilation operators for the Bosons, because $\hat{a}_{\mathbf{0}}|\mathbf{G}\rangle \neq 0$ and $\hat{a}_{\mathbf{0}}^\dagger|\mathbf{G}\rangle \neq 0$. In order to apply Wick's theorem (see below), it is, however, essential to have a complete set of annihilation operators. For this reason, already in 1947 Bogoliubov [77] proposed to treat the single particle ground state separately. He argued that $\langle\mathbf{G}|\hat{a}_{\mathbf{0}}^\dagger\hat{a}_{\mathbf{0}}|\mathbf{G}\rangle = N_B$ and $\langle\mathbf{G}|\hat{a}_{\mathbf{0}}\hat{a}_{\mathbf{0}}^\dagger|\mathbf{G}\rangle = N_B + 1$ are almost equal if $N_B \gg 1$. The same is of course also true for all other states, where the single-particle ground state is populated with macroscopic number of particles $N_0$ (but only for them!). For those states (i.e. all states with a BEC), the operators $\hat{a}_{\mathbf{0}}$ and $\hat{a}_{\mathbf{0}}^\dagger$ "almost commute". So it might be allowed to treat them as simple $c$-numbers: $\hat{a}_{\mathbf{0}} = \sqrt{N_0}$, $\hat{a}_{\mathbf{0}}^\dagger = \sqrt{N_0 + 1} \approx \sqrt{N_0}$. This approach has the advantage of algebraic simplicity over some more recent and elaborate prescriptions [78, 79, 80]. There are, however, some disadvantages. For example, after applying the Bogoliubov replacement for the ground state operators, the number operator for the Bosons does not commute with the Hamiltonian anymore and so the ground state is not automatically a fixed Boson number state. This is, because the ground state particles are so to say excluded from the quantum field and transformed into a classical field. But there will be always a particle exchange between those two fields. Thus, one has to impose the condition of correct number of Bosons by a Lagrange multiplier. In the next section, we will apply the Bogoliubov replacement to the Bose–Fermi Hamiltonian, but first expressions of the field operators after the particle–hole transformation for the Fermions and the Bogoliubov replacement for the Bosons are listed:

$$\hat{\phi}(\mathbf{x}) = \tfrac{1}{\sqrt{V}} \sum_{|\mathbf{k}|>0} e^{-i\mathbf{k}\mathbf{x}} \hat{a}_{\mathbf{k}}, \tag{2.50}$$

$$\hat{\psi}_1(\mathbf{x}) = \tfrac{1}{\sqrt{V}} \sum_{|\mathbf{k}|\leq k_F} e^{-i\mathbf{k}\mathbf{x}} \hat{c}_{\mathbf{k}}, \tag{2.51}$$

$$\hat{\psi}_2(\mathbf{x}) = \tfrac{1}{\sqrt{V}} \sum_{|\mathbf{k}|>k_F} e^{-i\mathbf{k}\mathbf{x}} \hat{c}_{\mathbf{k}}, \tag{2.52}$$

where the factors $\frac{1}{\sqrt{V}}$ were inserted in order to talk about particle densities rather than particle numbers. Then, the old field–operators in terms of the new ones read:

$$\hat{\Phi}(\mathbf{x})/\sqrt{V} = \sqrt{n_0} + \hat{\phi}(\mathbf{x}), \tag{2.53}$$

$$\hat{\Psi}(\mathbf{x})/\sqrt{V} = \hat{\psi}_1^\dagger(\mathbf{x}) + \hat{\psi}_2(\mathbf{x}), \tag{2.54}$$

where $n_0 = N_0/V$ is the density of the BEC, i.e. the density of the Bosons in the single-particle ground state. Treating the BEC separately, there is no need to include the lowest energy state in the description of the states. So we introduce a new ground state

$$|\mathbf{0}\rangle = |\cdot, 0, 0, \ldots\rangle \otimes |0, 0, \ldots\rangle = \hat{c}_{\mathbf{0}} ... \hat{c}_{\mathbf{k}_F} |\rangle, \tag{2.55}$$

where the $\cdot$ indicates that the single particle ground state is omitted. In the labeling of the Fermion states we switched into a particle–hole picture for the Fermions, so the 1's in $|\mathbf{G}\rangle$ turned into 0's. In this picture the operators of kinetic energy densities read

$$\hat{T}_B/V = \frac{\hbar^2 \mathbf{0}^2}{2m_B} n_0 + \sum_{|\mathbf{k}|>0} \frac{\hbar^2 \mathbf{k}^2}{2m_B} \hat{a}^\dagger_{\mathbf{k}} \hat{a}_{\mathbf{k}} = \sum_{|\mathbf{k}|>0} \frac{\hbar^2 \mathbf{k}^2}{2m_B} \hat{a}^\dagger_{\mathbf{k}} \hat{a}_{\mathbf{k}} \tag{2.56}$$

$$\hat{T}_F/V = \sum_{|\mathbf{k}|\leq k_F} \frac{\hbar^2 \mathbf{k}^2}{2m_F} \hat{c}_{\mathbf{k}} \hat{c}^\dagger_{\mathbf{k}} + \sum_{|\mathbf{k}|>k_F} \frac{\hbar^2 \mathbf{k}^2}{2m_F} \hat{c}^\dagger_{\mathbf{k}} \hat{c}_{\mathbf{k}}. \tag{2.57}$$

Passing to the limit $V \to \infty$ such that the densities $n_B = N_B/V$ and $n_F = N_F/V$ are finite we can see from Eqn. (2.42) that

$$d^3\mathbf{k} \to (2\pi)^3/V \tag{2.58}$$

and so $\sum_{\mathbf{k}} \to \frac{V}{(2\pi)^3} \int d^3\mathbf{k}$. Under these circumstances:

$$\begin{aligned} E_0 &= \langle \mathbf{0}|\hat{H}_0|\mathbf{0}\rangle \\ &= \frac{V}{(2\pi)^3} \int d^3\mathbf{k} \frac{\hbar^2 \mathbf{k}^2}{2m_B} \langle \mathbf{0}|\hat{a}^\dagger_{\mathbf{k}} \hat{a}_{\mathbf{k}}|\mathbf{0}\rangle \\ &\quad + \frac{V}{2\pi^2} \int_0^{k_F} dk\ k^2 \frac{\hbar^2 \mathbf{k}^2}{2m_F} \langle \mathbf{0}|\hat{c}_{\mathbf{k}} \hat{c}^\dagger_{\mathbf{k}}|\mathbf{0}\rangle + \frac{V}{2\pi^2} \int_0^{k_F} dk\ k^2 \frac{\hbar^2 \mathbf{k}^2}{2m_F} \langle \mathbf{0}|\hat{c}^\dagger_{\mathbf{k}} \hat{c}_{\mathbf{k}}|\mathbf{0}\rangle \\ &= 0 + \frac{3}{5} \frac{\hbar^2 k_F^2}{2m_F} k_F^3/(6\pi^2) + 0 \end{aligned} \tag{2.59}$$

So for the homogeneous, non-interacting system the only contribution to the ground state energy is the kinetic energy of the Fermions. $k_F$ can be easily determined from:

$$\begin{aligned} N_F &= \langle \mathbf{0}|\hat{N}_F|\mathbf{0}\rangle = \frac{V}{2\pi^2} \int_0^{k_F} dk\ k^2 \langle \mathbf{0}|\hat{c}_{\mathbf{k}} \hat{c}^\dagger_{\mathbf{k}}|\mathbf{0}\rangle \frac{V}{2\pi^2} \int_0^{k_F} dk\ k^2 \langle \mathbf{0}|\hat{c}^\dagger_{\mathbf{k}} \hat{c}_{\mathbf{k}}|\mathbf{0}\rangle \\ &= V k_F^3/(6\pi^2). \end{aligned} \tag{2.60}$$

Likewise, the number of condensed Bosons is determined from:

$$\begin{aligned} N_B &= N_0 + \langle \mathbf{0}|\hat{N}'_B|\mathbf{0}\rangle \\ &= N_0 + \sum_{|\mathbf{k}|>0} \langle \mathbf{0}|\hat{a}^\dagger_{\mathbf{k}} \hat{a}_{\mathbf{k}}|\mathbf{0}\rangle \\ &= N_0, \end{aligned} \tag{2.61}$$

where $\hat{N}'_B$ is the number operator of excited (also called thermal or non-condensed) Bosons. As expected, all Bosons are condensed in the absence of interactions.

## 2.3 Perturbation theory

### 2.3.1 The grand-canonical Hamiltonian

Now, we also allow for interactions among the particles. The resulting equations are by no means solvable exactly, so one has to use a perturbative approach assuming that

the interactions are weak in a sense that will be clarified below. We will also see below that the first correction terms to the noninteracting system involve the $s$-wave scattering lengths. Since, as we have seen in chapter 1, the Fermions do not $s$–wave scatter one can omit the Fermion–Fermion interactions from the very beginning. The Hamiltonian is thus:

$$\hat{H}_0 = \hat{T}_B + \hat{T}_F + \hat{U} + \hat{V}, \tag{2.62}$$

where $\hat{U}$ and $\hat{V}$ are defined in Sec. 2.1. As indicated before, we are going to apply a Bogoliubov replacement and so it is required to assure (average) particle conservation for the Bosons by introducing a Lagrangian multiplier $\mu_B$ and the grand-canonical Hamiltonian

$$\hat{K} = \hat{H} - \mu_B \hat{N}_B, \tag{2.63}$$

where $\mu_B$ is identified with the Boson chemical potential [58]. Substituting Eqn. (2.53) into Eqn. (2.63), the grand-canonical Hamiltonian reads

$$\hat{K} = \hat{K}_0 - \mu_B N_0 + \hat{W}, \tag{2.64}$$

where

$$\begin{aligned} \hat{K_0} &= \frac{\hbar^2}{2m_B}\int d^3\mathbf{x}\nabla\hat{\phi}^\dagger(\mathbf{x})\cdot\nabla\hat{\phi}(\mathbf{x}) + \frac{\hbar^2}{2m_F}\int d^3\mathbf{x}\nabla\hat{\Psi}^\dagger(\mathbf{x})\cdot\nabla\hat{\Psi}(\mathbf{x}) \\ &\quad -\mu_B\int d^3\mathbf{x}\hat{\phi}^\dagger(\mathbf{x})\hat{\phi}(\mathbf{x}), \end{aligned} \tag{2.65}$$

and

$$\hat{W} = \hat{U}_1 + \hat{U}_2 + \hat{U}_3 + \hat{V}_1 + \hat{V}_2 + \hat{V}_3 + \hat{V}_4 + \hat{V}_5 + \hat{V}_6 + \hat{V}_7 \tag{2.66}$$

with

$$\hat{U}_1 = n_0\int\int d^3\mathbf{x}d^3\mathbf{x}'\hat{\Psi}^\dagger(\mathbf{x}')U(|\mathbf{x}-\mathbf{x}'|)\hat{\Psi}(\mathbf{x}'), \tag{2.67}$$

$$\hat{U}_2 = \sqrt{n_0}\int\int d^3\mathbf{x}d^3\mathbf{x}'\hat{\Psi}^\dagger(\mathbf{x}')U(|\mathbf{x}-\mathbf{x}'|)\hat{\Psi}(\mathbf{x}')\hat{\phi}(\mathbf{x}) + \text{h.c.}, \tag{2.68}$$

$$\hat{U}_3 = \int\int d^3\mathbf{x}d^3\mathbf{x}'\hat{\phi}^\dagger(\mathbf{x})\hat{\Psi}^\dagger(\mathbf{x}')U(|\mathbf{x}-\mathbf{x}'|)\hat{\Psi}(\mathbf{x}')\hat{\phi}(\mathbf{x}), \tag{2.69}$$

$$\hat{V}_1 = \frac{1}{2}n_0^2\int\int d^3\mathbf{x}d^3\mathbf{x}'V(|\mathbf{x}-\mathbf{x}'|), \tag{2.70}$$

$$\hat{V}_2 = n_0\sqrt{n_0}\int\int d^3\mathbf{x}d^3\mathbf{x}'V(|\mathbf{x}-\mathbf{x}'|)\hat{\phi}(\mathbf{x}) + \text{h.c.}, \tag{2.71}$$

$$\hat{V}_3 = \frac{1}{2}n_0\int\int d^3\mathbf{x}d^3\mathbf{x}'V(|\mathbf{x}-\mathbf{x}'|)\hat{\phi}(\mathbf{x}')\hat{\phi}(\mathbf{x}) + \text{h.c.}, \tag{2.72}$$

$$\hat{V}_4 = n_0\int\int d^3\mathbf{x}d^3\mathbf{x}'\hat{\phi}^\dagger(\mathbf{x})V(|\mathbf{x}-\mathbf{x}'|)\hat{\phi}(\mathbf{x}'), \tag{2.73}$$

$$\hat{V}_5 = n_0\int\int d^3\mathbf{x}d^3\mathbf{x}'\hat{\phi}^\dagger(\mathbf{x})V(|\mathbf{x}-\mathbf{x}'|)\hat{\phi}(\mathbf{x}), \tag{2.74}$$

$$\hat{V}_6 = \sqrt{n_0}\int\int d^3\mathbf{x}d^3\mathbf{x}'\hat{\phi}^\dagger(\mathbf{x})V(|\mathbf{x}-\mathbf{x}'|)\hat{\phi}(\mathbf{x}')\hat{\phi}(\mathbf{x}) + \text{h.c.}, \tag{2.75}$$

$$\hat{V}_7 = \frac{1}{2}\int\int d^3\mathbf{x}d^3\mathbf{x}'\hat{\phi}^\dagger(\mathbf{x})\hat{\phi}^\dagger(\mathbf{x}')V(|\mathbf{x}-\mathbf{x}'|)\hat{\phi}(\mathbf{x}')\hat{\phi}(\mathbf{x}). \tag{2.76}$$

### 2.3.2 Pictures and Green's functions

According to the Schrödinger dynamics, an initial state vector $|\Phi(0)\rangle$ will develop as $|\Phi(t)\rangle = \exp(-i\hat{K}t/\hbar)|\Phi(0)\rangle$. The corresponding state in the Heisenberg picture $|\Phi(t)\rangle = \exp(i\hat{K}t/\hbar)|\Phi(t)\rangle = |\Phi(0)\rangle$ is time independent. In the interaction picture, the state at time $t$ is $|\Phi(t)\rangle_I = \exp(i\hat{K}_0 t/\hbar)\exp(-i\hat{K}t/\hbar)|\Phi(0)\rangle$.
Let $\hat{O}$ be a (time independent) operator in the Schrödinger-picture. Then the operator in the Heisenberg picture is $\hat{O}(t) = \exp(i\hat{K}t/\hbar)\hat{O}\exp(-i\hat{K}t/\hbar)$ and the same operator in the interaction picture: $\tilde{O}(t) = \exp(i\hat{K}_0 t/\hbar)\hat{O}\exp(-i\hat{K}_0 t/\hbar)$. From the notation, it is clear that all operators without the time argument are meant to be in the Schrödinger picture. The operator with a time argument are meant to be in the Heisenberg picture, whereas operators with a tilde are in the interaction picture. We note that in the Heisenberg picture, the canonical (anti–)commutation relations are the same as in the Schrödinger picture *only* if the operators are taken at equal times. At different times the (anti-)commutators are very hard to determine. And this is exactly the point where the interaction picture proves to be useful. To determine the commutation relations in the interaction picture we explicitly evaluate the time dependence of $\tilde{a}_{\mathbf{k}}(t)$ and $\tilde{c}_{\mathbf{k}}(t)$. For this purpose we write $\hat{K}_0 = \sum_{\mathbf{k}}(\frac{\hbar^2\mathbf{k}^2}{2m_B} - \mu_B)\hat{a}^\dagger_{\mathbf{k}}\hat{a}_{\mathbf{k}} + \frac{\hbar^2\mathbf{k}^2}{2m_F}\hat{b}^\dagger_{\mathbf{k}}\hat{b}_{\mathbf{k}}$.

$$\begin{aligned}
\frac{\partial\tilde{a}_{\mathbf{k}}(t)}{\partial t} &= \frac{\partial\exp(i\hat{K}_0 t/\hbar)\hat{a}_{\mathbf{k}}\exp(-i\hat{K}_0 t/\hbar)}{\partial t} \\
&= \frac{1}{i\hbar}\exp(i\hat{K}_0 t/\hbar)[\hat{a}_{\mathbf{k}}, \hat{K}_0]\exp(-i\hat{K}_0 t/\hbar) \\
&= \frac{1}{i\hbar}\exp(i\hat{K}_0 t/\hbar)(\frac{\hbar^2\mathbf{k}^2}{2m_B} - \mu)\hat{a}_{\mathbf{k}}\exp(-i\hat{K}_0 t/\hbar) \\
&= \frac{1}{i\hbar}(\frac{\hbar^2\mathbf{k}^2}{2m_B} - \mu)\tilde{a}_{\mathbf{k}}(t) \qquad (2.77)
\end{aligned}$$

With the boundary condition $\tilde{a}_{\mathbf{k}}(0) = \hat{a}_{\mathbf{k}}$ this differential equation has the solution

$$\tilde{a}_{\mathbf{k}}(t) = e^{-i(\frac{\hbar^2\mathbf{k}^2}{2m_B} - \mu)t/\hbar}\hat{a}_{\mathbf{k}}. \qquad (2.78)$$

Similarly, we get

$$\tilde{c}_{\mathbf{k}}(t) = e^{-i\mathrm{sgn}(|\mathbf{k}|-k_F)\frac{\hbar^2\mathbf{k}^2}{2m_F}t/\hbar}\hat{c}_{\mathbf{k}}, \qquad (2.79)$$

where $\mathrm{sgn}(|\mathbf{k}| - k_F)$ gives the sign of $|\mathbf{k}| - k_F$. Thus the field operators in the interaction picture are (upon using Eqns. (2.50)-(2.52)):

$$\begin{aligned}
\tilde{\phi}(\mathbf{x}, t) &= \sum_{|\mathbf{k}|>0} e^{-i\mathbf{k}\mathbf{x} - i(\frac{\hbar^2\mathbf{k}^2}{2m_B} - \mu)t/\hbar}\hat{a}_{\mathbf{k}}, \qquad (2.80) \\
\tilde{\psi}_1(\mathbf{x}, t) &= \sum_{|\mathbf{k}|\leq k_F} e^{-i\mathbf{k}\mathbf{x} + i\frac{\hbar^2\mathbf{k}^2}{2m_F}t/\hbar}\hat{b}^\dagger_{\mathbf{k}}, \qquad (2.81) \\
\tilde{\psi}_2(\mathbf{x}, t) &= \sum_{|\mathbf{k}|>k_F} e^{-i\mathbf{k}\mathbf{x} + i\frac{\hbar^2\mathbf{k}^2}{2m_F}t/\hbar}\hat{c}_{\mathbf{k}}. \qquad (2.82)
\end{aligned}$$

From this, it is easy to compute all possible (anti-)commutation relations of these operators, namely:

$$[\tilde{\phi}(\mathbf{x}, t), \tilde{\phi}^\dagger(\mathbf{x}', t')] = \frac{1}{V}\sum_{|\mathbf{k}|>0} e^{-i(\frac{\hbar^2\mathbf{k}^2}{2m_B} - \mu)(t-t')/\hbar}e^{i\mathbf{k}(\mathbf{x}-\mathbf{x}')}, \qquad (2.83)$$

$$\{\tilde{\psi}_1(\mathbf{x}',t'),\tilde{\psi}_1^\dagger(\mathbf{x},t)\} = \frac{1}{V}\sum_{|\mathbf{k}|\le k_F} e^{-i(\frac{\hbar^2\mathbf{k}^2}{2m_F})(t-t')/\hbar}e^{i\mathbf{k}(\mathbf{x}-\mathbf{x}')}, \tag{2.84}$$

$$\{\tilde{\psi}_2(\mathbf{x},t),\tilde{\psi}_2^\dagger(\mathbf{x}',t')\} = \frac{1}{V}\sum_{|\mathbf{k}|>k_F} e^{-i(\frac{\hbar^2\mathbf{k}^2}{2m_F})(t-t')/\hbar}e^{i\mathbf{k}(\mathbf{x}-\mathbf{x}')}, \tag{2.85}$$

for any $t$ and $t'$. The other commutation relations between the Boson operators or Boson and Fermion operators vanish as well as the other anti–commutators between Fermion operators.

Another nice property of the interaction picture is that a product operator in the interaction picture is just the product of its factors in the interaction picture (which is also true for the Heisenberg picture). For example, we can use this to express the interaction operator in the interaction picture in terms of field operators in the interaction picture:

$$\begin{aligned}\tilde{V}(t) &= n_0\int\int d^3\mathbf{x}d^3\mathbf{x}'\tilde{\Psi}^\dagger(\mathbf{x}',t)U(|\mathbf{x}-\mathbf{x}'|)\tilde{\Psi}(\mathbf{x}',t)\\ &+ \sqrt{n_0}\int\int d^3\mathbf{x}d^3\mathbf{x}'\tilde{\Psi}^\dagger(\mathbf{x}',t)U(|\mathbf{x}-\mathbf{x}'|)\tilde{\Psi}(\mathbf{x}',t)\tilde{\phi}(\mathbf{x},t)\\ &+ \sqrt{n_0}\int\int d^3\mathbf{x}d^3\mathbf{x}'\tilde{\phi}^\dagger(\mathbf{x},t)\hat{\Psi}_I^\dagger(\mathbf{x}',t)U(|\mathbf{x}-\mathbf{x}'|)\tilde{\Psi}(\mathbf{x}',t)\\ &+ \int\int d^3\mathbf{x}d^3\mathbf{x}'\tilde{\phi}^\dagger(\mathbf{x},t)\tilde{\Psi}^\dagger(\mathbf{x}',t)U(|\mathbf{x}-\mathbf{x}'|)\tilde{\Psi}(\mathbf{x}',t)\tilde{\phi}(\mathbf{x},t).\end{aligned} \tag{2.86}$$

The Green's functions are defined as:

$$iG_B(\mathbf{x},t,\mathbf{x}',t') = \langle\mathcal{F}(\mu_B)|T[\hat{\Phi}(\mathbf{x},t)\hat{\Phi}^\dagger(\mathbf{x}',t')]|\mathcal{F}(\mu_B)\rangle, \tag{2.87}$$

$$iG_F(\mathbf{x},t,\mathbf{x}',t') = \langle\mathcal{F}(\mu_B)|T[\hat{\Psi}(\mathbf{x},t)\hat{\Psi}^\dagger(\mathbf{x}',t')]|\mathcal{F}(\mu_B)\rangle. \tag{2.88}$$

Here $|\mathcal{F}(\mu_B)\rangle$ is the normalized ground state of $\hat{K}$. In the special case of a non-interacting system, we have already seen that $\mu_B = 0$ (cf. Eqn. (2.59)), which means that $|\mathcal{F}(\mu_B)\rangle = |\mathbf{0}\rangle$ is the ground state of $\hat{K}_0$). The $T$ denotes the time ordered product:

$$\begin{aligned}T[\hat{\Phi}(\mathbf{x},t)\hat{\Phi}^\dagger(\mathbf{x}',t')] &= \theta(t-t')\hat{\Phi}(\mathbf{x},t)\hat{\Phi}^\dagger(\mathbf{x}',t')\\ &\quad +(1-\theta(t-t'))\hat{\Phi}^\dagger(\mathbf{x}',t')\hat{\Phi}(\mathbf{x},t)\end{aligned} \tag{2.89}$$

$$\begin{aligned}T[\hat{\Psi}(\mathbf{x},t)\hat{\Psi}^\dagger(\mathbf{x}',t')] &= \theta(t-t')\hat{\Psi}(\mathbf{x},t)\hat{\Psi}^\dagger(\mathbf{x}',t')\\ &\quad -(1-\theta(t-t'))\hat{\Psi}^\dagger(\mathbf{x}',t')\hat{\Psi}(\mathbf{x},t).\end{aligned} \tag{2.90}$$

$\theta(t-t')$ is the step function, which is 1 for $t-t'>0$ and 0 for $t-t'\le 0$, so that in the $T$–ordered product the operator at the later time is on the left. Note that the sign conventions are different for Fermion and for Boson operators.

One can use the Bogoliubov replacement to write:

$$iG_B(\mathbf{x},t,\mathbf{x}',t') = n_0 + iG'_B(\mathbf{x},t,\mathbf{x}',t'), \tag{2.91}$$

where

$$iG'_B(\mathbf{x},t,\mathbf{x}',t') = \langle\mathcal{F}(\mu_B)|T[\hat{\phi}(\mathbf{x},t),\hat{\phi}^\dagger(\mathbf{x}',t')]|\mathcal{F}(\mu_B)\rangle \tag{2.92}$$

is the Green's function for the non-condensate Bosons. Directly from the definition of the Green's functions, it is easy to see that:

$$iG'_B(\mathbf{x},t,\mathbf{x},t) = n'_B(\mathbf{x}), \tag{2.93}$$

$$-iG_F(\mathbf{x},t,\mathbf{x},t) = n_F(\mathbf{x}), \tag{2.94}$$

where $n'_B(\mathbf{x})$ is the density of the non-condensed Bosons and $n_F(\mathbf{x})$ is the density of the Fermions.
For general $\mathbf{x}'$ and $t'$, the Green's functions can be evaluated in perturbation theory [58]. Thus

$$iG'_B(\mathbf{x},t,\mathbf{x}',t') = \frac{\sum_{n=0}^{\infty} i\tilde{G}_B^{(n)}(\mathbf{x},t,\mathbf{x}',t')}{\sum_{n=0}^{\infty}\langle\mathbf{0}|S^{(n)}|\mathbf{0}\rangle}, \tag{2.95}$$

$$iG_F(\mathbf{x},t,\mathbf{x}',t') = \frac{\sum_{n=0}^{\infty} i\tilde{G}_F^{(n)}(\mathbf{x},t,\mathbf{x}',t')}{\sum_{n=0}^{\infty}\langle\mathbf{0}|S^{(n)}|\mathbf{0}\rangle}, \tag{2.96}$$

where

$$i\tilde{G}_B^{(n)}(\mathbf{x},t,\mathbf{x}',t') = \langle\mathbf{0}|T[S^{(n)}\tilde{\phi}(\mathbf{x},t)\tilde{\phi}^\dagger(\mathbf{x}',t')]|\mathbf{0}\rangle, \tag{2.97}$$

$$i\tilde{G}_F^{(n)}(\mathbf{x},t,\mathbf{x}',t') = \langle\mathbf{0}|T[S^{(n)}\tilde{\Psi}(\mathbf{x},t)\tilde{\Psi}^\dagger(\mathbf{x}',t')]|\mathbf{0}\rangle, \tag{2.98}$$

$$S^{(n)} = \frac{1}{n!}\left(\frac{-i}{\hbar}\right)^n \int dt_1 \ldots \int dt_n T[\tilde{W}(t_1)\ldots\tilde{W}(t_n)]. \tag{2.99}$$

### 2.3.3 Evaluation of terms using Wick's theorem

Equations (2.97), (2.98), and (2.99) can be evaluated by Wick's theorem, which states that the vacuum (non-interacting ground state) expectation values of time ordered products of operators can be expressed as the sum of all products of contractions of pairs of operators in the time-ordered product. Contractions are defined in terms of time and normal ordered products:

$$\tilde{O}(t)^{(i)}\tilde{P}(t')^{(i)} = T[\tilde{O}(t)\tilde{P}(t')] - :\tilde{O}(t)\tilde{P}(t'):, \tag{2.100}$$

where $:\tilde{O}(t)\tilde{P}(t'):$ is the normal ordered product. From Eqns. (2.80)-(2.82)

$$\tilde{\phi}(\mathbf{x})|\mathbf{0}\rangle = \tilde{\psi}_1(\mathbf{x})|\mathbf{0}\rangle = \tilde{\psi}_2(\mathbf{x})|\mathbf{0}\rangle = 0 \tag{2.101}$$

and

$$\langle\mathbf{0}|\tilde{\phi}^\dagger(\mathbf{x}) = \langle\mathbf{0}|\tilde{\psi}_1^\dagger(\mathbf{x}) = \langle\mathbf{0}|\tilde{\psi}_2^\dagger(\mathbf{x}) = 0. \tag{2.102}$$

This defines a unique set of creation and destruction operators. Accordingly, the normal product is defined on pairs of creation and destruction operators:

$$\begin{aligned}
:\tilde{\phi}(\mathbf{x},t)\tilde{\phi}^\dagger(\mathbf{x}',t'): &= \tilde{\phi}^\dagger(\mathbf{x}',t')\tilde{\phi}(\mathbf{x},t),\\
:\tilde{\psi}_j(\mathbf{x},t)\tilde{\psi}_k^\dagger(\mathbf{x}',t'): &= -\tilde{\psi}_k^\dagger(\mathbf{x}',t')\tilde{\psi}_j(\mathbf{x},t),\\
:\tilde{\phi}(\mathbf{x},t)\tilde{\psi}_j^\dagger(\mathbf{x}',t'): &= \tilde{\psi}_j^\dagger(\mathbf{x}',t')\tilde{\phi}(\mathbf{x},t),\\
:\tilde{\psi}_j(\mathbf{x},t)\tilde{\phi}^\dagger(\mathbf{x}',t'): &= \tilde{\phi}^\dagger(\mathbf{x}',t')\tilde{\psi}_j(\mathbf{x},t),
\end{aligned} \tag{2.103}$$

for $j,k \in \{1,2\}$. For all other pairs of creation and destruction operators, the normal product is the same as the ordinary operator product (because they commute and the order does not matter). The extension to arbitrary operators is done by linearity (every operator can be uniquely decomposed into a creation and a destruction part). Depending on the time arguments of the creation and destruction operators the contraction is either zero or the (anti-)commutator of the operators. Simply by keeping track of the order of the operators one gets the following results:

$$\tilde{\phi}(\mathbf{x},t)^{(i)}\tilde{\phi}^\dagger(\mathbf{x}',t')^{(i)} = \theta(t-t')[\tilde{\phi}(\mathbf{x},t),\tilde{\phi}^\dagger(\mathbf{x}',t')], \tag{2.104}$$

$$\begin{aligned}
\tilde{\phi}^\dagger(\mathbf{x}',t')^{(i)}\tilde{\phi}(\mathbf{x},t)^{(i)} &= \theta(t-t')[\tilde{\phi}(\mathbf{x},t),\tilde{\phi}^\dagger(\mathbf{x}',t')], && (2.105)\\
\tilde{\psi}_1(\mathbf{x}',t')^{(i)}\tilde{\psi}_1^\dagger(\mathbf{x},t)^{(i)} &= (1-\theta(t-t'))\{\tilde{\psi}_1(\mathbf{x}',t'),\tilde{\psi}_1^\dagger(\mathbf{x},t)\}, && (2.106)\\
\tilde{\psi}_1^\dagger(\mathbf{x},t)^{(i)}\tilde{\psi}_1(\mathbf{x}',t')^{(i)} &= -(1-\theta(t-t'))\{\tilde{\psi}_1(\mathbf{x}',t'),\tilde{\psi}_1^\dagger(\mathbf{x},t)\}, && (2.107)\\
\tilde{\psi}_2(\mathbf{x},t)^{(i)}\tilde{\psi}_2^\dagger(\mathbf{x}',t')^{(i)} &= \theta(t-t')\{\tilde{\psi}_2^\dagger(\mathbf{x},t),\tilde{\psi}_2(\mathbf{x}',t')\}, && (2.108)\\
\tilde{\psi}_2^\dagger(\mathbf{x}',t')^{(i)}\tilde{\psi}_2(\mathbf{x},t)^{(i)} &= -\theta(t-t')\{\tilde{\psi}_2^\dagger(\mathbf{x},t),\tilde{\psi}_2(\mathbf{x}',t')\}. && (2.109)
\end{aligned}$$

and all other contractions of pairs of operators $\in \{\tilde{\phi}(\mathbf{x},t),\tilde{\phi}^\dagger(\mathbf{x}',t'),\tilde{\psi}_i(\mathbf{x}'',t''),\tilde{\psi}_k^\dagger(\mathbf{x}''',t''')\}$ vanish. Using the linearity of the contraction we can further calculate:

$$\begin{aligned}
&\tilde{\Psi}(\mathbf{x},t)^{(i)}\tilde{\Psi}^\dagger(\mathbf{x}',t')^{(i)}\\
&= \tilde{\psi}_1^\dagger(\mathbf{x},t)^{(i)}\tilde{\psi}_1(\mathbf{x}',t')^{(i)} + \tilde{\psi}_2(\mathbf{x},t)^{(i)}\tilde{\psi}_1(\mathbf{x}',t')^{(i)} +\\
&\quad \tilde{\psi}_1^\dagger(\mathbf{x},t)^{(i)}\tilde{\psi}_2^\dagger(\mathbf{x}',t')^{(i)} + \tilde{\psi}_2(\mathbf{x},t)^{(i)}\tilde{\psi}_2^\dagger(\mathbf{x}',t')^{(i)}\\
&= \theta(t-t')\{\tilde{\psi}_2(\mathbf{x},t),\tilde{\psi}_2^\dagger(\mathbf{x}',t')\}\\
&\quad -(1-\theta(t-t'))\{\tilde{\psi}_1^\dagger(\mathbf{x}',t'),\tilde{\psi}_1(\mathbf{x}',t')|\} && (2.110)\\
&\tilde{\Psi}^\dagger(\mathbf{x}',t')^{(i)}\tilde{\Psi}(\mathbf{x},t)^{(i)}\\
&= \tilde{\psi}_1(\mathbf{x}',t')^{(i)}\tilde{\psi}_1^\dagger(\mathbf{x},t)^{(i)} + \tilde{\psi}_2^\dagger(\mathbf{x}',t')^{(i)}\tilde{\psi}_1^\dagger(\mathbf{x}',t')^{(i)} +\\
&\quad \tilde{\psi}_1(\mathbf{x}',t')^{(i)}\tilde{\psi}_2(\mathbf{x},t)^{(i)} + \tilde{\psi}_2^\dagger(\mathbf{x}',t')^{(i)}\tilde{\psi}_2(\mathbf{x},t)^{(i)}\\
&= -\theta(t-t')\{\tilde{\psi}_2(\mathbf{x},t),\tilde{\psi}_2^\dagger(\mathbf{x}',t')\}\\
&\quad +(1-\theta(t-t'))\{\tilde{\psi}_1^\dagger(\mathbf{x}',t'),\tilde{\psi}_1(\mathbf{x}',t')|\} && (2.111)
\end{aligned}$$

and all other contractions of pairs from $\tilde{\phi}(\mathbf{x},t),\tilde{\phi}^\dagger(\mathbf{x},t),\tilde{\Psi}(\mathbf{x},t),\tilde{\Psi}^\dagger(\mathbf{x},t)$ vanish.

Wick's theorem (see e.g. [58]) states how a time ordered product of arbitrary operators can be written in terms of normal ordered products and contractions. Loosely speaking: A time ordered product of operators is the same as the sum of all normal ordered products, where all possible contractions can be taken inside the normal ordered product. By definition of the normal ordered product, all terms in this sum vanish in the average regarding to the non-interacting ground state unless all factors are contracted. So we can write:

$$\begin{aligned}
&\langle\mathbf{0}|T[\tilde{O}(t)\tilde{P}(t')\tilde{Q}(t'')\ldots]|\mathbf{0}\rangle = && (2.112)\\
&\quad \sum(\text{all products of pairs of contractions of } \tilde{O}(t),\tilde{P}(t'),\tilde{Q}(t''),\ldots).
\end{aligned}$$

As an important example of Wick's theorem, we now evaluate the Green's functions in the limit of a non-interacting system ($\tilde{W}=0$). In this case, they reduce to the zeroth order terms in the expansions Eqns. (2.95) and (2.96), so that

$$\begin{aligned}
iG_B^0(\mathbf{x},t,\mathbf{x}',t') &= i\tilde{G}_B^{(0)}(\mathbf{x},t,\mathbf{x}',t')\\
&= \langle\mathbf{0}|T[\tilde{\phi}(\mathbf{x},t)\tilde{\phi}^\dagger(\mathbf{x}',t')]|\mathbf{0}\rangle, && (2.113)\\
iG_F^0(\mathbf{x},t,\mathbf{x}',t') &= i\tilde{G}_F^{(0)}(\mathbf{x},t,\mathbf{x}',t')\\
&= \langle\mathbf{0}|T[\tilde{\Psi}(\mathbf{x},t)\tilde{\Psi}^\dagger(\mathbf{x}',t')]|\mathbf{0}\rangle. && (2.114)
\end{aligned}$$

Upon applying Wick's theorem, one gets

$$\begin{aligned}
iG_B^0(\mathbf{x},t,\mathbf{x}',t') &= \tilde{\phi}(\mathbf{x},t)^{(i)}\tilde{\phi}^\dagger(\mathbf{x}',t')^{(i)}, && (2.115)\\
iG_F^0(\mathbf{x},t,\mathbf{x}',t') &= \tilde{\Psi}(\mathbf{x},t)^{(i)}\tilde{\Psi}^\dagger(\mathbf{x}',t')^{(i)}. && (2.116)
\end{aligned}$$

Using Eqns. (2.104)-(2.111) along with Eqns. (2.83)-(2.85) it follows:

$$iG_B^0(\mathbf{x},t,\mathbf{x}',t') = \theta(t-t')\frac{1}{V}\sum_{|\mathbf{k}|>0} e^{-i(\frac{\hbar^2\mathbf{k}^2}{2m_B}-\mu_B)(t-t')/\hbar}e^{i\mathbf{k}(\mathbf{x}-\mathbf{x}')}, \tag{2.117}$$

$$\begin{aligned} iG_F^0(\mathbf{x},t,\mathbf{x}',t') &= \theta(t-t')\frac{1}{V}\sum_{|\mathbf{k}|>k_F} e^{-i(\frac{\hbar^2\mathbf{k}^2}{2m_F})(t-t')/\hbar}e^{i\mathbf{k}(\mathbf{x}-\mathbf{x}')} \\ &+ (1-\theta(t-t'))\frac{1}{V}\sum_{|\mathbf{k}|\le k_F} e^{-i(\frac{\hbar^2\mathbf{k}^2}{2m_F})(t-t')/\hbar}e^{i\mathbf{k}(\mathbf{x}-\mathbf{x}')}, \end{aligned} \tag{2.118}$$

The last expressions are Fourier transforms in space but not in time. To also express them as Fourier transforms in time, one can use the following Fourier representations of the $\theta$-functions:

$$\theta(x) = -\lim_{\epsilon\to 0^+}\frac{1}{2\pi i}\int_{-\infty}^{+\infty} d\omega \frac{e^{-i\omega(x-\epsilon)})}{\omega+i\nu}$$

and similarly

$$1-\theta(x) = \lim_{\epsilon\to 0^+}\frac{1}{2\pi i}\int_{-\infty}^{+\infty} d\omega \frac{e^{-i\omega(x-\epsilon)}}{\omega-i\nu},$$

These lead to:

$$\begin{aligned} &G_B^0(\mathbf{x},t,\mathbf{x}',t') \\ &= \frac{1}{2\pi}\int d\omega \frac{e^{-i\omega(t-t'-\epsilon)}}{\omega+i\nu}\frac{1}{V}\sum_{|\mathbf{k}|>0} e^{-i(\frac{\hbar^2\mathbf{k}^2}{2m_B}-\mu)(t-t')/\hbar}e^{i\mathbf{k}(\mathbf{x}-\mathbf{x}')} \\ &= \frac{1}{2\pi V}\sum_{|\mathbf{k}|>0}\int d\omega e^{i\mathbf{k}(\mathbf{x}-\mathbf{x}')}\frac{e^{i(\omega-\frac{\hbar\mathbf{k}^2}{2m_B}+\mu/\hbar))(t-t')}}{\omega+i\nu}e^{i\omega\epsilon} \\ &= \frac{1}{2\pi V}\sum_{\mathbf{k}}\int d\omega e^{i\mathbf{k}(\mathbf{x}-\mathbf{x}')}e^{-i\omega(t-t')}\frac{e^{i\omega\epsilon}(1-\delta_{\mathbf{k}})}{\omega-\frac{\hbar\mathbf{k}^2}{2m_B}+\mu/\hbar+i\nu}, \end{aligned} \tag{2.119}$$

where the limit $\epsilon\to 0$ is implicit.
And for the Fermions:

$$\begin{aligned} &G_F^0(\mathbf{x},t,\mathbf{x}',t') \\ = &\frac{1}{2\pi}\int d\omega\frac{e^{-i\omega(t-t'-\epsilon)}}{\omega+i\nu}\frac{1}{V}\sum_{|\mathbf{k}|\le k_F} e^{-i(\frac{\hbar^2\mathbf{k}^2}{2m_F})(t-t')/\hbar}e^{i\mathbf{k}(\mathbf{x}-\mathbf{x}')} \\ &+\frac{1}{2\pi}\int d\omega\frac{e^{-i\omega(t-t'-\epsilon)}}{\omega-i\nu}\frac{1}{V}\sum_{|\mathbf{k}|>k_F} e^{-i(\frac{\hbar\mathbf{k}^2}{2m_F})(t-t')/\hbar}e^{i\mathbf{k}(\mathbf{x}-\mathbf{x}')} \\ = &\frac{1}{2V\pi}\sum_{\mathbf{k}}\int d\omega e^{i\mathbf{k}(\mathbf{x}-\mathbf{x}')}e^{i(-\omega-\frac{\hbar\mathbf{k}^2}{2m_F})(t-t')} \\ &\times(\frac{1-\theta(k_F-|\mathbf{k}|)}{\omega+i\nu}+\frac{\theta(k_F-|\mathbf{k}|)}{\omega-i\nu})e^{i\omega\epsilon} \\ = &\frac{1}{2\pi V}\sum_{\mathbf{k}}\int d\omega e^{i\mathbf{k}(\mathbf{x}-\mathbf{x}')}e^{-i\omega(t-t')}(\frac{1-\theta(k_F-|\mathbf{k}|)}{\omega-\frac{\hbar\mathbf{k}^2}{2m_F}+i\nu}+\frac{\theta(k_F-|\mathbf{k}|)}{\omega-\frac{\hbar\mathbf{k}^2}{2m_F}-i\nu})e^{i\omega\epsilon} \\ = &\frac{1}{2\pi V}\sum_{\mathbf{k}}\int d\omega e^{i\mathbf{k}(\mathbf{x}-\mathbf{x}')}e^{-i\omega(t-t')}\frac{e^{i\omega\epsilon}}{\omega-\frac{\hbar\mathbf{k}^2}{2m_F}+i\mathrm{sgn}(|\mathbf{k}|-k_F)\nu}, \end{aligned} \tag{2.120}$$

where $\mathrm{sgn}(x) = 1$ for $x \geq 0$ and $\mathrm{sgn}(x) = -1$ for $x < 0$.
We immediately recognize that the energy-momentum components of the Green's functions are

$$G_B^0(\mathbf{k},\omega) = \frac{e^{i\omega\epsilon}(1-\delta_{\mathbf{k}})}{\omega - \frac{\hbar\mathbf{k}^2}{2m_B} + \mu/\hbar + i\nu} \tag{2.121}$$

and

$$G_F^0(\mathbf{k},\omega) = \frac{e^{i\omega\epsilon}}{\omega - \frac{\hbar\mathbf{k}^2}{2m_F} + i\mathrm{sgn}(|\mathbf{k}| - k_F)\nu}. \tag{2.122}$$

These results could of course also have been obtained directly without using Wick's theorem. Usually, in literature the limits $\epsilon \to 0$ are carried out directly, in these expressions, even though this is strictly only correct *after* evaluating integrals which involve the Green's functions. If the volume $V \to \infty$, the $\delta_{\mathbf{k}}$ appearing in the Boson Green's function is only non-zero on a volume of measure 0 and may thus be replaced by 1.

### 2.3.4 Higher order terms and Feynman diagrams

Inserting Eqn. (2.66) into the perturbation series Eqns. (2.95) and (2.96) using Wick's theorem to evaluate the time ordered products and expressing the contractions via Eqns. (2.113) and (2.114), in principle all terms in the expansion of the Green's functions can be evaluated. The first order terms are readily determined to be:

$$\begin{aligned}
i\tilde{G}_B^{(1)}(x^\mu,y^\mu) &= \frac{-i}{\hbar}\int\int d^4x_1^\mu d^4y_1^\mu \\
&\Big\{U(x_1^\mu - y_1^\mu)\Big[-n_0 iG_F^0(y_1^\mu,y_1^\mu)iG_B^0(x^\mu,y^\mu) \\
&-iG_F^0(y_1^\mu,y_1^\mu)iG_B^0(x^\mu,x_1^\mu)iG_B^0(x_1^\mu,y^\mu)\Big] \\
&+V(x_1^\mu - y_1^\mu)\Big[\frac{n_0^2}{2}iG_B^0(x^\mu,y^\mu) + n_0 iG_B^0(x^\mu,x_1^\mu)iG_B^0(x_1^\mu,y^\mu) \\
&+n_0 iG_B^0(x^\mu,x_1^\mu)iG_B^0(x^\mu,x_2^\mu)\Big]\Big\}, \qquad (2.123) \\
i\tilde{G}_F^{(1)}(x^\mu,y^\mu) &= \frac{-i}{\hbar}\int\int d^4x_1^\mu d^4y_1^\mu \\
&\Big\{U(x_1^\mu - y_1^\mu)\Big[-n_0 iG_F^0(y_1^\mu,y_1^\mu)iG_F^0(x^\mu,y^\mu) \\
&-n_0 iG_F^0(x^\mu,y_1^\mu)iG_F^0(y_1^\mu,y^\mu)\Big] \\
&+V(x_1^\mu - y_1^\mu)\Big[\frac{n_0^2}{2}iG_F^0(x^\mu,y^\mu)\Big]\Big\}, \qquad (2.124) \\
S^{(1)} &= \frac{-i}{\hbar}\int\int d^4x_1^\mu d^4y_1^\mu\Big\{U(x_1^\mu - y_1^\mu)\Big[-in_0 G_F^0(y_1^\mu,y_1^\mu)\Big] \\
&+V(x_1^\mu - y_1^\mu)\Big[\frac{n_0^2}{2}\Big]\Big\}, \qquad (2.125)
\end{aligned}$$

where we have used the more compact four-vector notation [$x^\mu = (t,\mathbf{x})$], and defined $U(x^\mu - y^\mu) = U(\mathbf{x}-\mathbf{y})\delta(x^0 - y^0)$ and $V(x^\mu - y^\mu) = V(\mathbf{x}-\mathbf{y})\delta(x^0 - y^0)$. Note that $G_B^0(t,\mathbf{x},t,\mathbf{y}) = 0$ (i.e. there are no Boson loops at zero temperature).

Higher order terms may be similarly evaluated, and will similarly be expressed in terms of integrals over products of noninteracting Green's functions, condensate factors $n_0$, and interaction terms. We represent these graphically (see Fig. 2.1): straight lines for Fermions, wiggly lines for non-condensate Bosons, dashed lines for condensate Bosons, and zigzag lines for interaction terms (whether it is a Boson-Boson or Boson-Fermion interaction is clearly determined by the kinds of particle lines attached to the vertexes of the interaction line). Some terms in the numerators of the perturbation

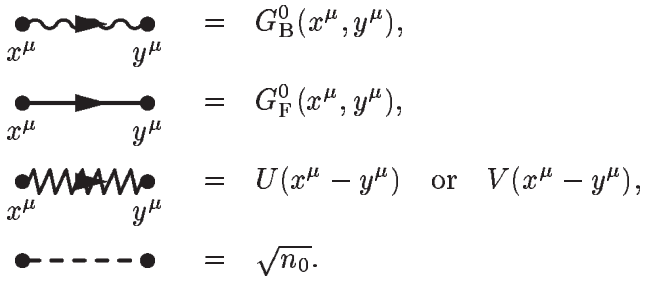


Figure 2.1: Definition of the diagram lines

series separate into products. They are called disconnected. To $(n+1)$st order they sum up to denominator $S^{(n)}$ times a connected term. This means that they cancel the denominator $S^{(n)}$ to order $n$. The proof for Bose–Fermi mixtures can be adapted from that of spin–$\frac{1}{2}$ Fermions in the following way: Considering Eqn. (7.12) of Ref. [58], we take $V(\mathbf{x},\mathbf{x}')_{\alpha\alpha',\beta\beta'} = U(\mathbf{x},\mathbf{x}')\delta_{\alpha\alpha'}\delta_{\beta\beta'}\delta_{\alpha(-\beta)} + V(\mathbf{x},\mathbf{x}')\delta_{\alpha\alpha'}\delta_{\beta\beta'}\delta_{\alpha\beta}\delta_{\alpha(1/2)}$, and replace $\hat{\psi}_{1/2}(\mathbf{x})$ by $\hat{\phi}(\mathbf{x})$ and $\hat{\psi}_{-1/2}(\mathbf{x})$ by $\hat{\Psi}(\mathbf{x})$. The derivation is then the same, apart from some sign factors. As a result, we only need to consider the connected diagrams, so that

$$G'_B(x^\mu, y^\mu) = \sum_{n=0}^{\infty} \tilde{G}_B^{(n)}(x^\mu, y^\mu)_{\text{connected}} , \tag{2.126}$$

$$G_F(x^\mu, y^\mu) = \sum_{n=0}^{\infty} \tilde{G}_F^{(n)}(x^\mu, y^\mu)_{\text{connected}} . \tag{2.127}$$

Noting that each connected graph essentially appears $n!$ times, with simple permutations on the labeling, when composing such graphs we integrate over all internal variables and affix a factor of $(i/\hbar)^n(-1)^F(-i)^C$, where $n$ is the number of interaction lines, $F$ is the number of closed Fermion loops, and $C$ is the number of dashed Boson lines.

Before we finally state the Feynman rules, we transform to energy–momentum space, which is appropriate for homogeneous systems, since the non–interacting Green functions look relatively simple in this space (see (2.121), (2.122)). If the Fourier components of the potential are defined by (here we use the Minkowski scalar product $k^\mu x_\mu = \mathbf{k}\cdot\mathbf{x} - k^0x^0$):

$$U(x^\mu - y^\mu) = \frac{1}{2\pi V}\sum_{\mathbf{k}} \int dk^0 e^{ik^\mu(x_\mu - y_\mu)} U(k^\mu) \tag{2.128}$$

(since $U(x^\mu - y^\mu) = U(\mathbf{x}-\mathbf{y})\delta(x^0 - y^0)$, $U(k^\mu)$ must be independent of $k^0$) and use (2.119) and (2.120) for the non-interacting Green functions, what reads in four-vector notation:

$$G^0_B(x^\mu, y^\mu) = \frac{1}{2\pi V}\sum_{\mathbf{k}} \int dk^0 e^{ik^\mu(x_\mu - y_\mu)} G^0_B(k^\mu) \tag{2.129}$$

and

$$G_F^0(x^\mu, y^\mu) = \frac{1}{2\pi V} \sum_{\mathbf{k}} \int dk^0 e^{ik^\mu (x_\mu - y_\mu)} G_F^0(k^\mu), \tag{2.130}$$

we can do the integration over the internal variables of the Feynman-diagrams. Those integrations gives a factor of

$$(2\pi)^{-4} \int d^4x^\mu e^{i(\sum k^\mu)x_\mu} = \delta(\sum k^\mu) \tag{2.131}$$

at every vertex, where by $\sum k^\mu$ we mean the sum over the momenta of all lines entering or leaving the vertex, where we count the momentum of the leaving lines negative. In other words: At every vertex energy-momentum is conserved.

Now, we state the Feynman-rules for the Boson (Fermion) Green's functions in momentum space, which are just a summary of this section:

1. Draw all topologically distinct connected diagrams with one outgoing external wiggly Boson (Fermion) line and one incoming external wiggly Boson (Fermion) line, no external Fermion (Boson) lines and no internal dashed Boson lines, $n$ zigzag interaction lines, each of which is attached at one vertex to an incoming and an outgoing Boson line (either wiggly or dashed), and at the other vertex either to an incoming and an outgoing Boson line, or to an incoming and an outgoing (not necessarily distinct) Fermion line. Each vertex must be attached to exactly one zigzag interaction line.
2. All wiggly Boson lines must run into the same direction and there are no closed Boson loops.
3. Each dashed Boson line corresponds to a factor of $\sqrt{n_0}$, each wiggly Boson line to a factor of $G_B^0(k^\mu)$, each Fermion line to a factor of $G_F^0(k^\mu)$, each Boson-Fermion interaction line to a factor of $U(k^\mu) = U(\mathbf{k})$, and each Boson-Boson interaction line to a factor of $V(k^\mu) = V(\mathbf{k})$.
4. Assign a direction to each interaction line; associate a directed four-momentum with each line and conserve four-momentum at each vertex. Each dashed Boson line carries four-momentum 0 and each wiggly Boson line has four-momentum $\neq 0$.
5. Integrate over the $n$ independent four-momenta.
6. Affix a factor of $(i/\hbar)^n (2\pi)^{-4(n)} (-1)^F (-i)^C$, where $F$ is the number of closed Fermion loops and $C$ is the number of dashed Boson lines.

### 2.3.5 The Dyson equations

The Dyson equation is a simple method to sum an infinite series of certain diagrams. As we will see, it also makes the pole structure of the Green's functions very transparent.

First, we consider the Fermion Green's function only. The proper self energy $\Sigma_F(p^\mu)$ is defined as a part of a Feynman diagram for the Fermion Green's function, which is connected to the rest of the diagram by an only *one* ingoing and an only *one* outgoing Fermion line, but which itself cannot be split into two diagrams by cutting *one* single Fermion line. So without the danger of double counting one can generate an infinite series of diagrams by:

$$\begin{aligned} G_F(p^\mu) &= G_F^0(p^\mu) + G_F^0(p^\mu)\Sigma_F(p^\mu)G_F^0(p^\mu) \\ &+ G_F^0(p^\mu)\Sigma_F(p^\mu)G_F^0(p^\mu)\Sigma_F(p^\mu)G_F^0(p^\mu) + \ldots \end{aligned}$$

which is an iterative form of the following Dyson equation for the Fermions:

$$G_F(p^\mu) = G_F^0(p^\mu) + G_F^0(p^\mu)\Sigma_F(p^\mu)G_F(p^\mu) \tag{2.132}$$

and has the solution:

$$G_F(p^\mu) = \frac{1}{[G_F^0(p^\mu)]^{-1} - \Sigma_F(p^\mu)}. \tag{2.133}$$

The spectrum is determined by the poles of the Green's function, which are determined by

$$p^0 = \frac{\hbar p^2}{2m_F} - \Sigma_F(p^\mu), \tag{2.134}$$

which clearly has the solution $p^0 = \frac{\hbar p^2}{2m_F}$, when the self energy vanishes. In the next chapter, we derive expansions which imply small self-energies, such that consistency only requires to use the zeroth order result (i.e. for vanishing self-energy) inside $\Sigma_F(p^\mu)$ in Eqn. (2.135) for $p^0$, which leads to the much simpler equation:

$$p^0 = \frac{\hbar p^2}{2m_F} - \Sigma_F(\hbar p^2/2m_F, \mathbf{p}). \tag{2.135}$$

For the Bosons the case is more complicated, since a wiggly Boson line not necessarily runs continuously through a diagram, because it can change into a dashed Boson line (this ultimately stems from the non particle-conservative structure of the Bogoliubov Hamiltonian). So, if we define the proper self energy as a part of a Feynman diagram for the Boson Green function, which is connected to the rest of the diagram by exactly two wiggly Boson lines, but which itself cannot be split into two diagrams by cutting a single wiggly Boson line, we basically have three proper self-energies, namely one with one incoming and one outgoing wiggly line ($\Sigma_B(p^\mu)$), one with two outgoing wiggly Boson lines and two incoming dashed Boson lines ($\Sigma_{12}(p^\mu)$), and another one with two incoming wiggly Boson lines and two outgoing dashed Boson lines ($\Sigma_{21}(p^\mu)$). Analogously, we have Green's functions representing $G_{12}(p^\mu)$ the scattering of two wiggly Boson lines into the condensate and $G_{21}(p^\mu)$ for the reverse process (defined as the Fourier transforms of $G_{12}(x^\mu, y^\mu) = \langle \mathbf{G}|T[\hat{\phi}(x^\mu)\hat{\phi}(y^\mu)]|\mathbf{G}\rangle$ and $G_{21}(x^\mu, y^\mu) = \langle \mathbf{G}|T[\hat{\phi}^\dagger(x^\mu)\hat{\phi}^\dagger(y^\mu)]|\mathbf{G}\rangle$, respectively). The Dyson equations for Bosons tells us how these quantities are related:

$$\begin{aligned} \begin{pmatrix} G_B'(p^\mu) & G_{12}(-p^\mu) \\ G_{21}(p^\mu) & G_B'(-p^\mu) \end{pmatrix} &= \begin{pmatrix} G_B^0(p^\mu) & 0 \\ 0 & G_B^0(-p^\mu) \end{pmatrix} \\ &+ \begin{pmatrix} G_B^0(p^\mu) & 0 \\ 0 & G_B^0(-p^\mu) \end{pmatrix} \begin{pmatrix} \Sigma_B(p^\mu) & \Sigma_{12}(p^\mu) \\ \Sigma_{21}(p^\mu) & \Sigma_B(-p^\mu) \end{pmatrix} \\ &\times \begin{pmatrix} G_B'(p^\mu) & G_{12}(p^\mu) \\ G_{21}(p^\mu) & G_B'(-p^\mu) \end{pmatrix}. \end{aligned} \tag{2.136}$$

The solution in terms of $G'_B(p^\mu)$ is:

$$G'_B(p^\mu) = \frac{1}{[G^0_B(p^\mu)]^{-1} - \Sigma_B(p^\mu) - \frac{\Sigma_{12}(p^\mu)\Sigma_{21}(p^\mu)}{[G^0_B(-p^\mu)]^{-1} - \Sigma_B(-p^\mu)}}. \tag{2.137}$$

### 2.3.6 The Hugenholtz-Pines theorem and Boson spectrum

According to the Hugenholtz-Pines theorem [81], the Bosonic chemical potential $\mu_B$ introduced in the Bogoliubov Hamiltonian (see Eqn. (2.63), is given by

$$\mu_B = \hbar\Sigma_B(0) - \hbar\Sigma_{12}(0), \tag{2.138}$$

where $\Sigma_B(0)$ and $\Sigma_{12}(0)$ are the proper self-energies for the Bosons due to their interaction with both Bosons and Fermions, evaluated at $p^\mu = 0$ (in what follows we call them the Bosonic self-energies). Furthermore, the chemical potential and the ground state energy are related in an obvious way:

$$\frac{\partial E/V}{\partial n_B} = \mu_B, \tag{2.139}$$

The proof of the validity of the Hugenholtz-Pines theorem can be adopted literally from the pure Boson case, since it is based on how to replace condensate lines by non-condensate propagators; a procedure which is unchanged in the present situation of Bose-Fermi mixtures.

With the Hugenholtz-Pines theorem we an derive the Boson spectrum simply by insertion of $\mu_B$ into Eqn. (2.119) and use it in Eqn.(2.137) to get:

$$\begin{aligned} G'_B(p^\mu) &= \Bigg[p^0 - \frac{\hbar p^2}{2m_B} + \Sigma_B(0) - \Sigma_B(p^\mu) - \Sigma_{12}(0) \\ &\quad - \frac{\Sigma_{12}(p^\mu)\Sigma_{21}(p^\mu)}{-p^0 - \hbar p^2/2m_B + \Sigma_B(0) - \Sigma_B(-p^\mu) - \Sigma_{12}(0)}\Bigg]^{-1}, \end{aligned} \tag{2.140}$$

Thus, we get the following pole equation

$$\begin{aligned} (p^0)^2 &= \left[\hbar p^2/2m_B + \Sigma_B(0) - \Sigma_B(p^0, \mathbf{p}) - \Sigma_{12}(0)\right]^2 \\ &\quad - \Sigma^2_{12}(p^0, \mathbf{p}), \end{aligned} \tag{2.141}$$

where we have assumed $\Sigma_B(p^\mu) = \Sigma_B(-p^\mu)$ and $\Sigma_{12}(p^\mu) = \Sigma_{21}(p^\mu)$, which will be always satisfied in the following.

# Chapter 3

# Results for dilute systems

## 3.1 The $T$–matrix in ladder approximation

As previously mentioned, dilute systems are defined as systems where the mean radius occupied by a particle is large compared to the characteristic length scale of the interactions. This means that processes, where three or more particles interact with each other at the same time are very rare. In turn, only two–particle scattering processes have to be considered. In terms of Feynman diagrams, it follows that only diagrams with interaction lines between two systems of connected propagators have to be taken into account (see Refs. [82, 58]). This approximation is called ladder approximation, because the Feynman diagrams look like ladders in this case as we will see in the following. The task is then to sum all the ladder diagrams.

Most easily this can be achieved if one expresses the self–energies in terms of the so-called $T$–matrices, which describe the two–particle scattering process in the medium, as shown in Fig. 3.1, where the Boson-Fermion $T$–matrix $T_{BF}$ in ladder approximation is defined in Fig. 3.2, the Boson-Boson $T$–matrix $T_{BB}$ (also in ladder approximation) is well known from studies of dilute pure Bose systems, and the normal (diagonal) Bosonic proper self–energy is given by

$$\Sigma_B(p^\mu) = \Sigma_{BF}(p^\mu) + \Sigma_{BB}(p^\mu). \tag{3.1}$$

The proper self–energies can thus be determined by adding the proper self–energies of a system of interacting Bosons to those of a hypothetical mixed Boson-Fermion system where there are Boson-Fermion interactions only. This result arises from our use of the ladder approximation, and is not in general true (there also exist, for example, inseparable three–legged "ladders" consisting of a Boson–Boson and a Boson–Fermion ladder joined by a common Boson leg, but these clearly describe higher order processes). For such a hypothetical mixed system, the only self–energies we need to consider and to evaluate are $\Sigma_{BF}(p^\mu)$ and $\Sigma_F(p^\mu)$, which can be written algebraically as:

$$\hbar\Sigma_{BF}(p^\mu) = -\frac{i}{(2\pi)^4}\int d^4k^\mu T_{BF}(p^\mu, k^\mu, p^\mu, k^\mu) G_F^0(k^\mu), \tag{3.2}$$

$$\hbar\Sigma_F(p^\mu) = T_{BF}(0, p^\mu, 0, p^\mu) n_0. \tag{3.3}$$

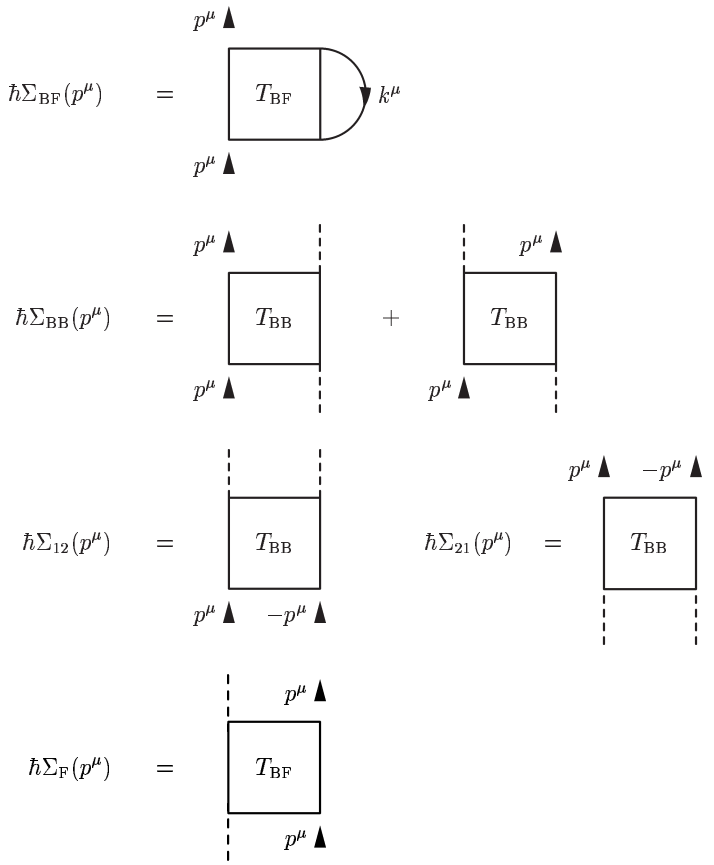


Figure 3.1: The self–energies in ladder approximation, expressed in terms of the $T$-matrices.

### 3.1.1 Bethe-Salpeter equation for $T_{BF}$

The Boson–Fermion $T$–matrix $T_{BF}$ can also be represented recursively, as shown in Fig. 3.3. If we now transform to center–of–mass coordinates,

$$\begin{aligned} P^\mu &= p_1^\mu + p_2^\mu = p_3^\mu + p_4^\mu, \\ k_1^\mu &= (p_1^\mu - p_2^\mu)/2, \\ k_2^\mu &= (p_3^\mu - p_4^\mu)/2, \end{aligned} \tag{3.4}$$

the algebraic form of the equation represented in Fig. 3.3 reads:

$$\begin{aligned} T_{BF}(k_1^\mu, k_2^\mu, P^\mu) &= U(\mathbf{k}_1 - \mathbf{k}_2) + \frac{i}{\hbar(2\pi)^4}\int d^3\mathbf{k} U(\mathbf{k}_1 - \mathbf{k}) \\ &\quad \times \int dk^0 G_B^0(P^\mu/2 + k^\mu) G_F^0(P^\mu/2 - k^\mu) \\ &\quad \times T_{BF}(k^\mu, k_2^\mu, P^\mu)\ . \end{aligned} \tag{3.5}$$

This is a kind of Bethe–Salpeter integral equation, which we will now solve recursively for low momenta, stopping at order $a_{BF}^2$, where $a_{BF}$ is the Boson-Fermion scattering length.

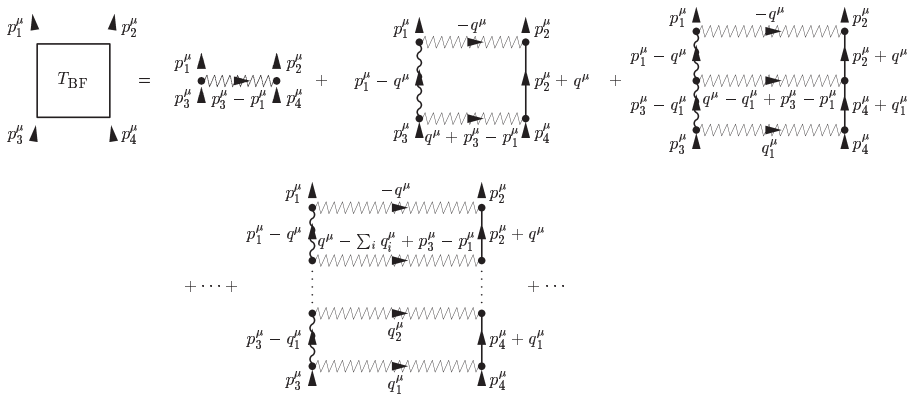


Figure 3.2: The Boson-Fermion $T$-matrix.

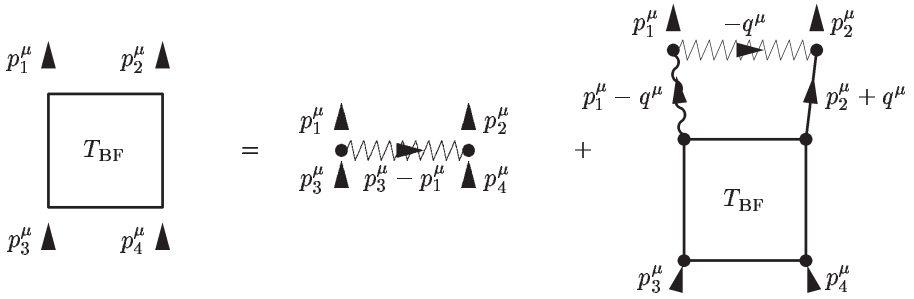


Figure 3.3: The integral equation for $T_{BF}$.

As the interactions are instantaneous, the only frequency dependence in $T_{BF}(k_1^\mu, k_2^\mu, P^\mu)$ is in $P^0$ [82, 58]. Thus, a contour integration over $k^0$ in Eqn. (3.5) yields:

$$T_{BF}(\mathbf{k}_1, \mathbf{k}_2, P^\mu) = U(\mathbf{k}_1 - \mathbf{k}_2) + \frac{1}{(2\pi)^3}\int d^3\mathbf{k} \times \frac{U(\mathbf{k}_1 - \mathbf{k})T_{BF}(\mathbf{k}, \mathbf{k}_2, P^\mu)\theta(|\mathbf{P}/2 - \mathbf{k}| - k_F)}{\hbar P^0 - \hbar^2(\mathbf{P}/2 + \mathbf{k})^2/2m_B - \hbar^2(\mathbf{P}/2 - \mathbf{k})^2/2m_F + \mu_B + i\nu}. \tag{3.6}$$

We now make use of Eqn. (1.38) in order to point out, that to lowest order $T_{BF}(\mathbf{k}_1, \mathbf{k}_2, P^\mu)$ is linear in $a_{BF}$ and thus iteration of Eqn. (3.6) produces an expansion in $a_{BF}$, which is correct to second order in $a_{BF}$, if one stops after two iteration steps. We insert Eqn. (1.38) into Eqn. (3.6) (remembering that $U(\mathbf{p}) = \frac{\hbar^2}{2m}u(\mathbf{p})$) keeping only terms up to second order in $a_{BF}$: This produces

$$T_{BF}(\mathbf{k}_1, \mathbf{k}_2, P^\mu) \approx \frac{2\pi\hbar^2}{m}[a_{BF} - ia_{BF}^2 k_1] + \frac{4\pi^2\hbar^4 a_{BF}^2}{(2\pi)^3 m^2}\int d^3\mathbf{k} \times \left[\frac{\theta(|\mathbf{P}/2 - \mathbf{k}| - k_F)}{\hbar P^0 - \hbar^2(\mathbf{P}/2 + \mathbf{k})^2/2m_B - \hbar^2(\mathbf{P}/2 - \mathbf{k})^2/2m_F + \mu_B + i\nu}\right.$$

$$-\frac{1}{\hbar^2\mathbf{k}_1^2/2m - \hbar^2\mathbf{k}^2/2m + i\nu}\Bigg] , \tag{3.7}$$

the renormalized second order expansion of the Boson–Fermion $T$–matrix. The integral can be evaluated (see Appendix B) to give

$$\begin{aligned} T_{BF}(\mathbf{k}_1, \mathbf{k}_2, P^\mu) \approx & \frac{2\pi\hbar^2}{m} a_{BF} + \frac{2\hbar^2 a_{BF}^2 k_F}{m} \\ & + \frac{a_{BF}^2\hbar^2}{2m^2}\left(\frac{m_B k_F^2}{P} - \frac{m^2 P}{m_B} - 2m\sqrt{D} - \frac{m_B D}{P}\right) \\ & \times \ln\frac{k_F + mP/m_B + \sqrt{D} + i\nu/2a_{BF}\sqrt{D}}{k_F - mP/m_B - \sqrt{D} - i\nu/2a_{BF}\sqrt{D}} \\ & - \frac{a_{BF}^2\hbar^2}{2m^2}\left(\frac{m_B k_F^2}{P} - \frac{m^2 P}{m_B} + 2m\sqrt{D} - \frac{m_B D}{P}\right) \\ & \times \ln\frac{k_F - mP/m_B + \sqrt{D} + i\nu/2a_{BF}\sqrt{D}}{k_F + mP/m_B - \sqrt{D} - i\nu/2a_{BF}\sqrt{D}} , \end{aligned} \tag{3.8}$$

where

$$D = -\frac{m}{m_B + m_F} P^2 + \frac{2mP^0}{\hbar} + \frac{2m\mu_B}{\hbar^2} . \tag{3.9}$$

The $T$–matrix is the analog of the vacuum scattering amplitude taking into account the many–particle background. All quantities that depend on the particle interactions processes are derived from the $T$–matrix. To lowest order in $a_{BF}$, the scattering amplitude and the $T$–matrix are the same. In this case, the many–particle background can be ignored. This is consistent on a mean–field level. Beyond the mean–field approximation, we have to consider also higher order terms as we shall do in the following.

## 3.2 Physical quantities

### 3.2.1 Bosonic chemical potential

In the following, we use the above expression for the $T$–matrix to evaluate the Boson self–energies. Then, we use the Hogenholtz–Pines theorem to calculate the Boson chemical potential, which we can use to find expressions for the Bosonic Green's functions. In the mean–field approximation, we will see that the Boson Green's functions do *not* depend on the Fermions. In a later section, we reconsider the dependence of Bosonic Green's functions on the Fermions to a higher order to see how the spectral properties of the Bosons are modified due to the presence of the Fermions.

Substituting Eqn. (2.122) into Eqn. (3.2) the equation for $\Sigma_{BF}(p^\mu)$ can be rewritten as

$$\hbar\Sigma_{BF}(p^\mu) = -\frac{i}{(2\pi)^4}\int d^4q^\mu \frac{T_{BF}[(\mathbf{p}-\mathbf{q})/2, (\mathbf{p}-\mathbf{q})/2, p^\mu + q^\mu]}{q^0 - \hbar\mathbf{q}^2/2m_F + i\mathrm{sgn}(q-k_F)\nu} . \tag{3.10}$$

To evaluate this, we substitute Eqn. (3.7) into Eqn. (3.10), and first carry out the frequency integral. As the pole in the complex $q^0$–plane of the integrand in Eqn. (3.7) is below the real axis, in order to get a non vanishing result the pole of $[q^0 - \hbar q^2/2m_F - i\mathrm{sgn}(q-k_F)\nu]^{-1}$ must be above the real axis ($q < k_F$). The frequency integral is thus readily solved by contour integration. The $\mathbf{k}$ integration in Eqn. (3.7) is then very similar

to that leading to Eqn. (3.8). The resulting expression for $\hbar\Sigma_{BF}(p^\mu)$ is then

$$\begin{aligned}\hbar\Sigma_{BF}(p^\mu) &= \frac{1}{(2\pi)^3}\int d^3\mathbf{q}\theta(k_F-q) \\ &\quad \times T_{BF}\left[\frac{\mathbf{p}-\mathbf{q}}{2},\frac{\mathbf{p}-\mathbf{q}}{2},\left(p^0+\frac{\hbar\mathbf{q}^2}{2m_F},\mathbf{p}+\mathbf{q}\right)\right]. \end{aligned} \tag{3.11}$$

We wish to similarly solve this integral to second order in $a_{BF}$. In Eqn. (3.8), all terms which depend on $D$ have a factor $a_{BF}^2$. Thus, in order to get a result for Eqn. (3.11) that is correct to second order in $a_{BF}$, it is sufficient to use the zeroth order expression for $D$. Specializing to the case where $p^\mu = 0$ this can be written as

$$D^0 = \frac{m_B^2}{(m_B+m_F)^2}q^2. \tag{3.12}$$

We now substitute $D^0$ for $D$ in Eqn. (3.8), and, after a straightforward (if lengthy) integration over $\mathbf{q}$, arrive at

$$\hbar\Sigma_{BF}(0) = \frac{2\pi\hbar^2 a_{BF}}{m}n_F\left[1+\frac{a_{BF}k_F}{\pi}f(\delta)\right], \tag{3.13}$$

where

$$f(\delta) = 1-\frac{3+\delta}{4\delta}+\frac{3(1+\delta)^2(1-\delta)}{8\delta^2}\ln\frac{1+\delta}{1-\delta}, \tag{3.14}$$

$\delta = (m_B-m_F)/(m_B+m_F)$, and we have used

$$(2\pi)^{-4}\int d^4k^\mu G_F(k^\mu) = G_F(x^\mu,x^\mu) = in_F.$$

Note that in this integration we need only consider the real part of the Boson-Fermion $T$–matrix, as within the range of the integration the imaginary part is zero (see Appendix B.1). The necessary expression for the $T$–matrix is then just given by Eqn. (3.8), where we take the absolute values of the arguments of the logarithms and set $\nu = 0$. From the Hugenholtz–Pines theorem [Eqn. (2.138)]:

$$\mu_B = \hbar\Sigma_{BF}(0)+\hbar\Sigma_{BB}(0)-\hbar\Sigma_{12}(0). \tag{3.15}$$

Thus, using the expression for $\Sigma_{BF}(0)$ in Eqn. (3.13), and the results from Ref. [83] for $\Sigma_{BB}(0)$ and $\Sigma_{12}(0)$ (neglecting corrections of the order of the Boson gas parameter),

$$\mu_B = \frac{4\pi\hbar^2 a_{BB}}{m_B}n_B+\frac{2\pi\hbar^2 a_{BF}}{m}n_F\left[1+\frac{a_{BF}k_F}{\pi}f(\delta)\right]. \tag{3.16}$$

This is exactly equivalent to adding $\hbar\Sigma_{BF}(0)$ to the standard mean field result for the Bosonic chemical potential for a pure, self–interacting Bosonic system.

Considering for the moment only mean–field terms (i.e. terms to first order in the scattering lengths), the Bosonic self energy matrix reads:

$$\mathbf{\Sigma_B}(p^\mu) = \begin{bmatrix} \frac{8\pi\hbar^2 n_0 a_B}{m_B}+\frac{2\pi\hbar^2 n_F a}{m} & \frac{4\pi\hbar^2 n_0 a_B}{m_B} \\ \frac{4\pi\hbar^2 n_0 a_B}{m_B} & \frac{8\pi\hbar^2 n_0 a_B}{m_B}+\frac{2\pi\hbar^2 n_F a}{m_B} \end{bmatrix}, \tag{3.17}$$

Looking at the pole equation Eqn. (2.141), we can see that to the mean–field level, there is no change in the Bose-spectrum as compared to the pure Bose gas, since there is no

off–diagonal self–energy contribution coming from Bose–Fermi interaction, and the self–energies are independent of the four–momentum. Consequently, also all quantities that are derived from the spectrum are not changed compared to the pure Boson case in the mean–field approximation. Thus, to mean–field order, we can copy the results for pure Bosons and get the following diagonal and off–diagonal Green's functions:

$$G_B(p^\mu) = \frac{u_p^2}{p^0 - E_p/\hbar + i\nu} - \frac{v_p^2}{p^0 - E_p/\hbar - i\nu}, \tag{3.18}$$

$$G_{12}(p^\mu) = G_{12}(p^\mu) = \frac{-u_p v_P}{p^0 - E_p/\hbar + i\nu} + \frac{u_p v_p}{p^0 - E_p/\hbar - i\nu}, \tag{3.19}$$

where

$$u_p^2 = \frac{1}{2}\left[E_p^{-1}\left(\hbar^2 p^2/2m_B + 4\pi n_0 a_B \hbar^2/m_B\right) + 1\right],$$

$$v_p^2 = \frac{1}{2}\left[E_p^{-1}\left(\hbar^2 p^2/2m_B + 4\pi n_0 a_B \hbar^2/m_B\right) - 1\right],$$

and

$$E_p = \sqrt{\left(\hbar^2 p^2/2m_B\right)\left(\hbar^2 p^2/2m_B + 8\pi n_0 a_B \hbar^2/m_B\right)},$$

which is derived from the expression Eqn. (2.140) by a factorization of the denominator into parts that are linear in $p^0$. This leads to the following spectrum:

$$p^0 = \sqrt{\hbar p^2/2m_B(\hbar p^2/2m_B + 8\pi\hbar^2 a_B n_B/m_B)},$$

which is again the same as if no Fermions were present. Also all other quantities, that are calculated from the first–order Bosonic Green function are consequently the same as in the pure Boson case. For example, the depletion of the BEC which is (cf. [58])

$$n_0 = n_B / \left(1 + \frac{8}{3}\sqrt{\frac{n_B a_B^3}{\pi}}\right) \approx n_B \left(1 - \frac{8}{3}\sqrt{\frac{n_B a_B^3}{\pi}}\right). \tag{3.20}$$

To the issue of the Bose spectrum beyond mean–field we come later. We will see that via induced interactions the Fermions indeed have an effect on the Bose spectrum. But before we focus on the Fermionic properties. There, one can neglect induced interactions, since just as the direct interactions, they are not relevant for spin–polarized Fermions.

### 3.2.2 The Fermionic spectrum

According to Eqns. (3.4) and (3.3) the Fermion self–energy is

$$\Sigma_F(p^\mu) = n_0 T(-\frac{\mathbf{p}}{2}, -\frac{\mathbf{p}}{2}, p^\mu)\ . \tag{3.21}$$

One can improve on this, if diagrams involving the mean-field Bosonic Green's functions, that we have found before, are also included. With the due modification the self–energy then reads

$$\begin{aligned}\Sigma_F(p^\mu) &= n_0 T(-\frac{\mathbf{p}}{2}, -\frac{\mathbf{p}}{2}, p^\mu) \\ &\quad + i(2\pi)^{-4}\int d^4 q^\mu T_{BF}\left(\frac{1}{2}(\mathbf{p}-\vec{q}), \frac{1}{2}(\mathbf{p}-\vec{q}), p^\mu + q^\mu\right) G_B^{(1)}(q^\mu),\end{aligned} \tag{3.22}$$

where $G_B^{(1)}(q^\mu)$ is taken from Eqn. (3.18).
We now split the $T$–matrix into its first–order part (which is independent of the four-momentum) and the second order part in the following way:

$$T^{(1)} = \frac{2\pi\hbar^2}{m} a_{BF}, \tag{3.23}$$

$$\begin{aligned} T^{(2)}(P^\mu) = \frac{2a_{BF}^2\hbar^2 k_F}{m} &+ \frac{a_{BF}^2\hbar^2}{2m^2}\left(\frac{m_B k_F^2}{P} - \frac{m^2 P}{m_B} - 2m\sqrt{D} - \frac{m_B D}{P}\right) \\ &\times \ln \frac{k_F + \frac{mP}{m_B} + \sqrt{D} + \frac{i\nu}{2a_{BF}\sqrt{D}}}{k_F - \frac{mP}{m_B} - \sqrt{D} - \frac{i\nu}{2a_{BF}\sqrt{D}}} \\ &- \frac{a_{BF}^2\hbar^2}{2m^2}\left(\frac{m_B k_F^2}{P} - \frac{m^2 P}{m_B} + 2m_+\sqrt{D} - \frac{m_B D}{P}\right) \\ &\times \ln \frac{k_F - \frac{mP}{m_B} + \sqrt{D} + \frac{i\nu}{2a_{BF}\sqrt{D}}}{k_F + \frac{mP}{m_B} - \sqrt{D} - \frac{i\nu}{2a_{BF}\sqrt{D}}} \, . \end{aligned} \tag{3.24}$$

$\Sigma_F(p^\mu)$ in terms of $T^{(1)}$ and $T^{(2)}(P^\mu)$ reads:

$$\begin{aligned} \Sigma_F(p^\mu) &= n_0 T^{(1)} + n_0 T^{(2)}(p^\mu) + \left[ i(2\pi)^{-4} \int d^4q^\mu G_B^{(1)}(q^\mu) \right] T^{(1)} \\ &\quad + i(2\pi)^{-4} \int d^4q^\mu T^{(2)}(p^\mu + q^\mu) G_B^{(1)}(q^\mu) \, . \end{aligned} \tag{3.25}$$

From Eqn. (3.20) we can see that $n_B - n_0$ is of higher than first order in $a_B$. But by definition $T^{(2)}(p^\mu)$ is of second order in $a_{BF}$. So $(n_B - n_0)T^{(2)}(p^\mu)$ is of higher than second order in the scattering lengths and can thus be neglected in our present approximation. This means that we can replace $n_0 T^{(2)}(p^\mu)$ by $n_B T^{(2)}(p^\mu)$.
Since $G_B^{(1)}(q^\mu) - G_B^0(q^\mu)$ is also of higher than zeroth order in $a_B$ and $T^{(2)}(p^\mu)$ is already second order in $a_B$, we can replace $G_B^{(1)}(q^\mu)$ by $G_B^0(q^\mu)$ in the last term in the equation for $\Sigma_F(p^\mu)$. But since $T^{(2)}(p^\mu + q^\mu)$ and $G_B^0(q^\mu)$ have both poles below the real axis in the $q^0$-plane, the $q^0$-integration in $i(2\pi)^{-4}\int d^4q^\mu T^{(2)}(p^\mu + q^\mu) G_B^0(q^\mu)$ is zero (because we close the integration contour above the real axis). This means that the last term in (3.25) can be approximated as zero.
From Eqn. (2.94) it is clear that

$$i(2\pi)^{-4} \int d^4q^\mu G_B^{(1)}(q^\mu) = iG_B^{(1)}(x^\mu, x^\mu) = n_B - n_0,$$

so that the third term in (3.25) is $(n_B - n_0)T^{(1)}$.
Putting all this together we get:

$$\Sigma_F(p^\mu) = n_B T^{(1)} + n_B T^{(2)}(p^\mu) = n_B T_{BF}(-\frac{\mathbf{p}}{2}, -\frac{\mathbf{p}}{2}, p^\mu) \, . \tag{3.26}$$

The only difference of this improved equation to Eqn. (3.21) is that $n_0$ is replaced by $n_B$. This we use in Eqn. (2.135) to get the following pole equation:

$$\hbar p^0 - \frac{\hbar^2\mathbf{p}^2}{2m_F} - n_B T_{BF}(-\frac{\mathbf{p}}{2}, -\frac{\mathbf{p}}{2}, \hbar p^2/2m_F, \mathbf{p}) + i\nu \mathrm{sgn}(p - k_F) = 0 \, . \tag{3.27}$$

In evaluating the $T$–matrix consistently to second order in $a_{BF}$ one may use as in the previous section $D = D^0 = \left(\frac{m_B}{m_B + m_F}\right)^2 p^2$. The solution of the pole equation is then

$$\hbar p^0 = \frac{\hbar^2 p^2}{2m_F} + \frac{2\pi\hbar^2}{m} a_{BF} n_B + \frac{2a_{BF}^2\hbar^2 k_F n_B}{m}$$

$$
\begin{aligned}
&+ \quad \frac{a_{BF}^2\hbar^2 n_B}{m(1-\delta)p}\left(k_F^2-p^2\right)\ln\frac{k_F+p+\frac{i\nu}{2a_{BF}\sqrt{D}}}{k_F-p-\frac{i\nu}{2a_{BF}\sqrt{D}}} \\
&- \quad \frac{a_{BF}^2\hbar^2 n_B}{m(1-\delta)p}\left(k_F^2-\delta^2p^2\right)\ln\frac{k_F-\delta p+\frac{i\nu}{2a_{BF}\sqrt{D}}}{k_F+\delta p-\frac{i\nu}{2a_{BF}\sqrt{D}}} \\
&- \quad i\nu\mathrm{sgn}(p-k_F)\,. \qquad (3.28)
\end{aligned}
$$

It follows that

$$
\mathrm{Im}\hbar p^0 = \begin{cases} \nu & : \quad p \le k_F, \\ -\frac{\pi a_{BF}^2\hbar^2 n_B}{m(1-\delta)p}(p^2-k_F^2) & : \quad k_F < p < |\delta|\,k_F, \\ -\frac{\pi a_{BF}^2\hbar^2 n_B(1+\delta)}{m}p & : \quad p \ge |\delta|\,k_F. \end{cases} \qquad (3.29)
$$

This means that the lifetime of the excitations are infinite for $p \le k_F$ and positive for $p > k_F$.
The quasiparticle energies are given by the real part of the spectrum:

$$
\begin{aligned}
\mathrm{Re}\hbar p^0 \quad = \quad & \frac{\hbar^2k_F^2}{2m_F}+\frac{2\pi\hbar^2}{m}a_{BF}n_B+\frac{2a_{BF}^2\hbar^2k_Fn_B}{m} \\
& +\frac{a_{BF}^2\hbar^2n_B}{m(1-\delta)p}\left(k_F^2-p^2\right)\ln\frac{k_F+p}{k_F-p} \\
& -\frac{a_{BF}^2\hbar^2n_B}{m(1-\delta)p}\left(k_F^2-\delta^2p^2\right)\ln\frac{k_F-\delta p}{k_F+\delta p}\,. \qquad (3.30)
\end{aligned}
$$

Performing an expansion to linear order in $p-k_F$ around $k_F$ yields:

$$
\begin{aligned}
\mathrm{Re}\hbar p^0 \quad \approx \quad & \frac{\hbar^2k_F^2}{2m_F}\left(2(p/k_F-1)+1\right)+\frac{2\pi\hbar^2}{m}a_{BF}n_B \\
& +\frac{a_{BF}^2\hbar^2n_Bk_F}{m}\left(2+(1+\delta)\ln\frac{1+\delta}{1-\delta}\right) \qquad (3.31) \\
& +\frac{a_{BF}^2\hbar^2n_Bk_F}{m(1-\delta)}\left(2\delta-(1+\delta^2)\ln\frac{1+\delta}{1-\delta}-2\ln 2\right)(p/k_F-1)\,.
\end{aligned}
$$

The effective mass of the particles on the Fermi surface is thus

$$
\begin{aligned}
\frac{1}{m_F^*} \quad = \quad & \frac{1}{m_F} \qquad (3.32) \\
& +\frac{a_{BF}^2n_B}{k_Fm(1-\delta)}\left(2\delta-(1+\delta^2)\ln\frac{1+\delta}{1-\delta}-2\ln 2\right)(p/k_F-1)\,.
\end{aligned}
$$

One might be tempted to calculate the chemical potential of the Fermions via $\mu_F = \mathrm{Re}\hbar p^0|_{p=k_F}$ [84]. This, however, is not correct, since this expression was derived for pure Fermions and is not applicable to Bose–Fermi mixtures, since it does not take into account the dependence of the Bose chemical potential on the Fermions.

### 3.2.3 Ground state energy density and derived quantities

There are two different ways to calculate the ground state energy with the results we already have. The most easy one is to integrate the Boson chemical potential with respect to the Boson density. This approach we present here. The other one by using the Green's functions to evaluate the ground state energy in shown in the appendix C.

Now, we integrate Eqn. (2.139):

$$\frac{E}{V} = \int_0^{n_B} \mu(n'_B) dn'_B + C(n_F), \tag{3.33}$$

where $C(n_F)$ is a quantity that can depend on the Fermion density $n_F$ only. Considering the limit $a_{BF} \to 0$, we see that $C(n_F)$ can only be the kinetic energy of free Fermions (the Fermi energy density $\epsilon_F$) that was calculated before as the only non–vanishing term in Eqn. (2.59):

$$C(n_F) = \epsilon_F = \frac{3}{5}\frac{\hbar^2 k_F^2}{2m_F} n_F. \tag{3.34}$$

Substituting this and Eqn. (3.16) into Eqn. (3.33), and integrating gives

$$\frac{E}{V} = \epsilon_F + \epsilon_B + \frac{2\pi\hbar^2 a_{BF}}{m} n_F n_B \left[1 + \frac{a_{BF} k_F}{\pi} f(\delta)\right], \tag{3.35}$$

where $\epsilon_B = 2\pi\hbar^2 a_{BB} n_B^2 / m_B$ is the Bosonic mean–field energy density. Eqn. (3.35) is the main result of this chapter. The Bose–Fermi interaction term splits into a mean–field part given by

$$\epsilon_{MF} = \frac{2\pi\hbar^2 a_{BF}}{m} n_F n_B \tag{3.36}$$

and another part which is of second order in $a_{BF}$ and is due to quantum correlation effects. Clearly, there is no contribution due to Boson–Fermion exchange, since the Bosons are distinguishable from the Fermions. In analogy to the terminology used for pure systems, we still call it exchange–correlation energy:

$$\epsilon_{xc} = \frac{2\pi\hbar^2 a_{BF}}{m} n_F n_B \frac{a_{BF} k_F}{\pi} f(\delta). \tag{3.37}$$

The function $f(\delta)$ is given by Eqn. (3.14). Fig. 3.4 shows it dependence on $\delta$.

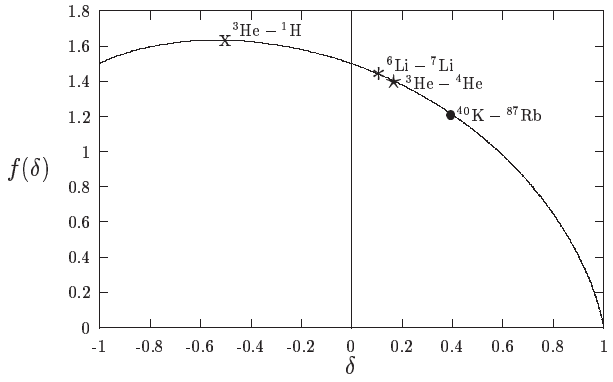


Figure 3.4: Plot of $f(\delta)$, where $\delta = (m_B - m_F)/(m_B + m_F)$, proportional to the exchange correlation energy in Eqn. 3.37 The relevant values of $f(\delta)$ for mixtures of $^3$He and $^1$H, $^6$Li and $^7$Li, $^3$He and $^4$He, and $^{40}$K and $^{87}$Rb are indicated. Quantities are dimensionless.

Note that in the limit $m_B/m_F \to \infty$, one has $\delta \to 1$ and $f(\delta) \to 0$. Thus, the second–order correction to the Boson–Fermion interaction energy and the total Boson–Boson interaction energy disappear. This is because if the Bosons are infinitely massive

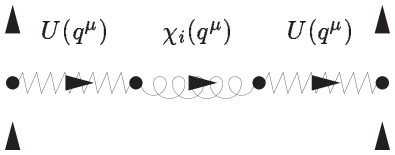


Figure 3.5: The induced interaction

(compared to a fixed, finite Fermion mass), then it is impossible for them to be scattered out of the condensate by the lighter Fermions, and only the Boson-Fermion mean field interaction remains, since *all* the Bosons populate the classical condensate field. In the opposite limit of $m_B/m_F \to 0$, the situation is different, because of the Pauli exclusion principle.

Directly from the ground state energy, we obtain

$$\begin{aligned} \mu_F &= \left(\frac{\partial E/V}{\partial n_F}\right)_{N_B,V} \\ &= \frac{\hbar^2 k_F^2}{2m_F} + \frac{2\pi\hbar^2 a_{BF}}{m} n_B \left[1 + \frac{4a_{BF}k_F}{3\pi} f(\delta)\right], \qquad (3.38) \\ P &= -\left(\frac{\partial E}{\partial V}\right)_{N_B,N_F} \qquad (3.39) \\ &= \frac{2}{5}\frac{\hbar^2 k_F^2}{2m_F} n_F + \frac{2\pi\hbar^2 a_{BB}}{m_B} n_B^2 + \frac{2\pi\hbar^2 a_{BF}}{m} n_F n_B \left[1 + \frac{4a_{BF}k_F}{3\pi} f(\delta)\right] \end{aligned}$$

for the Fermionic chemical potential and the ground state pressure.

We must mention that in this section all terms of the order of the Bose gas parameter $\sqrt{n_B a_{BB}^3} = (n_B^{(1/3)} a_{BB})^{3/2}$ were neglected. These terms are of order 3/2 in the small "diluteness parameter" and thus half an order more than $k_F a_{BF} \propto (n_F^{(1/3)} a_{BF})$. Because of this, in the dilute limit, the Bose gas parameter is in general smaller that $k_F a_{BF} \propto (n_F^{(1/3)} a_{BF})$. Of course, when the Boson density is a lot higher than the Fermion density then the also terms of the order of the Bose gas parameter become important. For a more detailed discussion of this point, see chapter 4.

### 3.2.4 Induced interactions and related properties

Induced interactions can be derived from diagrams of the form shown in Fig. 3.5, where the intermediate line, labelled $\chi_i$, is the so–called density–density response function of the component that mediates the interaction.

For the floowing illustration we will temporarily assume the Fermions to be *not* spin–ploraized, because then an effective Fermi–Fermi interaction can be mediated by density fluctuations of the Bosons. In order to calculate the Boson density–density response function, we note that it consists of diagrams which can have interaction lines attached to their ends. The simplest diagrams of this form are shown in Fig. (3.6), where the double wiggly lines are the diagonal or off–diagonal Boson Green functions. There, we can use the mean–field expressions for the Green's function derived previously. We must

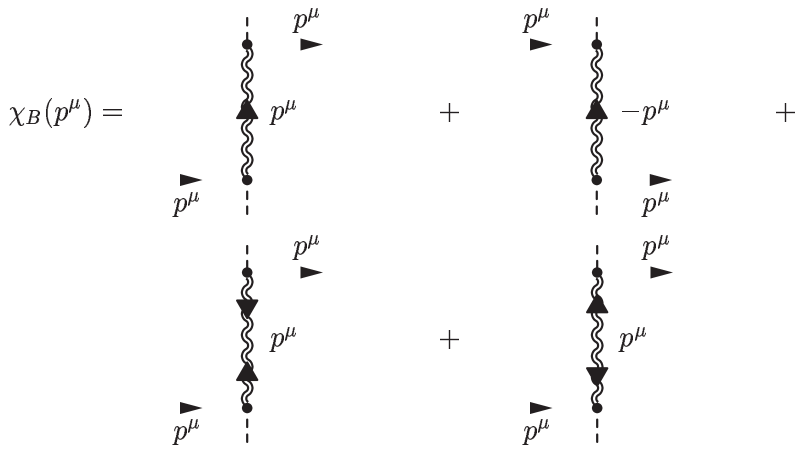


Figure 3.6: The Boson density-density response function

be aware, however, that this way we neglect all the modifications of the Bose density–density response function due to the presence of the Fermions, and thus the expression we get is just the lowest order term. Writing the above diagram as an equation, we get:

$$\chi_B(q^\mu) = G_B(q^\mu) + G_B(-q^\mu) + G_{12}(q^\mu) + G_{21}(q^\mu) \tag{3.40}$$

If we take the terms for the Bose Green's function in mean–field approximation from Eqns. (3.18) and (3.19) we get to lowest order in the Boson–Boson scattering length:

$$\chi_B(q^\mu) = \frac{n_B q^2}{m_B (q^0)^2 - q^4/4m_B + 4\pi n_B a_B q^2)} \tag{3.41}$$

For algebraic simplicity, we continue by considering the static limit (i.e. for $q^0 = 0$) only, even though very recently it was pointed out that this limit is not exactly appropriate for the parameters typical for current experiments, since the Boson sound velocity usually exceeds the Fermi velocity $v_F = \hbar k_F / m_F$ [85]. In the static limit, the induced interaction reads in the mean–field approximation for the Bose–Fermi interaction:

$$\begin{aligned} U_{FF}(\mathbf{q}) &= \left(\frac{2\pi\hbar^2 a_{BF}}{m}\right)^2 \chi_B(0,\mathbf{q}) \\ &= \left(\frac{2\pi\hbar^2 a_{BF}}{m}\right)^2 \frac{-n_B}{m_B(q^2/4m_B + 4\pi n_B a_B)}. \end{aligned} \tag{3.42}$$

This can be Fourier transformed to real-space to show that the induced interaction is of the Yukawa form as shown in Ref. [36]. The remarkable feature is that no matter what the sign of the Bose–Fermi interaction length is the induced interaction is always attractive. This opens the possibility of Cooper pairing. Nevertheless, the pairing has to take place in the $p$–wave channel since $s$–wave paring for spin-polarized Fermions is forbidden by the Pauli principle. Estimates of the critical temperature have lead to critical temperatures of about $0.5nK$ for optimal conditions [57]. This is to low to be reached in current experiments. An interesting perspective would be to find systems with higher critical temperatures by using Feshbach resonances or optical lattices. In optical lattices, the Boson density–density response function which is related to the dynamical structure factor changes compared to the homogeneous case we considered here

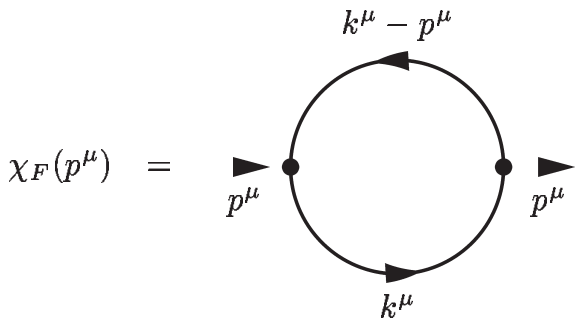


Figure 3.7: The Fermion density-density response function

as pointed out in Ref. [86] and Fermions in an optical lattice can be tuned to have a comparatively high critical temperature of BCS [87]. Together those two effects, could lead to a critical temperature which could be reached under the conditions of the current experiments. In the last chapter of this thesis, Boson–Fermion mixtures in optical lattices are introduced. Issues related to the Cooper pairing, however, are not treated there.

If we now turn the attention on the reverse process, namely the Fermion induced interaction on the Bosons, we need the Fermion density–density response function, which is given to lowest order by the diagram of Fig. 3.7 and its algebraic form can be taken from Ref. [58]. The Fermion induced interaction has three major consequences. First, just as the direct Bose–Bose interactions the induced one leads to a modification of the Bose excitation spectrum and thus also to a depletion of the condensate. Second, the induced interaction can cause an instability of the system. We first consider the effect on the excitation spectrum.

Previously, we have seen that to a mean–field level there is no change in the Bose spectrum according to the presence of the Fermions. This was because on this level there was no off–diagonal contribution and also the Boson self–energies were independent of the four momentum. Now, we will see that beyond mean-field the self–energies are momentum dependent and there is also an off–diagonal self–energy term coming from the induced interaction. The latter one gives rise to a change in the phonon sound velocity and the first one to an effective change in the Bose particle mass. Therefore we now revisit the Bose spectrum, this time to higher order than mean–field. We start again from Eqn. (2.140). We recall that the mean—field spectral equation for the Bosons is

$$p^0 = E_p = \sqrt{\hbar p^2/2m_B(\hbar p^2/2m_B + 8\pi\hbar^2 a_B n_B/m_B)}.$$

To get the spectrum to next order, we have to solve the pole equation (2.141), but it is enough to insert the mean–field excitation frequency on the right hand side of this equation, such that we get the following spectrum:

$$\begin{aligned}(p^0)^2 &= \left[\hbar p^2/2m_B + \Sigma_B(0) - \Sigma_B(E_p,\mathbf{p}) - \Sigma_{12}(0)\right]^2 \\ &\quad -\Sigma_{12}^2(E_p,\mathbf{p}),\end{aligned} \tag{3.43}$$

The off–diagonal self–energy term due to the Fermions is solely due to the induced interaction and reads to lowest order:

$$\Sigma_{12}^{BF}(E_p,\mathbf{p}) = \left(\frac{2\pi\hbar^2 a_{BF}}{m}\right)^2 \chi_F(E_p,\mathbf{p}) \tag{3.44}$$

Also the diagonal part of the self-energy is modified by the induced interaction:

$$\begin{aligned}\hbar\Sigma_{BF}(E_p,\mathbf{p}) &= \frac{1}{(2\pi)^3}\int d^3\mathbf{q}\theta(k_F-q)\\ &\quad\times T_{BF}\left[\frac{\mathbf{p}-\mathbf{q}}{2},\frac{\mathbf{p}-\mathbf{q}}{2},\left(E_p+\frac{\hbar\mathbf{q}^2}{2m_F},\mathbf{p}+\mathbf{q}\right)\right]\\ &\quad+\left(\frac{2\pi\hbar^2 a_{BF}}{m}\right)^2\chi_F(E_p,\mathbf{p}) \qquad (3.45)\end{aligned}$$

In the Hugenholtz–Pines theorem, the two modifications of the self–energy terms according to the induced interaction exactly cancel, so it is a posteriori justified that we did not consider them in order to calculate the Boson chemical potential. For the spectrum, in contrast, they are important. Also, for the spectrum we need the momentum dependence of the self–energy terms at least in the low–momentum limit and not just the value at zero momentum as in the Hugenholtz–Pines theorem. For general momentum, the integrals cannot be evaluated analytically. We may, however, do a low-momentum expansion to quadratic order, thus writing:

$$\begin{aligned}\Sigma_{12}^{BF}(E_p,\mathbf{p}) &\approx \Sigma_{12}^{BF}(0)+p\cdot\frac{d}{dp}\Big|_{p=0}\Sigma_{12}^{BF}(E_p,\mathbf{p})\\ &\quad+\frac{1}{2}p^2\cdot\frac{d^2}{dp^2}\Big|_{p=0}\Sigma_{12}^{BF}(E_p,\mathbf{p}) \qquad (3.46)\\ \Sigma_{BF}(E_p,\mathbf{p}) &\approx \Sigma_{BF}(0)+p\cdot\frac{d}{dp}\Big|_{p=0}\Sigma_{BF}(E_p,\mathbf{p})\\ &\quad+\frac{1}{2}p^2\cdot\frac{d^2}{dp^2}\Big|_{p=0}\Sigma_{BF}(E_p,\mathbf{p}). \qquad (3.47)\end{aligned}$$

The Fermion density–desnity response functions is well known (cf. e.g. Ref. [58]). In different contexts, it is also called polarization propagator or structure factor and denoted by $\Pi^0$. We find

$$\Sigma_{12}^{BF}(E_p,\mathbf{p})=-\frac{m_F k_F}{2\pi^2\hbar^2}\left(2-x\ln\left|\frac{1+x}{1-x}\right|+\frac{p^2}{6(x^2-1)}+i\pi x\theta(1-x)\right), \qquad (3.48)$$

where $x=m_F/\sqrt{2}m_B k_F\xi_B$ with $\xi_B=1/\sqrt{8\pi a_{BB}n_B}$ being the Boson healing length. We note that the linear term in $p$ vanishes and now show that the same is also true for $\Sigma_{BF}(E_p,\mathbf{p})$. Looking at Eqns. (3.45) and (3.8), we can observe, that the first term of Eqn. (3.45) is of the form

$$\frac{1}{(2\pi)^2}\int_0^{k_F}dq\;q^2\int_1^{-1}d\cos\theta\;T_{BF}\left(p^2,pq\cos\theta,q^2\right). \qquad (3.49)$$

The derivative with respect to $p$ at zero is thus

$$\begin{aligned}&\frac{1}{(2\pi)^2}\int_0^{k_F}dq\;q^2\int_1^{-1}d\cos\theta\left[p\;\partial_1 T_{BF}\left(p^2,pq\cos\theta,q^2\right)\right.\\ &\left.+\;q\cos\theta\;\partial_2 T_{BF}\left(p^2,pq\cos\theta,q^2\right)\right]\Big|_{p=0} \qquad (3.50)\end{aligned}$$

The first term is zero after setting $p=0$ and the second after integration over $\cos\theta$. The second derivative we do not evaluate, but just observe that the spectral equation (3.43)

can now be written to second order in the momentum as:

$$(p^0)^2 = \hbar\Sigma_{12}(0)p^2/m_B^*, \tag{3.51}$$

where the modified mass is defined as:

$$\begin{aligned}\frac{1}{m_B^*} &= \frac{1}{m_B} - \frac{8\hbar m_F k_F a_{BF}^2}{m^2}\frac{p^2}{6(x^2-1)} \\ &\quad -\frac{1}{2\pi^2\hbar}\int_0^{k_F} dqq^2\int_1^{-1} d\cos\theta \frac{d^2}{dp^2}\bigg|_{p=0} T_{BF}\left(p^2, pq\cos\theta, q^2\right),\end{aligned} \tag{3.52}$$

and the off–diagonal self–energy term is, upon including Bose–Bose interactions on a mean–field level,

$$\begin{aligned}\Sigma_{12}(0) &= \frac{2\hbar m_F k_F a_{BF}^2}{m^2}\left(2 - x\ln\left|\frac{1+x}{1-x}\right| + i\pi x\theta(1-x)\right) \\ &\quad + \frac{4\pi\hbar^2 a_{BB} n_B}{m_B}.\end{aligned} \tag{3.53}$$

Thus the spectrum is still phononic, but compared to the pure Bose case the mass and the sound velocity are modified. The new sound velocity is $c_B = \sqrt{\hbar \mathrm{Re}\Sigma_{12}(0)/m_B^*}$. and the lifetimes of the phonon excitations are $\propto \mathrm{Im}\Sigma_{12}(0)$ Neglecting mass modification, this was first found in Ref. [88]. There, by integrating the off–diagonal Green's function including the induced interaction, the depletion of the condensate was found in the limit of small Fermion density (which is not considered in the present chapter) and in the opposite limit. In the first case, as expected, the depletion is dominated by the direct Boson–Boson interaction and in the second case, the depletion caused by the Fermions is of order $\propto (k_F a_{BF})^2$.

The other effect due to Fermion induced interaction is to cause a potential instability of the system. Although we assume a repulsive direct Boson–Boson interaction, the net interaction (i.e. direct plus induced) can indeed be attractive, due to the attractive nature of the induced interaction. Since we know, that attractive Bosons are unstable (see Refs. [89, 90]), the Fermions could cause the Bosons to collapse. Exactly this argument was used in Ref. [91] to explain the collapse of the system observed in Ref. [92]. In the experiment, however, only the collapse of the Fermions can be clearly identified, not of the Bosons. Motivated by this observation an interesting alternative procedure would the be use the Bose induced interaction among the Fermions, which we have calculated above, to find a criterion of collapse of the Fermions. That also attractive spin–polarized Fermions can be unstable for an attractive $p$-wave interaction as has been shown in Ref. [93]. There is, however, a technical difficulty since the length scale of the Boson induced Fermi–Fermi interaction is of order of the Boson healing length $\xi_B$. Then, depending on the magnitude $k_F\xi_B$ one has to find an energy functional for either high, low or intermediate momentum $p$–wave scattering. This we will not carry out here. But yet another kind of collapse, a simultaneous collapse, of both, Fermions and the Bosons, as explained in the introductory chapter of this thesis was predicted in [33]. In the next chapter, this latter kind of collapse is investigated in more detail.

# Part III

# Inhomogenous Boson-Fermion systems

# Chapter 4

# Density functional theory

## 4.1 The Hohenberg-Kohn theorem

In this section, we shall treat the full problem, i.e. we include all relevant energy contributions to the Hamiltonian, thus in addition to the particle-particle interaction terms also the external potentials. The Hamiltonian now reads:

$$\hat{H} = \hat{T}_B + \hat{T}_F + \hat{V}_B + \hat{V}_F + \hat{U} + \hat{V}, \tag{4.1}$$

where we recall that the external potential operators are:

$$\hat{V}_B = \int d^3\mathbf{r}\hat{\Phi}^\dagger(\mathbf{r})V_B(\mathbf{r})\hat{\Phi}(\mathbf{r}) \tag{4.2}$$

and

$$\hat{V}_F = \int d^3\mathbf{r}\hat{\Psi}^\dagger(\mathbf{r})V_F(\mathbf{r})\hat{\Psi}(\mathbf{r})\ . \tag{4.3}$$

The effects of the interaction terms have been extensively studied in the previous chapter. Now, we consider these interactions to be fixed and explore how the ground state properties depend on the external potential. This investigation will lead to the Hohenberg-Kohn theorem, which we formulate here for Bose-Fermi mixtures.

Let the ground state of the system be $|\mathbf{G}\rangle$, and define the ground state energy

$$E_0 = \langle \mathbf{G}|\hat{H}|\mathbf{G}\rangle \tag{4.4}$$

and the Boson and Fermion densities, which we write for brevity as a tuple:

$$\begin{pmatrix} n_B(\mathbf{r}) \\ n_F(\mathbf{r}) \end{pmatrix} = \begin{pmatrix} \langle \mathbf{G}|\hat{\Phi}^\dagger(\mathbf{r})\hat{\Phi}(\mathbf{r})|\mathbf{G}\rangle \\ \langle \mathbf{G}|\hat{\Psi}^\dagger(\mathbf{r})\hat{\Psi}(\mathbf{r})|\mathbf{G}\rangle \end{pmatrix} \tag{4.5}$$

Clearly, considering $\hat{H}_0 = \hat{T}_B + \hat{T}_F + \hat{U} + \hat{V}$ to be fixed, the tuple of potential energies

$$\begin{pmatrix} V_B(\mathbf{r}) \\ V_F(\mathbf{r}) \end{pmatrix} \in \mathcal{V} \tag{4.6}$$

maps on the set of ground states via the eigenvalue equation (we always assume the Hamiltonian to be bounded from below).[1]

$$\hat{H}|\mathbf{G}\rangle = E_0|\mathbf{G}\rangle \tag{4.7}$$

[1] $\mathcal{V}$ is an appropriate set which is specified in mathematically rigorous treatments (see e.g. [94]).

Thus we define the map:

$$C: \quad \begin{pmatrix} V_B(\mathbf{r}) \\ V_F(\mathbf{r}) \end{pmatrix} \mapsto |\mathbf{G}\rangle. \tag{4.8}$$

The definition of the densities (4.8) can be considered as another map:

$$D: \quad |\mathbf{G}\rangle \mapsto \begin{pmatrix} n_B(\mathbf{r}) \\ n_F(\mathbf{r}) \end{pmatrix}, \tag{4.9}$$

The composite map $D \circ C$ describes the dependence of the ground state densities with respect to the external potentials. We shall see that this relation is invertible, which we prove by showing that the maps $D$ and $C$ are invertible.

- $C$ is invertible:
  In the following we will see that two different tuples of external potentials, $(V_B(\mathbf{r}), V_F(\mathbf{r}))$ and $(V'_B(\mathbf{r}), V'_F(\mathbf{r}))$, that lead to the same ground state $|\mathbf{G}\rangle$ are necessary related by an additive constant. This additive constant is not observable and thus the potentials are considered to be equivalent. $C$ is invertible on this equivalence class. The formal proof starts with the definition of $C$ for the two different tuples, which are assumed be mapped onto the same ground state $|\mathbf{G}\rangle$:

$$\begin{aligned} (\hat{H}_0 + \hat{V}_B + \hat{V}_F)|\mathbf{G}\rangle &= E_0|\mathbf{G}\rangle \\ (\hat{H}_0 + \hat{V}'_B + \hat{V}'_F)|\mathbf{G}\rangle &= E'_0|\mathbf{G}\rangle. \end{aligned} \tag{4.10}$$

  The difference of these equations is:

$$(\hat{V}_B + \hat{V}_F - \hat{V}'_B - \hat{V}'_F)|\mathbf{G}\rangle = (E_0 - E'_0)|\mathbf{G}\rangle. \tag{4.11}$$

  Multiplication from the left by the following state

$$\int d^3\mathbf{y}_1 \dots d^3\mathbf{y}_{N_B} \langle|\Psi(\mathbf{r}_{N_F}) \dots \Psi(\mathbf{r}_1)\Phi(\mathbf{y}_{N_B}) \dots \Phi(\mathbf{y}_1) \tag{4.12}$$

  projects out the Boson sector and leads after making extensive use of the (anti-)-commutation relations to an equation in terms of the many–Fermion wave function

$$\begin{aligned} &\Psi(\mathbf{r}_1, \dots, \mathbf{r}_{N_F}) \\ &= \int d^3\mathbf{y}_1 \dots d^3\mathbf{y}_{N_B} \langle|\Psi(\mathbf{r}_{N_F}) \dots \Psi(\mathbf{r}_1)\Phi(\mathbf{y}_{N_B}) \dots \Phi(\mathbf{y}_1)|\mathbf{G}\rangle, \end{aligned}$$

  which reads:

$$\left(\sum_{i=1}^{N_F} [V_F(\mathbf{r}_i) - V'_F(\mathbf{r}_i)]\right) \Psi(\mathbf{r}_1, \dots, \mathbf{r}_{N_F}) = (E_0 - E'_0)\Psi(\mathbf{r}_1, \dots, \mathbf{r}_{N_F})$$

  For arbitrary coordinates $\mathbf{r}_1, \dots, \mathbf{r}_{N_F}$, this can only be satisfied if

$$V_F(\mathbf{r}) - V'_F(\mathbf{r}) = (E_0 - E'_0)/N_F. \tag{4.13}$$

  Applying analogous arguments for the Bosons many–particle wave functions leads a similar condition:

$$V_B(\mathbf{r}) - V'_B(\mathbf{r}) = (E_0 - E'_0)/N_B. \tag{4.14}$$

  Eqns. (4.13) and (4.14) show that the respective Bosonic and Fermionc potentials are equivalent and hence the proof is completed.

- $D$ is invertible:
  The proof is by reductio ad absurdum. We assume two non-equivalent tuples of potentials $(V_B(\mathbf{r}), V_F(\mathbf{r}))$ and $(V'_B(\mathbf{r}), V'_F(\mathbf{r}))$, which lead to different ground states $|\mathbf{G}\rangle$ and $|\mathbf{\Psi}\rangle$, respectively. We show that the assumption that the two ground states give rise to the same Boson and the same Fermion densities leads to a contradiction. In the following we assume a non-degenerate ground states $|\mathbf{G}\rangle$ and $|\mathbf{\Psi}\rangle$. The case of a degenerate ground state complicates matters slightly, but the essential result does not change. For more details, the reader may refer to the book Ref. [94]. To proceed with the proof, we make use of Ritz-principle which states that the ground state energy is smaller than the expectation value with respect to any other states. This is in particular true for the state $|\mathbf{\Psi}\rangle$:

$$\begin{aligned} E_0 = \langle \mathbf{G}|\hat{H}|\mathbf{G}\rangle &< \langle \mathbf{\Psi}|\hat{H}|\mathbf{\Psi}\rangle \\ &= \langle \mathbf{\Psi}|\hat{H}' + \hat{V}_B + \hat{V}_F - \hat{V}'_B - \hat{V}'_F|\mathbf{\Psi}\rangle \\ &= E'_0 + \int d^3\mathbf{r}[V_F(\mathbf{r}) - V'_F(\mathbf{r})]n'_F(\mathbf{r}) \\ &\quad + \int d^3\mathbf{r}[V_B(\mathbf{r}) - V'_B(\mathbf{r})]n'_B(\mathbf{r}) \, . \end{aligned} \tag{4.15}$$

  In the same way, one can derive

$$\begin{aligned} E'_0 = \langle \mathbf{G}'|\hat{H}'|\mathbf{G}'\rangle < E_0 \quad &+ \quad \int d^3\mathbf{r}[V'_F(\mathbf{r}) - V_F(\mathbf{r})]n_F(\mathbf{r}) \\ &+ \quad \int d^3\mathbf{r}[V'_B(\mathbf{r}) - V_B(\mathbf{r})]n_B(\mathbf{r}) \, . \end{aligned} \tag{4.16}$$

  The assumption

$$\begin{pmatrix} n_B(\mathbf{r}) \\ n_F(\mathbf{r}) \end{pmatrix} = \begin{pmatrix} n'_B(\mathbf{r}) \\ n'_F(\mathbf{r}) \end{pmatrix} \tag{4.17}$$

  leads to a contradiction, which becomes obvious by adding the two inequalities. Thus, the density profiles have to be different and the proof is completed.

We have just shown that given the interaction potentials the external potentials uniquely determine the Boson and Fermion densities. In turn, knowing the density profiles one can in principle the external potentials that gave rise to the given densities. Thus, the Hamiltonian is uniquely determined (remember we considered the interactions to be fixed) by the Boson and Fermion density distribution and thus all observables in particular the ground state energy are functionals of the density profiles:

$$E_0 = E_0[n_B, n_F], \tag{4.18}$$

which is the Hohenberg-Kohn theorem (HKT) and was originally formulated for an inhomogeneous electron gas already in 1964 [26].

In order for the HKT to be useful, one has to know (at least good approximations) for the energy functional. The above proof was merely a proof of existence and gives no hint how to construct the energy functional. Besides some ad-hoc expressions for the energy functional (Thomas–Fermi approximations), Kohn and Sham [95] presented a systematic scheme to construct this functional.

## 4.2 The Kohn-Sham scheme

Kohn and Sham proposed to invent a hypothetical *non-interacting* reference system, described by the Hamiltonian

$$\hat{H}^{ref} = \hat{T}_B + \hat{T}_F + \hat{V}_B^{ref} + \hat{V}_F^{ref}, \tag{4.19}$$

such that the exact density profiles of the original interacting system and the reference system are identical:

$$\begin{pmatrix} n_B(\mathbf{r}) \\ n_F(\mathbf{r}) \end{pmatrix} = \begin{pmatrix} n_B^{ref}(\mathbf{r}) \\ n_F^{ref}(\mathbf{r}) \end{pmatrix} . \tag{4.20}$$

The point of this procedure is that the non–interacting reference system can be solved at least numerically and with the above requirements for the densities, one int turn known the density distribution even for the original interacting system. Existence of this reference system will be shown in this section by construction. However, we do not address mathematically subtle questions here. For details the reader is again referred to Ref. [94]. According to the HKT, the potentials of the reference system $V_B^{ref}(\mathbf{r})$ and $V_F^{ref}(\mathbf{r})$ are unique functionals of the reference densities $n_B^{ref}(\mathbf{r})$ and $n_F^{ref}(\mathbf{r})$ and thus by construction also of the original densities $n_B(\mathbf{r})$ and $n_F(\mathbf{r})$, so that the reference system is unique. Once $V_B^{ref}(\mathbf{r})$ and $V_F^{ref}(\mathbf{r})$ are known, the ground state of the reference system simply factorizes into a product wave function for the Bosons and a Slater determinant for the Fermions:

$$|\mathbf{G}\rangle^{ref} = \frac{1}{\sqrt{N_B!}}\phi(\mathbf{r}_1)\cdots\phi(\mathbf{r}_{N_B}) \times \frac{1}{\sqrt{N_F!}} \begin{vmatrix} \psi_1(\mathbf{r}_1) & \dots & \psi_1(\mathbf{r}_N) \\ \vdots & & \vdots \\ \vdots & \ddots & \vdots \\ \vdots & & \vdots \\ \psi_N(\mathbf{r}_1) & \dots & \psi_N(\mathbf{r}_N) \end{vmatrix} \tag{4.21}$$

where the wave Boson ($\phi(\mathbf{r})$) and Fermion ($\psi_i(\mathbf{r})$) functions are determined via:

$$\left(\frac{\hbar^2}{2m_B} + V_B^{ref}(\mathbf{r})\right)\phi(\mathbf{r}) = \mu_B\phi(\mathbf{r}), \tag{4.22}$$

$$\left(\frac{\hbar^2}{2m_F} + V_F^{ref}(\mathbf{r})\right)\psi_i(\mathbf{r}) = \epsilon_i\psi_i(\mathbf{r}), \tag{4.23}$$

where $\epsilon_i$ are the lowest $N_F$ energy eigenvalues. The densities are easily obtained from these wave functions:

$$\begin{pmatrix} n_B^{ref}(\mathbf{r}) \\ n_F^{ref}(\mathbf{r}) \end{pmatrix} = \begin{pmatrix} N_B|\phi(\mathbf{r})|^2 \\ \sum_{i=1}^{N_F}|\psi_i(\mathbf{r})|^2 \end{pmatrix} . \tag{4.24}$$

At this point, we do not bother very much about the problem of degeneracies of the highest occupied energy level of the Fermions which in principle causes an ambiguity in determining the densities. Considering the fact that we mostly deal with a large number particles and expecting only a small portion of them occupying the highest energy level we note that this ambiguity can only slightly change the final outcome. Also, one can partially overcome this ambiguity if one imposes the same symmetry of the density profiles as of the external potentials.

Employing again the HKT, one knows that the wave functions $\phi(\mathbf{r})$ and $\psi_i(\mathbf{r})$ are functionals of the densities[2] and consequently also the kinetic energies:

$$T_B^{ref}[n_B, n_F] = N_B \int d^3\mathbf{r}\phi^*(\mathbf{r}) \left(-\frac{\hbar^2\nabla^2}{2m_B}\right) \phi(\mathbf{r}) \,, \tag{4.25}$$

$$T_F^{ref}[n_B, n_F] = \sum_{i=1}^{N_F} \int d^3\mathbf{r}\psi_i^*(\mathbf{r}) \left(-\frac{\hbar^2\nabla^2}{2m_F}\right) \phi_i(\mathbf{r}) \,. \tag{4.26}$$

In order to determine $\hat{V}_B^{ref}$ and $\hat{V}_F^{ref}$ one has to establish a connection between the reference system and the original interacting system.

In this spirit, we express the ground state energy functional of the interacting system as:

$$\begin{aligned} E_0[n_B, n_F] = {} & T_B^{ref}[n_B, n_F] + T_F^{ref}[n_B, n_F] + \\ & \int d^3\mathbf{r} V_B(\mathbf{r}) n_B(\mathbf{r}) + \int d^3\mathbf{r} V_F(\mathbf{r}) n_F(\mathbf{r}) \\ & + \tfrac{1}{2} \tfrac{4\pi\hbar^2 a_{BB}}{m_B} \int d^3\mathbf{r} n_B^2(\mathbf{r}) \\ & + \tfrac{2\pi\hbar^2 a_{BF}}{m} \int d^3\mathbf{r} n_B(\mathbf{r}) n_F(\mathbf{r}) \\ & + E_{xc}[n_B, n_F]. \end{aligned} \tag{4.27}$$

Here, the first two terms are the kinetic energies of the reference system, the next two terms is the potential energy, the fourth and fifth term is mean-field part of the interaction energy, where we have used the $s$-wave approximation of the interaction potentials to first order only, which are given by:

$$\begin{aligned} U(|\mathbf{r} - \mathbf{r}'|) &= \tfrac{4\pi\hbar^2 a_{BB}}{m_B} \delta(\mathbf{r} - \mathbf{r}'), \\ V(|\mathbf{r} - \mathbf{r}'|) &= \tfrac{2\pi\hbar^2 a_{BF}}{m} \delta(\mathbf{r} - \mathbf{r}'). \end{aligned} \tag{4.28}$$

These equations can be verified by a Fourier transformation of Eqn. (1.38) and keeping only the first order term in the scattering length. The last term in the above expression for the energy functional is the so-called exchange-correlation energy an contains all higher order terms in the scattering length. The expression is as it stands merely a definition of the exchange-correlation energy functional $E_{\rm xc}[n_B, n_F]$. But since for weakly correlated systems the major contribution of the kinetic energy is contained in the first two terms and the major part of the interaction energy consists of the mean-field part one hopes that the exchange-correlation energy is small. Thus by finding suitable approximations of $E_{\rm xc}[n_B, n_F]$ one can hope to find a very precise description of the system. In fact, if $E_{\rm xc}[n_B, n_F]$ is neglected altogether one simply obtains a sum of the well-known Gross-Pitaevskii energy functional for the Bosons, the energy functional obtained by the self-consistent Hartree Ansatz for the Fermions, and a mean-field Boson-Fermion coupling term. This was the basis of the calculations of the density distribution for Boson-Fermion mixtures done so far [31, 33]. Here we want to go a step further and carry out the full Kohn-Sham scheme.

[2]One might be tempted to identify the wave functions $\phi(\mathbf{r})$ and $\psi_i(\mathbf{r})$ with states that are occupied by the particles, but this identification is not correct. The only physical meaning that can be ascribed to the wave function is that they reproduce the correct densities

We go on by imposing the saddle point condition on $E_0[n_B, n_F]$, namely $\delta E_0[n_B, n_F] = 0$ using (see Ref. [94])

$$\delta T_B^{ref} = -\int d^3\mathbf{r} V_B^{ref}(\mathbf{r})\delta n_B(\mathbf{r}), \tag{4.29}$$

$$\delta T_F^{ref} = -\int d^3\mathbf{r} V_F^{ref}(\mathbf{r})\delta n_F(\mathbf{r}). \tag{4.30}$$

Then the saddle point condition yields

$$\begin{aligned} 0 = \delta E_0[n_B, n_F] &= \delta T_B^{ref} + \delta T_F^{ref} \\ &+ \int d^3\mathbf{r} V_B(\mathbf{r})\delta n_B(\mathbf{r}) + \int d^3\mathbf{r} V_F(\mathbf{r})\delta n_F(\mathbf{r}) \\ &+ \tfrac{4\pi\hbar^2 a_{BB}}{m_B}\int d^3\mathbf{r}\delta n_B(\mathbf{r}) n_B(\mathbf{r}) \\ &+ \tfrac{2\pi\hbar^2 a_{BF}}{m}\int d^3\mathbf{r}\left(\delta n_B(\mathbf{r}) n_F(\mathbf{r}) + \delta n_F(\mathbf{r}) n_B(\mathbf{r})\right) \\ &+ \int d^3\mathbf{r} V_B^{xc}(\mathbf{r})\delta n_B(\mathbf{r}) + \int d^3\mathbf{r} V_F^{xc}(\mathbf{r})\delta n_F(\mathbf{r}), \end{aligned} \tag{4.31}$$

with the definition of the exchange-correlation potentials

$$V_B^{xc}(\mathbf{r}) = \frac{\delta E_{xc}[n_B, n_F]}{\delta n_B(\mathbf{r})}, \tag{4.32}$$

$$V_F^{xc}(\mathbf{r}) = \frac{\delta E_{xc}[n_B, n_F]}{\delta n_B(\mathbf{r})}. \tag{4.33}$$

Solving for the reference potentials leads to:

$$\begin{aligned} V_B^{ref}(\mathbf{r}) &= V_B(\mathbf{r}) + \tfrac{4\pi\hbar^2 a_{BB}}{m_B} n_B(\mathbf{r}) \\ &\quad + \tfrac{2\pi\hbar^2 a_{BF}}{m} n_F(\mathbf{r}) + V_B^{xc}(\mathbf{r}), \end{aligned} \tag{4.34}$$

$$V_F^{ref}(\mathbf{r}) = V_F(\mathbf{r}) + \tfrac{2\pi\hbar^2 a_{BF}}{m} n_B(\mathbf{r}) + V_F^{xc}(\mathbf{r}). \tag{4.35}$$

These can be inserted into Eqns. (4.23) to lead to the Kohn-Sham equations for Bose-Fermi mixtures:

$$\begin{aligned} &\Big[-\tfrac{\hbar^2\nabla^2}{2m_B} + V_B(\mathbf{r}) + \tfrac{4\pi\hbar^2 a_{BB}}{m_B} n_B(\mathbf{r}) \\ &\qquad + \tfrac{2\pi\hbar^2 a_{BF}}{m} n_F(\mathbf{r}) + \tfrac{\delta E_{xc}[n_B, n_F]}{\delta n_B(\mathbf{r})}\Big]\phi(\mathbf{r}) = \mu_B\phi(\mathbf{r}), \\ &\Big[-\tfrac{\hbar^2\nabla^2}{2m_F} + V_F(\mathbf{r}) \\ &\qquad + \tfrac{2\pi\hbar^2 a_{BF}}{m} n_B(\mathbf{r}) + \tfrac{\delta E_{xc}[n_B, n_F]}{\delta n_F(\mathbf{r})}\Big]\psi_i(\mathbf{r}) = \epsilon_i\psi_i(\mathbf{r}). \end{aligned} \tag{4.36}$$

The conditions (4.20) introduce non-linearities:

$$n_B(\mathbf{r}) = N_B|\phi(\mathbf{r})|^2, \quad n_F(\mathbf{r}) = \sum_{i=1}^{N_F}|\psi_i(\mathbf{r})|^2, \tag{4.37}$$

where the sum in $n_F(\mathbf{r})$ runs over the $N_F$ states $\psi_i$ that have the *lowest* energies $\epsilon_i$.

## 4.3 The exchange–correlation energy

For the exchange-correlation energy, we resort to the so called local density approximation (LDA), i.e. we approximate the exchange–correlation energy as an integral over the exchange correlation energy density of a *homogeneous* system taken at the –yet unknown– densities $n_B(\mathbf{r})$ and $n_F(\mathbf{r})$:

$$E_{xc}[n_B, n_F] \approx \int d^3\mathbf{r}\epsilon_{xc}(n_B(\mathbf{r}), n_F(\mathbf{r})) \,. \tag{4.38}$$

This is very much in the spirit of Thomas–Fermi approximation, which is in fact a LDA on the kinetic energies. With this expression of $E_{xc}[n_B, n_F]$ the effective exchange–correlation potentials appearing in the Kohn-Sham equations (4.47) become:

$$V_B^{xc}(\mathbf{r}) = \frac{\delta E_{xc}[n_B, n_F]}{\delta n_B(\mathbf{r})} = \frac{\partial \epsilon_{xc}}{\partial n_B}(n_B(\mathbf{r}), n_F(\mathbf{r})) \,, \tag{4.39}$$

$$V_F^{xc}(\mathbf{r}) = \frac{\delta E_{xc}[n_B, n_F]}{\delta n_F(\mathbf{r})} = \frac{\partial \epsilon_{xc}}{\partial n_F}(n_B(\mathbf{r}), n_F(\mathbf{r})) \,. \tag{4.40}$$

As mentioned before, the exchange-correlation energy contains all terms in the energy functional which are of at least quadratic order in the coupling constants. A topic of the previous chapter was to find the lowest order expression for the exchange-correlation energy in the homogeneous case. We use Eqn. (3.37) for the exchange-correlation energy of a homogeneous system $\epsilon_{xc}(n_B, n_F)$:

$$\epsilon_{xc}(n_B, n_F) = \tfrac{2\hbar^2 a_{BF}}{m} f(\delta) a_{BF} k_F n_F n_B, \tag{4.41}$$

where we recall that $k_F = (6\pi n_F)^{1/3}$ is the Fermi wave vector, and that $f(\delta)$ (see Eqn. (3.14)) only depends on the masses of the Bosons and Fermions, respectively:

$$f(\delta) = 1 - \frac{3+\delta}{4\delta} + \frac{3(1+\delta)^2(1-\delta)}{8\delta^2} \ln \frac{1+\delta}{1-\delta} \,. \tag{4.42}$$

Viverit and Giorgini have recently shown [88] that Eqn. (4.41) is exact in the limit $k_F\xi_B \gg 1$, where $\xi_B$ is the Boson healing length. In order of magnitude, the homogeneous densities are $n_F \approx N_F/\ell^3$ and $n_B \approx N_B/\ell^3$, where $\ell$ is the characteristic length of the confining potential. The condition $k_F\xi_B \gg 1$ is then equivalent to $N_F \gg N_B^{3/2}(a_{BB}/\ell)^{3/2}$. On the other hand, LDA is correct for large $N_B$ and $N_F$, provided that $\ell \gg a_{BB}, a_{BF}$, i.e., the characteristic lengths of the confining potentials are much larger than the scattering lengths. In current experiments $N_F \approx N_B \approx 10^4$ and $a_{BF}/\ell \approx a_{BB}/\ell \approx 10^{-3}$, so that the condition $k_F\xi_B \gg 1$ is well satisfied. Moreover, the Boson-Boson exchange-correlation energy is $256\hbar^2 a_{BB} n_B^2 \sqrt{\pi n_B a_{BB}^3}/15 m_B$ (see e.g. [83]). This is much smaller than the exchange-correlation energy in Eqn. (4.41) if $N_F >> 5.4(a_{BB}/a_{BF})^{3/2}(a_{BB}/\ell)^{3/8}((1-\delta)/f(\delta))N_B^{9/8}$. Since $a_{BB}/a_{BF} = 0.13$ for the Paris experiment with $^6$Li-$^7$Li [21] and $a_{BB}/a_{BF} = 0.28$ for the Florence experiment with $^{40}$K-$^{87}$Rb [23] (these are the only two experiments where $a_{BF}$ has been measured), this condition is satisfied as well. Yet other higher order terms are due to direct Fermion–Fermion $p$-wave scattering. These terms are at least of the order of $(k_F a_{FF})^3$[96], where $a_{FF}$ is the Fermion–Fermion $p$–wave scattering length, and thus certainly negligible against the term we consider. Altogether, Eqn. (4.41) provides the most relevant contribution to the exchange–correlation energy for the current experimental situations. For more general situations, Eqn. (4.41) provides the most relevant contribution beyond mean field any time LDA is satisfied, $N_F$ is comparable or larger than $N_B$ in order of

magnitude, and perturbation theory holds, i.e. $k_F a_{BF}/\pi << 1$, and a sufficiently small Bose gas parameter. The final expressions for the exchange–correlation potentials are now:

$$V_B^{xc}(\mathbf{r}) = \frac{2a_{BF}^2 f(\delta)}{m} n_F(r) k_F(r), \tag{4.43}$$

$$V_F^{xc}(\mathbf{r}) = \frac{8a_{BF}^2 f(\delta)}{3m} n_B(r) k_F(r). \tag{4.44}$$

## 4.4 The numerical procedure

We now specialize to spherically symmetric, harmonically trapped systems:

$$V_B(\mathbf{r}) = \tfrac{1}{2} m_B \omega_B^2 r^2, \quad V_F(\mathbf{r}) = \tfrac{1}{2} m_F \omega_F^2 r^2, \tag{4.45}$$

where $\omega_B$ ($\omega_F$) are the harmonic oscillator frequencies for the Bosonic (Fermionic) atoms. As indicated in the introduction chapter, they are due to the external magnetic field and also depend on the magnetic moments of the atoms. If the magnetic moments are the same for both species, then the external potentials are also the same for the Bosons and the Fermions. Due to the spherical symmetry, we separate off the angular parts in the usual way by the Ansatz:

$$\phi[n_B, n_F](\mathbf{r}) = \frac{u(r)}{r} Y_{00}(\Theta, \Phi), \quad \psi_{nlm}[n_B, n_F](\mathbf{r}) = \frac{u_{nl}(r)}{r} Y_{lm}(\Theta, \Phi), \tag{4.46}$$

where $Y_{lm}$ are the spherical harmonics and the Kohn-Sham equations (4.36) become:

$$\left[-\frac{1}{2m_B}\frac{d^2}{dr^2}+\frac{m_B}{2}\omega_B^2 r^2+\frac{4\pi a_{BB}}{m_B}n_B(r)+\frac{2\pi a_{BF}}{m}n_F(r)\right.$$

$$\left.+\frac{2a_{BF}^2 f(\delta)}{m}n_F(r)k_F(r)\right]u(r)=\mu_B u(r)\,,$$

$$\left[-\frac{1}{2m_F}\frac{d^2}{dr^2}+\frac{l(l+1)}{2m_F r^2}+\frac{m_F}{2}\omega_F^2 r^2+\frac{2\pi a_{BF}}{m}n_B(r)\right.$$

$$\left.+\frac{8a_{BF}^2 f(\delta)}{3m}n_B(r)k_F(r)\right]u_{nl}(r)=\epsilon_{nl}u_{nl}(r)\,, \tag{4.47}$$

with $\int dr\ u^2(r)=1, \int dr\ u_{nl}^2(r)=1$ and $n$ denotes the number of nodes of the radial functions $u_{nl}$. Here we have chosen $\ell=\sqrt{\hbar/M\Omega}$ as the length unit, where $M$ and $\Omega$ are appropriate units of mass and frequency. Energies are expressed in units of $\hbar\Omega$. The density distributions read:

$$r^2 n_B(\mathbf{r})=\frac{N_B}{4\pi}u^2(r),\quad r^2 n_F(\mathbf{r})=\frac{1}{4\pi}\sum_{\epsilon_{nl}\le\mu_F}(2l+1)u_{nl}^2(r). \tag{4.48}$$

Eqns. (4.47) together with Eqns. (4.48) define a system of coupled non-linear differential equations. We solve them numerically by an iterative procedure. We initialize $n_B(\mathbf{r})$ and $n_F(\mathbf{r})$ to be the Thomas–Fermi density distribution with no Boson-Fermion coupling. We then use these as initial densities for Eqns. (4.47). The energy eigenvalues are found by a bi-section algorithm, i.e. we assume the correct energy eigenvalue to be in a certain interval. We take a trial energy in this interval and numerically integrate the differential equations from $r$ close to zero and from an outer (large) cut-off radius to the first classical turning point. We then compare the differences in the first logarithmic derivatives of the two computed parts of the wave function at the first classical turning point. If the difference is negative the trial energy eigenvalue was too small; if it is positive, the trial energy was too large. According to this, we adjust the new interval, where the true energy eigenvalue is supposed to be in. We then iterate the procedure with this new interval. The length of the interval tends to zero with the number of iterations and the true energy eigenvalue in this interval can be determined with better and better accuracy. Having found the states $u$ and $u_{nl}$, we only have to look for $N_F$ $u_{nl}$ with lowest energy $\epsilon_{nl}$. For the search, we use the fact that $\epsilon_{nl}$ grows with $n$ and $l$. When all the occupied Kohn-Sham states are determined the output densities are computed with Eqn. (4.48). We then compare the initial and output density distributions. If these are about the same, we have found a self-consistent solution and the procedure ends. If not, we mix new densities from the initial and output ones, i.e. we use $n_{B/F}^{new}(r)=(1-x)\cdot n_{B/F}^{initial}+x\cdot n_{B/F}^{output}$, where $0<x\le 1$. If $x$ is close to 0 then the convergence is very slow, if $x$ is too large the procedure does not converge or run into local minimums. We have found good convergence with $x=0.3$. Then we start a new iteration steps with the new densities $n_{B/F}^{new}(r)$.

If the number of Fermions is large (i.e. of order 1000) it is very time consuming to determine all the occupied Kohn-Sham states for the Fermions. Additionally, the more states are required, the higher is the number of nodes of the high energetic wave

functions. For the numerics, one has to discretise space and thus there is a maximum number of nodes that can be represented. For these reasons we use the Thomas–Fermi approximation of the kinetic energy part of the Fermions, when the number of Fermion is above 1000:

$$T_F^{\rm ref}[n_B, n_F] = \frac{3}{5}\int d^3\mathbf{r}\frac{\hbar^2 k_F^2(\mathbf{r})}{2m_F} n_F(\mathbf{r}), \tag{4.49}$$

instead of $T_F^{\rm ref}[n_B, n_F]$ from Eqn. (4.26). The Thomas–Fermi approximation is reasonably accurate for large Fermion numbers. A good agreement to the single-particle description was obtained for $N_F > 1000$.

## 4.5 Results

A comparison of our results with current experiments can be carried out for those systems whose Boson-Fermion scattering length has been measured. These are the $^6$Li-$^7$Li mixtures realized in the Paris experiment [21], and the $^{40}$K-$^{87}$Rb recently realized in the Florence experiment [23]. In the Paris experiment with Fermionic $^6$Li and Bosonic $^7$Li, the measured scattering lengths are $a_{BB} = 5.1a_0$ and $a_{BF} = 38.0a_0$, where $a_0$ is the Bohr radius. Here and in the description of the following experiment, we have restricted ourselves to spherically symmetric systems. Since the actual experiments are only axially symmetric we have taken the geometric mean of the axial trapping frequencies. The mean trapping frequencies are about $\omega_B = \omega_F = 7000Hz$. Taking the unit of frequency $\Omega = \omega_B$ and the mass unit $M = m_B$, the exchange-correlation energy turns out to be $\approx 50\hbar\Omega$, whereas the mean-field Boson-Fermion interaction energy is $\approx 7455\hbar\Omega$. Thus, only about 0.67% of the interaction energy is due to exchange correlations, it has the same sign of the mean-field energy, and the modification of the mean-field density profiles is negligible. In Fig. 4.1 we show a plot of our calculated density profiles for the Paris experiment. We can see almost no difference between the calculations neglecting the exchange correlation energy and the calculations including exchange correlation in LDA.

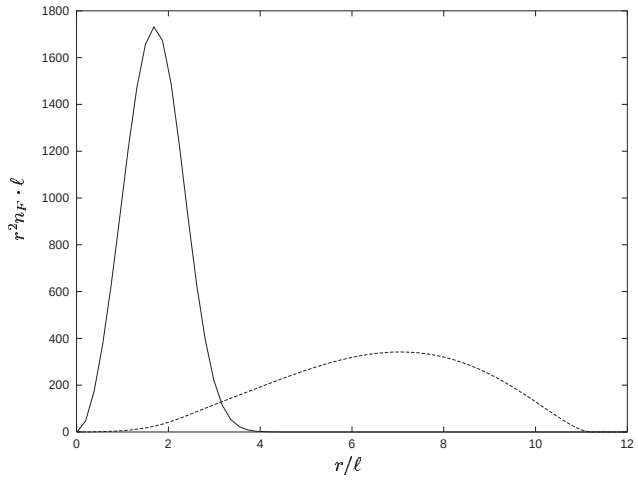


Figure 4.1: Solid line: Boson density (same with and without exchange-correlation), Fermion density (same with and without exchange-correlation). For better visibility of the Fermion density profile we multiplied the densities by $r^2$ in this plot.

However, in Fig. 4.2, one can see that there is a little effect in the Fermion density distribution close to the center of the trap. Since $a_{BF} > 0$ exchange correlation effects enhance the mean-field effects and the $^6$Li atoms are even more expelled to the outside of the trap than in the pure mean-field calculation.

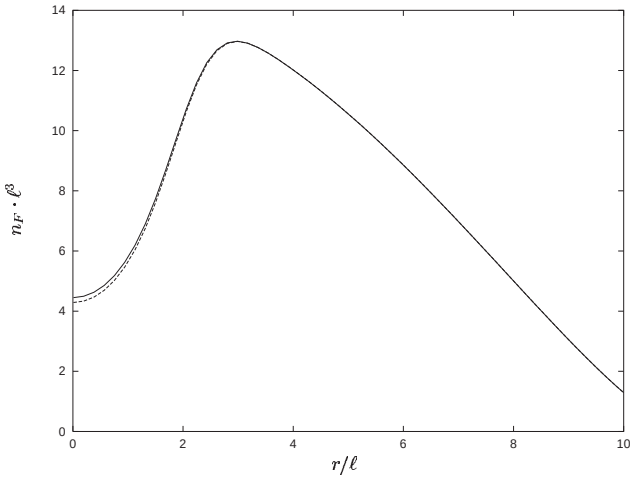


Figure 4.2: Solid line: Fermion density without exchange-correlation, dashed line: Fermion density with exchange-correlation

The situation is very different for the mixture of Fermionic $^{40}$K and Bosonic $^{87}$Rb realized in the Florence experiment, due to the large and negative Boson-Fermion scattering length giving rise both to a large attractive mean–field Boson–Fermion interaction potential, and to a non negligible exchange–correlation potential. The latter, being proportional to the square of the Boson-Fermion scattering length, is always repulsive. For this experiment, a typical stable configuration is achieved for $N_F = 10^4$, $N_B = 2 \times 10^4$. The Boson–Boson scattering length is $a_{BB} = 100.0a_0$, while the Boson–Fermion scattering length $a_{BF} \approx -400.0a_0$ is measured with an uncertainty of about 50%. The mean-field interaction energy is $\approx -98165\hbar\omega_B$, while the exchange-correlation energy is $\approx 6783\hbar\omega_B$. Thus, the relative correction in the interaction energy is about 7% of the mean-field result, going in opposite direction, and leads to a pronounced effect on the density profiles. Both the Boson and Fermion densities spread out and decrease substantially at the center of the trap with respect to the mean-field prediction, due to the repulsive exchange–correlation potential. This effect is shown in Figs. 4.3 and 4.4, where we show the Boson and Fermion density distributions with and without exchange correlations, calculated with the parameters fixed at the values measured in the Florence experiment. At the center of the trap, the Boson and Fermion densities are reduced, respectively, to about 85% and 78% of the mean-field result.

## 4.6 Stability and collapse

In general, there are two kinds of instabilities in a binary mixture (we do not consider instabilities due to Fermion pairing): demixing [28] and simultaneous collapse of both the Boson and the Fermion component [33]. The first can occur if the interaction between the two species is repulsive, and implies by definition a minimal overlap of the density distributions. In this case, we do not expect a significant change of the phase diagram

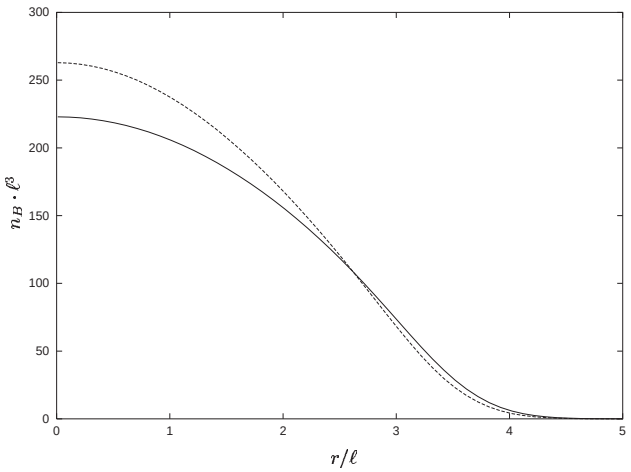


Figure 4.3: The Boson density profile for the Florence experiment. Solid line: without exchange correlations; dashed line: with exchange correlations. Quantities are dimensionless, rescaled in units of $\ell = (\hbar/m_B\omega_B)^{1/2}$.

by repulsive exchange–correlation interactions, but only for a small enhancement of the phase separation.

In the collapse regime, which can occur if the interaction between the two species is attractive, the situation is radically different, as in this case one has indeed a very high overlap of the densities in the center of the trap. The exchange–correlation interaction, which is always repulsive to second order in the Boson-Fermion scattering length, opposes the propensity to collapse due to the attractive mean-field contribution. If the coupling strength between the two components of the mixture is sufficiently strong, the exchange–correlation can significantly modify the phase diagram.

In Fig. 4.5, we provide the mean–field phase diagram of a binary Boson–Fermion mixture, with the physical parameters of the Florence experiment [92]. The plot shows the behavior of the critical number of Bosons $N_B^{cr}$, i.e., the threshold number for the onset of collapse , as a function of the number of Fermions $N_F$. Collapse occurs at any point of the phase plane above the critical curve, while the mixture is stable at all points below it. For low Fermion numbers $N_F \leq 8\times10^3$, the critical number of Bosons $N_B^{cr}$ begins to grow so fast that to all practical purposes collapse is inhibited. The inversion regime between the number of Fermions and the critical number of Bosons takes place at $N_F \simeq N_B^{cr} \simeq 5\times10^4$. For a typical number of Fermions $N_F \simeq 2\times10^4$ one has a critical Boson number $N_B^{cr} \simeq 7\times10^4$. The situation in the mean-field approximation is to be compared with the prediction obtained by including exchange–correlation. Fig. 4.6 shows the same phase diagram as in Fig. 4.5 but with the inclusion of exchange–correlation. We clearly see a significant increase in the critical number of the Bosons due to exchange–correlation. The inversion regime between the number of Fermions and the critical number of Bosons takes place at $N_F \simeq N_B^{cr} \simeq 1.2\times10^5$, and for a typical Fermion number $N_F \simeq 2\times10^4$ the critical Boson number $N_B^{cr} \simeq 1.5\times10^5$, i.e., a much larger number of Bosons is needed to produce a collapse of the Fermion component. This behavior was qualitatively expected since the effective exchange-correlation potentials are always repulsive to second order in the Boson-Fermion scattering length.

Due to the large difference between the mean-field and the exchange-correlation phase

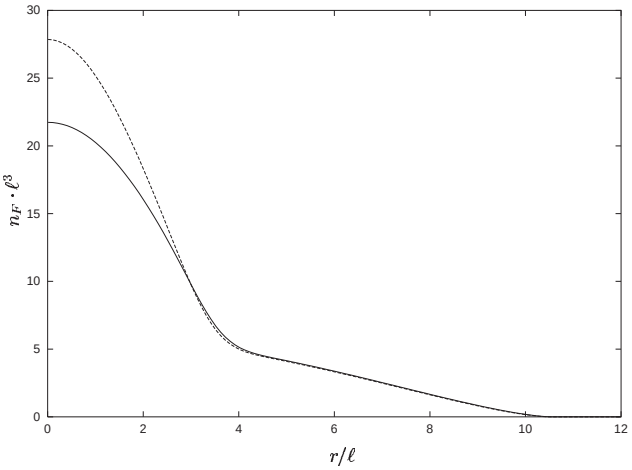


Figure 4.4: The Fermion density profile for the Florence experiment. Solid line: without exchange correlations; dashed line: with exchange correlations. Quantities are dimensionless, rescaled in units of $\ell = (\hbar/m_B\omega_B)^{1/2}$.

diagram, some comments are in order. First of all, the determination of the critical line for simultaneous collapse of the mixture is very sensitive to the exact value of the Boson-Fermion scattering length. Since this value is experimentally known with a large uncertainty, it would be crucial to know it with a much greater precision. This could be achieved by tuning the scattering length in order to fit the experimental data on the onset of collapse [97]. Moreover, for large interaction strengths, such as that in the Florence experiment, the second–order term in the exchange–correlation energy might overestimate the effect of stabilization. In fact, in these cases, the attractive third–order term could possibly give rise to a non negligible contribution, so that the mean–field critical line of Fig. 4.5 and the second–order critical line of Fig. 4.6 would provide, respectively, a lower and an upper bound. The true phase–diagram would, therefore, lie in between the two. A more detailed analysis than that provided in the present thesis requires, however, knowledge of the third–order interaction energy in powers of $k_F a_{BF}$, and this is a formidable task, even numerically. One might also ask in what respect the anisotropy plays a role. We have assumed a spherically symmetric trapping potential. In actual experiments, the traps are only axially symmetric. The system is thus more accurately described by external potentials of the form given in Eqn. (1.40). even if the anisotropy parameter $\lambda = \omega_x/\omega_{yz}$ deviated from 1 not so much that we are in the confinement dominated (or even quasi-low dimensional) regime. In Figs. 4.7 and 4.8 we show plots of the density distributions for $\lambda =$ in a stable regime.

In order to simplify the numerics, we also used a Thomas–Fermi approximation also for the Bosons. Thomas–Fermi approximation is a local density approximation on the kinetic energy. From Eqn. (2.59), we can see that in this approximation the Boson kinetic energy is zero. The exploration how the collapse regime depends on the anisotropy will be subject of a future work.

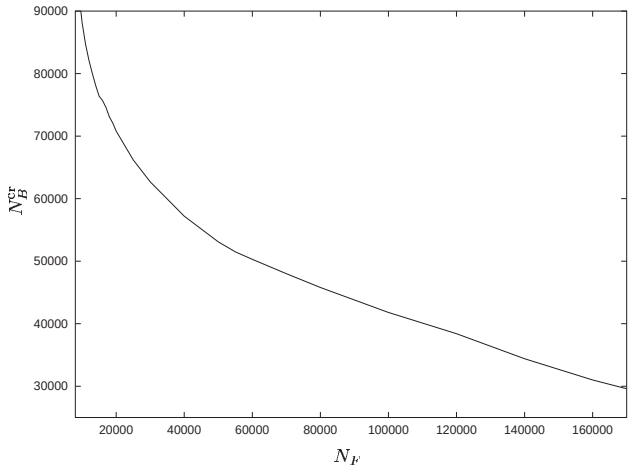


Figure 4.5: The critical number of Bosons $N_B^{cr}$ for the onset of collapse as a function of the number of Fermions $N_F$ in mean–field approximation.

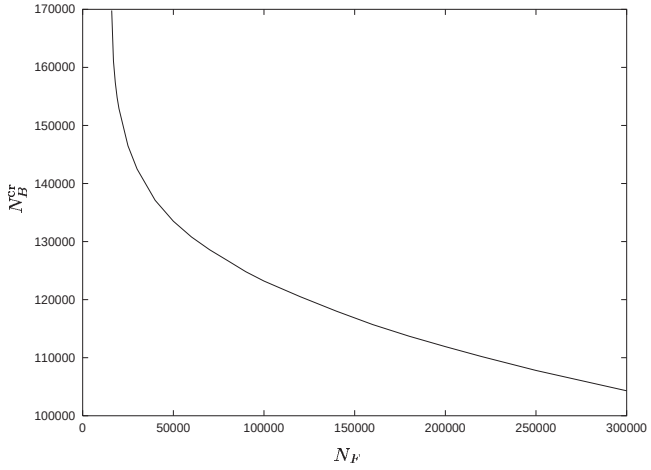


Figure 4.6: The critical number of Bosons $N_B^{cr}$ for the onset of collapse as a function of the number of Fermions $N_F$ including exchange–correlation.

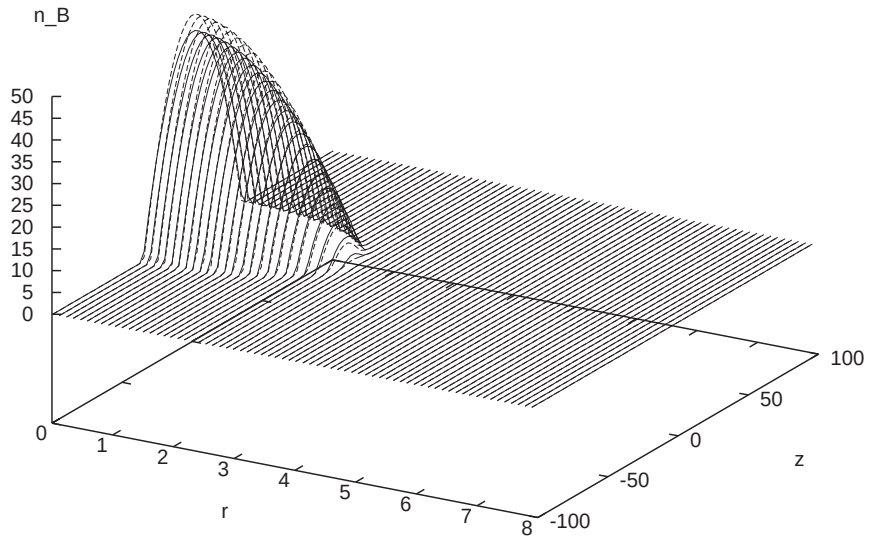


Figure 4.7: The Boson densities including exchange–correlation (solid lines, below) and in mean-field approximation (dahed lines, above) in a cylindrical trap

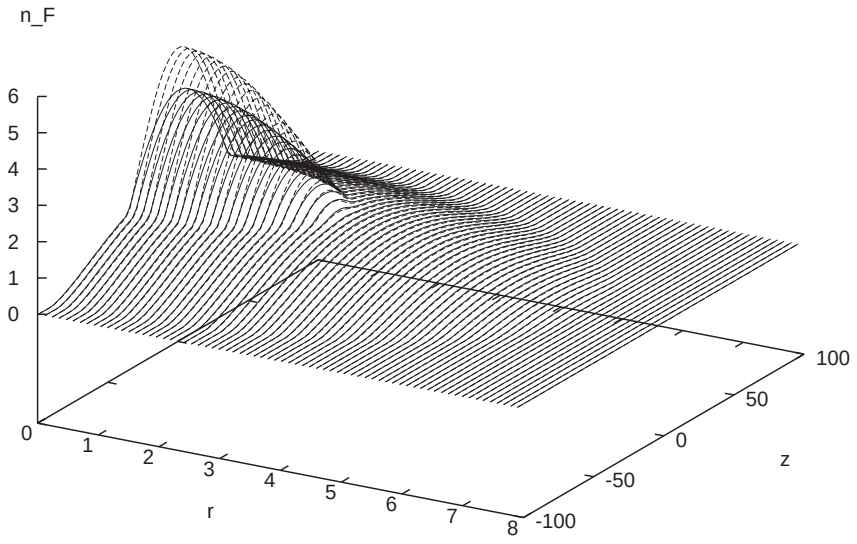


Figure 4.8: The Fermion densities including exchange–correlation (solid lines, below) and in mean-field approximation (dahed lines, above) in a cylindrical trap

# Chapter 5

# The critical temperature of BEC

Up to this point, the discussions were mostly restricted the case of zero temperature. We briefly mentioned the possibility of a BSC phase transition of the Fermions due to exchange of phonon fluctuations in the Bose gas. In this chapter, the phase transition for the Bosons from an (almost classical) Bose gas to a BEC in the presence of Fermions is studied in more detail. Whereas previously, we have assumed the existence of a BEC, we here give an estimate of how low the temperature has to be in order for this assumption to be satisfied. As in the previous chapter, the harmonically trapped systems are considered and we also make extensive use of LDA. Unlike before we do not consider exchange and correlation effects, thus restrict the discussion to mean-field approximation for the interaction terms. Our aim is to calculate the critical temperature $T_c$ of BEC. Within our mean-field approach the contribution to the critical temperature is due to re-distribution of density profiles caused by particle-particle interactions. In homogeneous systems, the situation is far more complicated since mean-field does not lead to a temperature shift and corrections are due to beyond mean-field effects. Some work on this issues has been done for the case of pure Bosonic systems and the interested reader is referred to the literature (Refs. [98, 99], and references therein).

## 5.1 Thermodynamics of inhomogeneous Bose-Fermi mixtures

We start with the well-known equation of state relating the chemical potentials $\mu_B$ and $\mu_F$ to the particle densities $n_B$ and $n_F$ in the grand–canonical ensemble for homogeneous non-interacting Bose and Fermi gases, respectively, in a large volume. The expressions can be found in any standard textbook about Quantum Statistical Mechanics, e.g. Ref. [100]:

$$n_B = \frac{1}{2\pi^2\hbar^3}\int_0^\infty dp\,\frac{p^2}{\exp\left((p^2/2m_B-\mu_B)/k_BT\right)-1}+n_0, \tag{5.1}$$

$$n_F = \frac{1}{2\pi^2\hbar^3}\int_0^\infty dp\,\frac{p^2}{\exp\left((p^2/2m_F-\mu_F)/k_BT\right)+1}. \tag{5.2}$$

Here $T$ is the temperature of the system and $k_B$ is the Boltzmann constant. $n_0$ denotes the BEC density. The critical temperature $T_c$ is defined as the minimal temperature

with $n_0 = 0$. The difference in the signs in the denominators under the integrals is due to the different statistics for the Bosons and Fermions.

A spatially uniform external potential can be easily included in the above expressions for the density distributions, since it can be easily absorbed by a shift in the chemical potential. However, we consider cases when the Bosons and Fermions are trapped by the respective (not necessarily isotropic) harmonic potentials:

$$V^B_{ext}(\mathbf{r}) = m_B(\omega_x^2 x^2 + \omega_y^2 y^2 + \omega_z^2 z^2)/2, \tag{5.3}$$
$$V^F_{ext}(\mathbf{r}) = m_F(\omega_x'^2 x^2 + \omega_y'^2 y^2 + \omega_z'^2 z^2)/2. \tag{5.4}$$

Local density approximation (LDA) in this context consist of dividing the inhomogeneous system into hypothetical (small) boxes in which the external potentials and the densities can be considered to be almost constant (at respective values $n_B(\mathbf{r}), n_F(\mathbf{r}), V_B(\mathbf{r}), V_F(\mathbf{r})$, where $\mathbf{r}$ is a position inside the box). Then the above equations of state turn into local equations of state:

$$n_B(\mathbf{r}) = (\lambda_T^F)^{-3} g_{3/2}(\exp\{-[V^B_{eff}(\mathbf{r}) - \mu_B]/k_B T\}) \tag{5.5}$$
$$n_F(\mathbf{r}) = (\lambda_T^F)^{-3} f_{3/2}(\exp\{-[V^F_{eff}(\mathbf{r}) - \mu_F]/k_B T\}), \tag{5.6}$$

where we have replaced the momentum by a dimensionless integration variable $x = p^2/(2m_B kT)$ in the Boson equation of state and $x = p^2/(2m_F kT)$ in the Fermion equation of state and well-known Bose and Fermi functions of order 3/2 are given by:

$$g_{3/2}(x) = \frac{2}{\sqrt{\pi}} \int_0^\infty \frac{\sqrt{z}}{e^z/x - 1} \tag{5.7}$$

and

$$f_{3/2}(x) = \frac{2}{\sqrt{\pi}} \int_0^\infty \frac{\sqrt{z}}{e^z/x + 1}. \tag{5.8}$$

Also, we have introduced the Boson and Fermion thermal wavelengths $\lambda_T^B = \hbar(2\pi/m_B k_B T)^{1/2}$ and $\lambda_T^F = \hbar(2\pi/m_F k_B T)^{1/2}$. The effective potentials take into account the external potential energies and the inter-particle interactions in mean-field approximation:

$$V^B_{eff}(\mathbf{r}) = V^B_{ext}(\mathbf{r}) + 2g_{BB} n_B(\mathbf{r}) + g_{BF} n_F(\mathbf{r}) \,, \tag{5.9}$$
$$V^F_{eff}(\mathbf{r}) = V^F_{ext}(\mathbf{r}) + g_{BF} n_B(\mathbf{r}) \,. \tag{5.10}$$

Notice the factor 2 present in the Bose-Bose contribution and absent in the Bose-Fermi term due to exchange effects. In the above equation $g_{BB} = 4\pi\hbar^2 a_{BB}/m_B$ and $g_{BF} = 2\pi\hbar^2 a_{BF}/m$ are the Bose-Bose and Bose-Fermi coupling constants. In principle also the exchange–correlation potentials from Eqns. (4.43) and (4.44) could be included here, but since we perform a first order expansion in the coupling constants for the critical temperature all higher order terms my be neglected. The above Eqns. (5.5) and (5.6) determine the density profiles for an inhomogeneous Bose-Fermi mixture at finite temperature *above* $T_c$.

In using the equations of state (5.1) and (5.1) along with LDA, we face the dilemma that we have to fit the large volume, which is required in order for Eqns. (5.1) and (5.1) to hold into the "small boxes" we needed for LDA. So are the approximations we use incompatible? No, because the volume needs to be large compared to the third power of the thermal wavelengths, but for LDA the size of the boxes have to be small compared to the third power of the characteristic length scale of the external potentials (i.e. the harmonic oscillator length for harmonic potentials), which are usually orders magnitude larger

than the thermal wavelengths: $\{\lambda_T^B, \lambda_T^B\} \gg \{l_{x,y,z}, l'_{x,y,z}\}$, where the harmonic oscillator length are $l_{x,y,z} = \sqrt{\hbar/m_B\omega_{x,y,z}}$, $l'_{x,y,z} = \sqrt{\hbar/m_F\omega'_{x,y,z}}$. The above conditions of validity for LDA can also be written in terms of energy quantities: $k_BT \gg \{\hbar\omega_{x,y,z}, \hbar\omega'_{x,y,z}\}$. Also LDA requires that the energy associated with the Fermi temperature of the Fermionic system to be much larger than the harmonic oscillator energies $k_BT_F \gg \hbar\omega'_{x,y,z}$. For a non-interacting trapped Fermi system the Fermi temperature, or equivalently the Fermi energy, is given by [101] $k_BT_F = \epsilon_F = \hbar\omega_F(6N_F)^{1/3}$, where $\omega_F = (\omega'_x\omega'_y\omega'_z)^{1/3}$ is the geometric mean of the Fermion oscillator frequencies. The density profiles without making use of LDA were recently determined numerically in Ref. [102] confirming the above and following results under the restrictions we have stated above.

## 5.2 Introduction to $T_c$

For the most simple case of a non-interacting pure Bose gas confined by an external harmonic potential the density distribution reads

$$n_B^0(\mathbf{r}) = (\lambda_T^B)^{-3} g_{3/2}(\exp\{-[V_{ext}^B(\mathbf{r}) - \mu_B]/k_BT\}) \tag{5.11}$$

in the LDA. In this case, the critical temperature for BEC is given by [103]:

$$k_BT_c^0 = \hbar\omega_B \left(\frac{N_B}{\zeta(3)}\right)^{1/3} \simeq 0.94\hbar\omega_B\, N_B^{1/3}\,, \tag{5.12}$$

where $\omega_B = (\omega_x\omega_y\omega_z)^{1/3}$ is the geometric mean of the oscillator frequencies and $m_B$, $N_B$ are respectively the particle mass and the number of Bosons in the trap. At $T = T_c^0$ the Boson chemical potential takes the critical value $\mu_B = \mu_c^0 = 0$, corresponding to the bottom of the external potential, and the density $n_B^0(0)$ in the center of the trap satisfies the critical condition $n_B^0(0)(\lambda_{T_c^0}^B)^3 = \zeta(3/2) \simeq 2.61$ holding for a homogeneous system [100].

Finite size effects modify the prediction of the critical temperature (5.12) resulting in a reduction of $T_c^0$. The first correction due to the finite number of atoms in the trap is given by [104]:

$$\left(\frac{\delta T_c}{T_c^0}\right)_{fs} = -\frac{\zeta(2)}{2\zeta(3)^{2/3}}\frac{\bar\omega_B}{\omega_B}N_B^{-1/3} \simeq -0.73\frac{\bar\omega_B}{\omega_B}N_B^{-1/3}\,, \tag{5.13}$$

where $\bar\omega_B = (\omega_x + \omega_y + \omega_z)/3$ is the arithmetic mean of the oscillator frequencies.

Interparticle interactions have an effect on the BEC transition temperature as well. The presence of repulsive interactions has the effect of expanding the atomic cloud, with a consequent decrease of the density. Lowering the peak density has then the effect of lowering the critical temperature. On the contrary, attractive interactions produce an increase of the density and thus an increase of $T_c$. This effect, which is absent in the case of a uniform gas where the density is kept fixed, can be easily estimated within mean-field theory. For pure Bosonic systems the shift $\delta T_c = T_c - T_c^0$ has been calculated in Ref. [105],

$$\left(\frac{\delta T_c}{T_c^0}\right)_{BB} = -1.33\,\frac{a_{BB}}{\ell_B}\,N_B^{1/6}\,, \tag{5.14}$$

to first order in the coupling constant $g_{BB}$. In the above equation $\ell_B = \sqrt{\hbar/m_B\omega_B}$ is the (mean) harmonic oscillator length. Result (5.14) has been obtained within LDA and neglects finite size effects.

In the case of trapped Bose-Fermi mixtures, the shift of $T_c$ due to both Bose-Bose and Bose-Fermi couplings can be calculated in mean-field approximation using the methods of Ref. [105]. The transition temperature $T_c$ of a trapped Bose gas is defined by the normalization condition

$$N_B = \int d\mathbf{r}\; n_B(\mathbf{r}, T_c, \mu_c)\;. \tag{5.15}$$

For a fixed value of the Boson chemical potential $\mu_B$ and a fixed temperature $T$, the Boson density (5.5) can be expanded to first order in $g_{BB}$ and $g_{BF}$ as

$$n_B(\mathbf{r}, T, \mu_B) = n_B^0(\mathbf{r}, T, \mu_B) - [2g_{BB}n_B^0(\mathbf{r}) + g_{BF}n_F^0(\mathbf{r})]\frac{\partial n_B^0}{\partial \mu_B}\;, \tag{5.16}$$

in terms of the non-interacting Boson (5.11) and Fermion density. The Fermion chemical potential $\mu_F$ is fixed by the normalization condition

$$N_F = \int d\mathbf{r}\; n_F^0(\mathbf{r})\;, \tag{5.17}$$

where $N_F$ is the total number of Fermions in the trap.

To first order in $g_{BB}$ and $g_{BF}$, the critical value $\mu_c$ of the Boson chemical potential can be written as

$$\mu_c = \mu_c^0 + 2g_{BB}n_B^0(\mathbf{r}=0) + g_{BF}n_F^0(\mathbf{r}=0)\;. \tag{5.18}$$

By writing $T_c = T_c^0 + \delta T_c$, one can expand Eqn. (5.15) obtaining the following result for the total relative shift of the condensation temperature:

$$\begin{aligned}\frac{\delta T_c}{T_c^0} &= \left(\frac{\delta T_c}{T_c^0}\right)_{BB} + \left(\frac{\delta T_c}{T_c^0}\right)_{BF} \\ &= -\frac{2g_{BB}}{T_c^0}\frac{\int d\mathbf{r}\;\partial n_B^0/\partial\mu_B[n_B^0(\mathbf{r}=0) - n_B^0(\mathbf{r})]}{\int d\mathbf{r}\;\partial n_B^0/\partial T} \\ &\quad -\frac{g_{BF}}{T_c^0}\frac{\int d\mathbf{r}\;\partial n_B^0/\partial\mu_B[n_F^0(\mathbf{r}=0) - n_F^0(\mathbf{r})]}{\int d\mathbf{r}\;\partial n_B^0/\partial T}\;,\end{aligned} \tag{5.19}$$

where the derivatives of the non-interacting Boson and Fermion densities $n_B^0$ and $n_F^0$ are evaluated at the ideal critical point $\mu_c^0 = 0$, $T = T_c^0$. The first term $\left(\delta T_c/T_c^0\right)_{BB}$ in the above equation accounts for interaction effects among the Bosons and coincides with the shift (5.14). The second term $\left(\delta T_c/T_c^0\right)_{BF}$ accounts instead for interaction effects between Bosons and Fermions, and its determination will constitute the main result of the present chapter. Some comments are in order here. (i) The shift $\delta T_c$ derived above is a mean-field effect which originates from the fact that in a trapped Bose-Fermi mixture the total number of Bosons and the total number of Fermions are fixed, but not the density profiles of the two species. This effect is peculiar of trapped systems, since it vanishes identically in the case of uniform systems, and should not be confused with the shift of $T_c$ occurring in homogeneous Bose systems, which is instead due to many-body effects (see Ref. [99]). (ii) The shift originating from the Bose-Fermi coupling, similarly to the one arising from the Bose-Bose one, is negative if $g_{BF} > 0$ and is positive if $g_{BF} < 0$. If $a_{BB}$ and $a_{BF}$ have opposite sign, the corresponding shifts of $T_c$ go in opposite directions. (iii) Result (5.19) holds to lowest order in $g_{BB}$ and $g_{BF}$ and, since it has been obtained using LDA, is exact if the number of Bosons and Fermions is large. Finite-size corrections are not included in (5.19). For a finite system, a reasonable estimate of the total shift of the critical temperature can be obtained by adding to result (5.19) the finite-size correction (5.13) of the non-interacting model.

## 5.3 Results

We now concentrate on the relative shift $\left(\delta T_c/T_c^0\right)_{BF}$ due to the Boson-Fermion interaction. First of all we observe that

$$\frac{\partial n_B^0(\mathbf{r})}{\partial \mu_B} = \frac{1}{(\lambda_{T_c^0}^B)^3 k_B T_c^0}\, g_{1/2}(\exp[-V_{ext}^B(\mathbf{r})/k_B T_c^0]) \;, \tag{5.20}$$

and $T_c^0 \int d\mathbf{r}\, \partial n_B^0/\partial T = 3N_B$, where the derivatives are evaluated at the condensation point of the non-interacting gas $\mu_c^0 = 0$, $T = T_c^0$. Using the zeroth order Fermi density distribution, i.e.

$$n_F^0(\mathbf{r}) = (\lambda_T^F)^{-3} f_{3/2}(\exp\{-[V_{ext}^F(\mathbf{r}) - \mu_F]/k_B T\}) \;, \tag{5.21}$$

the relative shift can then be rewritten as:

$$\begin{aligned}\left(\frac{\delta T_c}{T_c^0}\right)_{BF} &= -\frac{g_{BF}}{3N_B}\frac{1}{(\lambda_{T_c^0}^B)^3(\lambda_{T_c^0}^F)^3 k_B T_c^0} \\ &\times \int d\mathbf{r}\; g_{1/2}(\exp[-V_{ext}^B(\mathbf{r})/k_B T_c^0]) \\ &\times \left[f_{3/2}(\exp\{\mu_F/k_B T_c\}) - f_{3/2}(\exp\{[\mu_F - V_{ext}^F(\mathbf{r})]/k_B T_c^0\})\right] .\end{aligned} \tag{5.22}$$

In the following, we shall assume that even if the trapping potentials of Bosons and Fermions can have different oscillator frequencies, nevertheless
$\omega_x/\omega_x' = \omega_y/\omega_y' = \omega_z/\omega_z' = \omega_B/\omega_F$, i.e. the anisotropy is the same for the Bosonic and Fermionic trapping potentials. This is always the case in today's experiments, and assuming otherwise would introduce unnecessary complications. In fact, the assumption of equal anisotropies holds in general in magnetic traps since the confining potentials depend only on the (common) external magnetic field, the magnetic moments, and the masses of the atoms. Eqn. (5.22) contains the Fermion chemical potential $\mu_F(N_F, T_c^0)$ which has to be determined from Eqn. (5.17). Eqns. (5.22) and (5.17) have then to be solved simultaneously. We notice that Eqn. (5.17) can be rewritten in dimensionless form as

$$\tilde{T}_F^3 = 3\int_0^\infty dt\; \frac{t^2}{\exp(t - \tilde{\mu}_F) + 1} \;, \tag{5.23}$$

where we have introduced the reduced chemical potential $\tilde{\mu}_F = \mu_F/k_B T_c^0$ and the reduced Fermi temperature $\tilde{T}_F = T_F/T_c^0$. Eqn. (5.23) reveals that $\tilde{\mu}_F$ is only a function of $\tilde{T}_F$, which in turn is a measure of the degeneracy of the Fermi gas at $T = T_c^0$. In terms of $\tilde{\mu}_F$ and $\tilde{T}_F$ Eqn. (5.22) then becomes

$$\begin{aligned}\left(\frac{\delta T_c}{T_c^0}\right)_{BF} &= -\frac{4\pi g_{BF}}{3N_B}\frac{R_F^3}{(\lambda_{T_c^0}^B)^3(\lambda_{T_c^0}^F)^3 k_B T_c^0} \\ &\times \int ds\; s^2\, g_{1/2}(\exp\{-\tilde{T}_F\,\alpha\, s^2\}) \\ &\times \left[f_{3/2}(\exp\{\tilde{\mu}_F\}) - f_{3/2}(\exp\{\tilde{\mu}_F - \tilde{T}_F\, s^2\})\right] .\end{aligned} \tag{5.24}$$

In writing Eqn. (5.24), we have rescaled each integration coordinate by the appropriate Thomas-Fermi radius of the Fermion cloud $R_i' = (2\epsilon_F/m_F\omega_i'^2)^{1/2}$. We have then introduced the mean Fermi radius $R_F = (R_x' R_y' R_z')^{1/3}$ and named $\alpha = m_B\omega_B^2/m_F\omega_F^2$. Since $\tilde{\mu}_F$ depends only on $\tilde{T}_F$ through Eqn. (5.23), the integral in Eqn. (5.24) above depends only on the values of the two parameters $\tilde{T}_F$ and $\alpha$.

The system of Eqns. (5.24) and (5.23) for general $\tilde{T}_F$ and $\alpha$ can only be solved numerically, and later we shall present the full numerical results for some specific choices of the parameters. However, approximate analytical solutions exist in two limits: when $\tilde{T}_F \gg 1$ (i.e. $T_F \gg T_c^0$) where the Fermi gas is completely degenerate at $T = T_c^0$ (Fermi-Dirac regime), and when $\tilde{T}_F \ll 1$ (i.e. $T_F \ll T_c^0$) so that at $T_c^0$ Fermions behave as a classical thermal gas (Boltzmann regime).

In order to clarify the connection between the two limits and the general numerical solution, it is useful to further manipulate Eqn. (5.24). By explicitly evaluating the prefactor, it can be finally recast in the convenient form

$$\left(\frac{\delta T_c}{T_c^0}\right)_{BF} = -\frac{2^{5/3}}{3^{5/6}\pi\zeta(3)}\left(\frac{m_F}{m_B}+1\right)\,\frac{a_{BF}}{\ell_F}N_F^{1/6}\,\cdot F(\tilde{T}_F,\alpha)\;, \tag{5.25}$$

where

$$\begin{aligned} F(\tilde{T}_F,\alpha) &= \alpha^{3/2}\tilde{T}_F\int ds\; s^2\, g_{1/2}(\exp\{-\tilde{T}_F\,\alpha\, s^2\}) \\ &\times \left[f_{3/2}(\exp\{\tilde{\mu}_F\}) - f_{3/2}(\exp\{\tilde{\mu}_F - \tilde{T}_F\, s^2\})\right]\;, \end{aligned} \tag{5.26}$$

and $\ell_F = \sqrt{\hbar/m_F\omega_F}$ is the Fermionic oscillator length. Notice the formal analogy between Eqn. (5.25) and Eqn. (5.14) for the shift $(\delta T_c/T_c^0)_{BB}$ due to the Boson-Boson interactions alone.

Let us begin by considering the Thomas-Fermi limit ($\tilde{T}_F \gg 1$). In this limit, the chemical potential of the Fermions $\mu_F$ tends to the Fermi energy $\epsilon_F = k_B T_F$. Thus $\tilde{\mu}_F \simeq \tilde{T}_F \gg 1$. The limit of the Fermi functions in Eqn. (5.8) for $x \to \infty$ is $f_{3/2}(x) \approx 4(\ln x)^{3/2}/3\sqrt{\pi}$. This implies that the density profile of the Fermion cloud takes the well known Thomas-Fermi shape

$$n_F^0(\mathbf{r}) = n_F^0(0)\,\left[1 - (x/R'_x)^2 - (y/R'_y)^2 - (z/R'_z)^2\right]^{3/2}\;, \tag{5.27}$$

with $n_F^0(0) = (2\epsilon_F m_F/\hbar^2)^{3/2}/(6\pi^2)$, whenever the expression inside the square brackets is positive, and $n_F^0(\mathbf{r}) = 0$ otherwise.

The function $F(\tilde{T}_F,\alpha)$ then goes to the limiting form

$$\begin{aligned} F(\tilde{T}_F,\alpha) &\to \frac{4}{3\sqrt{\pi}}\,\alpha^{3/2}(\tilde{T}_F)^{5/2}\sum_{n=1}^{\infty}\frac{1}{n^{1/2}}\int_0^1 ds\, s^2 \\ &\times e^{-n\,\tilde{T}_F\alpha\, s^2}[1-(1-s^2)^{3/2}]\;. \end{aligned} \tag{5.28}$$

In the above expression, we have expanded the Bose function (5.7) as $g_{1/2}(x) = \sum_{n=1}^{\infty} x^n/n^{1/2}$, which is allowed since the argument $x$ is always smaller than 1 in the present situation. We cannot perform a similar expansion for the Fermi function since $\tilde{\mu}_F$ can take any positive or negative values. We obtained Eqn. (5.28) in the limit $\tilde{T}_F \gg 1$. Therefore, if $\alpha$ is not too small (so that $\tilde{T}_F\alpha \gg 1$ still holds), then, for every $n$ in the series, the exponential is non-vanishing only for values of $s \ll 1$, and we can adopt the expansion $1-(1-s^2)^{3/2} \simeq 3s^2/2$. The integral in Eqn. (5.28) becomes $\int_0^1 ds\, s^4\, e^{-n\,\tilde{T}_F\,\alpha\, s^2} \simeq 3\sqrt{\pi}/[8(n\,\tilde{T}_F\,\alpha)^{5/2}]$. Finally, therefore, $F(\tilde{T}_F,\alpha) \to 3\zeta(3)/4\alpha$ and the Thomas-Fermi prediction for the relative shift reads

$$\left(\frac{\delta T_c}{T_c^0}\right)_{BF} = -\frac{3^{1/6}}{2^{1/3}\pi}\left(\frac{m_F}{m_B}+1\right)\frac{m_F\omega_F^2}{m_B\omega_B^2}\,\frac{a_{BF}}{\ell_F}\,N_F^{1/6}\;, \tag{5.29}$$

where $3^{1/6}/(2^{1/3}\pi) \simeq 0.304$. We notice that in the Thomas-Fermi regime the shift is independent of the number of Bosons $N_B$ and varies as the first inverse power of the parameter $\alpha = m_B\omega_B^2/m_F\omega_F^2$.

We now consider the Boltzmann limit for the Fermi gas ($\tilde{T}_F \ll 1$). In this case, the chemical potential $\tilde{\mu}_F$ is large and negative and depends on $\tilde{T}_F$ as: $\tilde{\mu}_F \approx \ln\{(\tilde{T}_F)^3/6\}$. In the limit $x \to 0$, $f_{3/2}(x) \approx x$, and then

$$\begin{aligned} F(\tilde{T}_F,\alpha) \quad &\to \quad \frac{\alpha^{3/2}(\tilde{T}_F)^4}{6}\sum_{n=1}^{\infty}\frac{1}{n^{1/2}}\int_0^{\infty} ds\, s^2 \\ &\times \quad \left[e^{-n\tilde{T}_F\alpha s^2} - e^{-(n\tilde{T}_F\alpha+\tilde{T}_F)s^2}\right] . \end{aligned} \tag{5.30}$$

Evaluation of the integrals is straightforward and yields

$$F(\tilde{T}_F,\alpha) \to \frac{\sqrt{\pi}}{24}(\tilde{T}_F)^{5/2}\cdot f(\alpha) , \tag{5.31}$$

with

$$f(\alpha) = \sum_{n=1}^{\infty}\left(\frac{1}{n^2} - \frac{1}{n^{1/2}(n+\alpha^{-1})^{3/2}}\right) , \tag{5.32}$$

so that:

$$\left(\frac{\delta T_c}{T_c^0}\right)_{BF} = -\frac{1}{2^{4/3}\pi^{1/2}3^{11/6}\zeta(3)}\left(\frac{m_F}{m_B}+1\right)\frac{a_{BF}}{\ell_F}\,N_F^{1/6}(\tilde{T}_F)^{5/2}\cdot f(\alpha) , \tag{5.33}$$

where the numerical prefactor is $\simeq 0.025$.

We notice that $f(\alpha)$ in Eqn. (5.32) is a monotonically decreasing function of $\alpha$. In particular, one finds the following behaviors: $f(\alpha \to 0) = \pi^2/6$, $f(1) \simeq 0.85$, and $f(\alpha \to \infty) = 3\zeta(3)/2\alpha$. As one should expect, in the Boltzmann limit ($\tilde{T}_F \ll 1$), the Bose-Fermi shift is negligible.

We now turn to the full numerical solution of Eqns. (5.25), (5.26), and (5.23) for more general values of the degeneracy parameter $\tilde{T}_F$. In Fig. 5.1, we show the dimensionless function $F(\tilde{T}_F,\alpha)$ as a function of $\tilde{T}_F$ for three different values of the parameter $\alpha = m_B\omega_B^2/m_F\omega_F^2$, $\alpha = 0.1$, 1, and 10. For fixed $\alpha$, $F(\tilde{T}_F,\alpha)$ is a monotonically non-decreasing function of $\tilde{T}_F$, which saturates for $\tilde{T}_F \to \infty$ at the value predicted in the Thomas-Fermi regime $3\zeta(3)/4\alpha \simeq 0.9\ \alpha^{-1}$. For fixed $\tilde{T}_F$, $F(\tilde{T}_F,\alpha)$ increases by decreasing $\alpha$. For the largest value of $\alpha$ ($\alpha = 10$) the function $F$ reaches its asymptotic Thomas-Fermi value already at $\tilde{T}_F \simeq 5$. For $\alpha = 1$ and $\alpha = 0.1$ the function saturates for larger values of $\tilde{T}_F$ not shown in the figure. The reason for this difference can be understood by recalling that the Thomas-Fermi result requires not only $\tilde{T}_F \gg 1$, but also $\tilde{T}_F \gg \alpha^{-1}$ (see the discussion below Eqn. (5.28)).

The physically relevant regimes in current experiments fall roughly around $\alpha \simeq 1$ and $\tilde{T}_F \simeq 1$. In this respect, a particularly interesting situation is the one realized in the Florence experiment [23], where a quantum degenerate trapped atomic mixture of Fermionic $^{40}$K and Bosonic $^{87}$Rb has been recently produced. One of the appealing features of this system is that the measured Boson-Fermion scattering length is large and negative: $a_{BF} = -22$ nm, giving rise to a fairly strong attractive Boson-Fermion interaction. The shift $\left(\delta T_c/T_c^0\right)_{BF}$ is thus positive and opposite to the shift $\left(\delta T_c/T_c^0\right)_{BB}$, since for pure $^{87}$Rb the Boson-Boson scattering length is $a_{BB} = 6$ nm, giving rise to a repulsive Boson-Boson interaction. In the Florence experiment, the two atomic species are magnetically trapped, and are both prepared in their doubly polarized spin state. These states experience the same trapping potential so that $\alpha = m_B\omega_B^2/m_F\omega_F^2 = 1$, while the

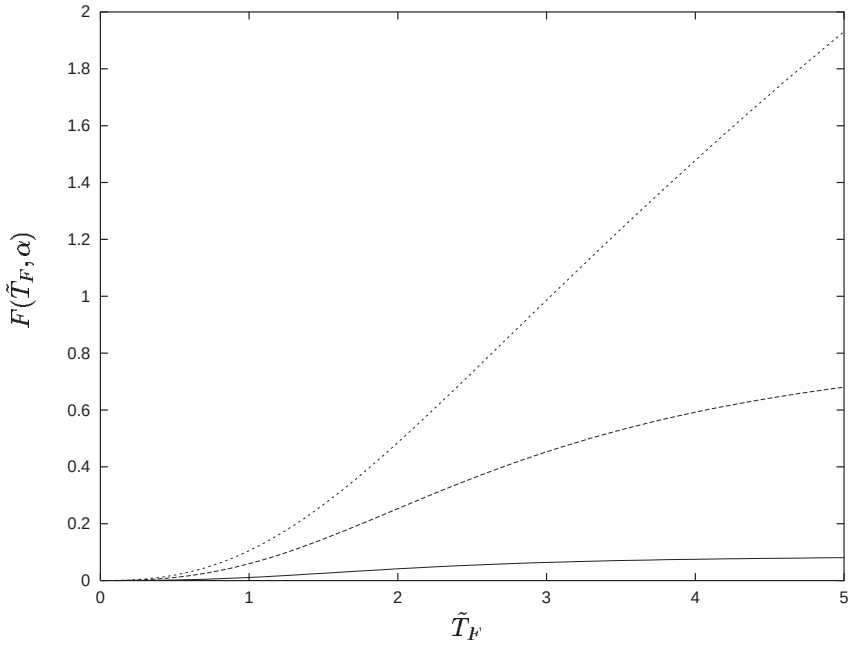


Figure 5.1: Dimensionless function $F(\tilde{T}_F, \alpha)$ as a function of $\tilde{T}_F$ for the values $\alpha = 0.1$ (dotted line), $\alpha = 1.0$ (dashed line), and $\alpha = 10$ (solid line).

number of Bosons and of Fermions are respectively $N_B = 2 \times 10^4$, $N_F = 10^4$, so that $N_F/N_B = 0.5$, and $\tilde{T}_F = T_F/T_c^0 \simeq 2.3$. For the conditions of the Florence experiment the shift (5.14) due to the Boson-Boson coupling turns out to be: $\left(\delta T_c/T_c^0\right)_{BB} \simeq -0.037$, and is comparable with the shift (5.13) due to finite size effects, which is given by: $\left(\delta T_c/T_c^0\right)_{fs} = -0.044$. For $\alpha = 1$ at $\tilde{T}_F \simeq 2.3$, the function $F$ is at about 1/3 of its asymptotic value in the Thomas-Fermi regime, resulting in a Bose-Fermi shift considerably smaller than the Bose-Bose one: $\left(\delta T_c/T_c^0\right)_{BF} \simeq 0.012$. In Fig. 2 we show the shift $\left(\delta T_c/T_c^0\right)_{BF}$ as a function of the ratio $N_F/N_B$, with all the other parameters entering Eqn. (5.25) fixed at the values of the Florence experiment [23]. In the same figure, we include as a reference value the modulus of the Boson-Boson relative shift $|\left(\delta T_c/T_c^0\right)_{BB}|$, calculated using the values of the parameters given by the Florence experiment.

From Fig. 5.2, we see that, while in the present experimental situation the Boson-Fermion shift is about 1/3 of the Boson-Boson one, by increasing the number of trapped Fermions the two shifts become comparable at $N_F \simeq 5N_B$. The Boson-Fermion shift is instead dominant at still larger values of $N_F$. It is important to remark that, even if the Bose-Fermi shift of the critical temperature is a small effect for the present experimental conditions, it might be observable. Since the Fermions can be eliminated from the trap, one can look for the differences in the transition temperature with and without Fermions.

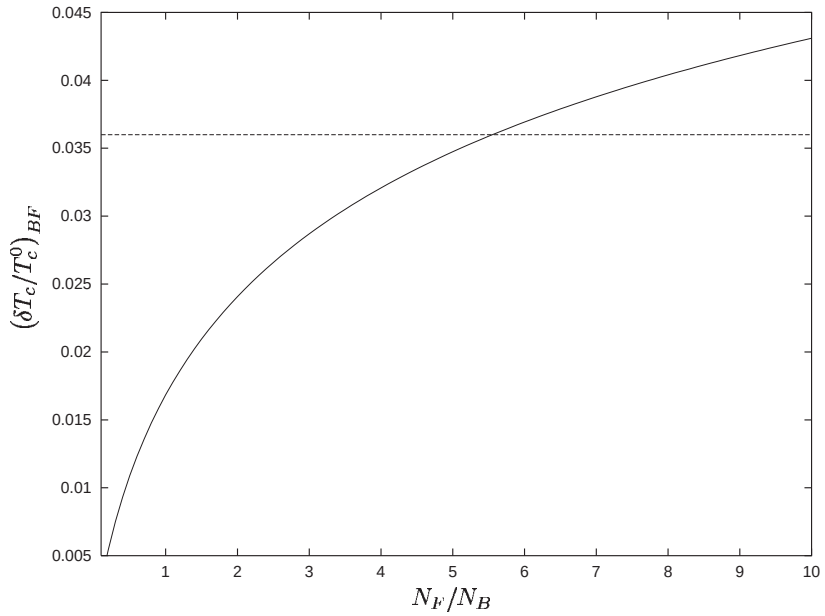


Figure 5.2: Boson-Fermion relative shift $\left(\delta T_c/T_c^0\right)_{BF}$ from Eqn. (5.25) (solid line) as a function of the ratio $N_F/N_B$. Horizontal dashed line: value of the modulus $|\left(\delta T_c/T_c^0\right)_{BB}|$ of the Boson-Boson shift (5.14). All other parameters, except the number of Fermions $N_F$, have been fixed at the values of the Florence experiment.

# Chapter 6

# Bose–Fermi Mixtures in optical lattices

## 6.1 Introduction to optical lattices

Recent spectacular progress in the manipulation of neutral atoms in optical lattices [106, 107, 108] has opened the way to the simulation of complex quantum systems of condensed matter physics, such as high–$T_c$ superconductors, Hall systems, and superfluid $^4$He, by means of atomic systems with perfectly controllable physical parameters [109]. Optical lattices are stable periodic arrays of microscopic potentials created by the standing waves of intersecting laser beams [110]. Atoms can be confined to different lattice sites, and by varying the strength of the periodic potential it is possible to tune the inter-atomic interactions with great precision. They can be enhanced well into regimes of strong correlation, even in the dilute limit. The transition to a strong coupling regime can be realized by increasing the depth of the lattice potential wells, a quantity that is directly proportional to the intensity of the laser light. This is an experimental parameter that can be controlled with great precision. For this reason, besides the fundamental interest for the investigation of quantum phase transitions [111] and other basic quantum phenomena [112, 113, 114, 87, 115, 116, 117], optical lattices have become an important practical tool for applications, ranging from laser cooling [118] to quantum control and information processing [119], and quantum computation [120, 121, 122, 123, 124, 125].

As compared to systems with no optical lattices that have been considered in the previous chapters, the new phases present in optical lattices are the superfluid phase and the Mott–insulating phase. In the former, the particles can easily hop from lattice site to lattice site and thus behave as a superfluid (SF). As the lattice strength is increased, tunneling is inhibited due to a larger potential barrier between the lattice sites. At some critical lattice strength, the particles are completely localized at a certain lattice site and tunneling is completely suppressed. This is the so-called Mott-insulator (MI) phase. The present chapter is concerned with the study of dilute mixtures of interacting Bosonic and Fermionic neutral atoms subject to an optical lattice and a superimposed trapping harmonic potential at zero temperature. Again, we assume the Fermions to be identical, so that there are only $s$–wave Boson–Boson and Fermion–Boson contact interactions present. Mixing vs. demixing phase transitions a nd phase transitions of the type SF–MI are investigated in this setting. Due to the approximations we use in the following we will not be able to describe phase transitions to the collapse regime that has been studied in previous chapters for continuous systems. In this case, the reader is

referred to future work.

The theory of Bosonic atoms in optical lattices has been developed [112] by assuming that the atoms are confined to the lowest Bloch band of the periodic potential. It can then be shown that the system is effectively described by a single–band Bose–Hubbard model Hamiltonian [126]. In such a model, the superfluid–insulator transition is predicted to occur when the on site Boson–Boson interaction energy becomes comparable to the hopping energy between adjacent lattice sites. This situation can be experimentally achieved by increasing the strength of the lattice potential, which results in a strong suppression of the kinetic (hopping) energy term. In this way, the superfluid–Mott-insulator quantum phase transition has been realized by loading an ultracold atomic Bose–Einstein condensate in an optical lattice [107]. The system of interacting Fermions in optical lattices was exactly solved in 1968 by Lieb and Wu [127] by means of a Bethe Ansatz. Since we treat the Fermions to be non-interacting the latter work has not so many implications to the work presented here, while we will often refer to methods uses for the Bosonic systems.

## 6.2 The Hubbard Hamiltonian

We start by introducing the Hamiltonian for a Bose–Fermi mixture loaded into optical lattice potentials and confined by additional, slowly varying, external (harmonic) trapping potentials. The Hamiltonian is similar to the one of chapter 4, only that now the external potentials are of the following form:

$$\hat{V}_B = \int d^3\mathbf{r}\hat{\Phi}^\dagger(\mathbf{r})\left(V_B(\mathbf{r}) + P_B(\mathbf{r})\right)\hat{\Phi}(\mathbf{r})\,, \tag{6.1}$$

$$\hat{V}_F = \int d^3\mathbf{r}\hat{\Psi}^\dagger(\mathbf{r})\left(V_F(\mathbf{r}) + P_F(\mathbf{r})\right)\hat{\Psi}(\mathbf{r})\,, \tag{6.2}$$

and are due to the magnetic trapping and standing laser waves. In the subsequent analysis, we will consider the harmonic approximation of a typical quadrupolar magnetic field with strong anisotropy in the transverse directions $y$ and $z$, i.e.,

$$V_B(\mathbf{r}) \simeq m_B\omega_B^2(x^2 + \lambda^2y^2 + \lambda^2z^2)/2\,, \tag{6.3}$$

and

$$V_F(\mathbf{r}) \simeq m_F\omega_F^2(x^2 + \lambda^2y^2 + \lambda^2z^2)/2\,, \tag{6.4}$$

where $\lambda \gg 1$ is the anisotropy parameter. Moreover, if we assume trapping in the same magnetic state for the Bosons and the Fermions, then the trapping frequencies are related according to $\omega_F/\omega_B = (m_B/m_F)^{1/2}$, so that the two potentials coincide: $V_B(\mathbf{r}) = V_F(\mathbf{r})$. The ground–state harmonic oscillator lengths, however, are different due to the different masses, and also differ for the $x$-direction on the one hand and the $y$ and $z$-directions on the other hand:

$$\ell^{\parallel}_{B/F} = \sqrt{\hbar/(m_{B/F}\omega_{B/F})} \tag{6.5}$$

in the $x$ direction, and $\ell^{\perp}_{B/F} = \ell^{\parallel}_{B/F}/\sqrt{\lambda}$ in the $y$ and $z$ directions. We next consider a lattice structure for the Bosons and the Fermions in the $x$–direction, associated to the corresponding Bosonic and Fermionic one–dimensional optical lattice potentials $P_B(x)$ and $P_F(x)$ are

$$\begin{aligned} P_B(x) &= V_B^0\sin^2(\pi x/a)\,, \\ P_F(x) &= V_F^0\sin^2(\pi x/a)\,, \end{aligned} \tag{6.6}$$

where $a$ is the lattice spacing associated to the frequency $\omega_L = \pi c/a$ of the laser light with $c$ being the speed of light. The optical potentials are due to the AC Stark shift and their strengths are [9]

$$V^0_{B/F} \approx \frac{6\pi c^2}{\omega^3_{B/F}} \frac{\Gamma_{B/F} I}{\omega_L - \omega_{B/F}}, \tag{6.7}$$

where the intensity at the maximum of the standing wave is four times the intensity $I$ of a laser beam. Usually the natural width $\Gamma_{B/F}$ and the atomic frequencies $\omega_{B/F}$ differ only slightly. If the lattice potentials are produced by a far off–resonant laser for both species, then also the ration of the two detuning frequencies $\omega_L - \omega_{B/F}$ is close to one and we can approximate that the lattice potential strengths are equal for both Fermions and Bosons: $V^0_F = V^0_B = V_0$, and the two optical lattices coincide. This is the situation we will always consider in the following.

In the presence of a strong optical lattice and a sufficiently shallow external confinement, to incorporate the localization of the particles at the lattice sites, one can choose a different expansion of the field operators as before (cf. Eqns. (2.27) and (2.28)), namely in terms of the so-called Wannier functions. We write:

$$\hat{\Phi}(\mathbf{r}) = \sum_{i,j} \hat{a}_{ij} w^B_j(\mathbf{r} - \mathbf{r}_i), \tag{6.8}$$

$$\hat{\Psi}(\mathbf{r}) = \sum_{i,j} \hat{b}_{ij} w^F_j(\mathbf{r} - \mathbf{r}_i)\,, \tag{6.9}$$

where the Wannier functions are defined as the eigenfunctions of the "local single-particle Hamilton operators":

$$\left[\frac{\hbar^2\nabla^2}{2m_{B/F}} + P_{B/F}(\mathbf{r}) + V_{B/F}(\mathbf{r})\right] w^{B/F}_j(\mathbf{r} - \mathbf{r}_i) = E^{B/F}_{i,j} w^{B/F}_j(\mathbf{r} - \mathbf{r}_i), \tag{6.10}$$

with the boundary conditions that the Wannier functions $w^{B/F}_j(\mathbf{r} - \mathbf{r}_i)$ are strongly localized at $\mathbf{r}_i$. Then $i$ is the site index, the points $x_i = ia$ indicate the minima of the lattice potential, and the index $i$ runs on positive and negative integers, the origin of the lattice being fixed at $i = 0$ so that it coincides with the center (the minimum) of the external trapping potential. $j$ is the so-called band index. We agree that $j$ is defined in such a way that $E^{B/F}_{i,j}$ grows with $j$. In writing the above expansion we have already assumed that the $E^{B/F}_{i,j}$ depends on the lattice site only by and additive constant of $m_{B/F}\omega^2_{B/F}x^2_i/2$ and $w^{B/F}_j(\mathbf{r} - \mathbf{r}_i)$ only by a shift of the origin. This assumption is satisfied if the external potential can be assumed to be constant between two neighboring lattice sites which is the case if the trapping potentials are very shallow in the lattice direction. This is again a sort of local density approximation, and we comment on it later in more detail. To further simplify we retain only the lowest band $j = 0$ at each site. This way the Wannier basis is by no means complete anymore and the restricted Hilbert space that is spanned by the lowest band Wannier functions is much smaller than the full Hilbert space. We assume, however, that the ground state of the system is contained in the restricted Hilbert space, which is assured if the excitation energies $E^{B/F}_j - E^{B/F}_0$ are larger that the typical on-site interaction energies. We also discuss the implications of this condition on our model below. To simplify even more we use the observation that if the Wannier functions are very much localized at a site $\mathbf{r}_i = (x_i, y, z)$ only the behavior of the potential in Eqn. (6.10) very close to the point $\mathbf{r}_i$ is relevant and thus it is sufficient to expand the potential to second order in $\mathbf{r} - \mathbf{r}_i$. We than have a harmonic potential

also in the $x$-direction and the lowest band Wannier functions factorize into Gaussian states:

$$w_j^{B/F}(\mathbf{r}-\mathbf{r}_i) = w_x^{B/F}(x-x_i)w_y^{B/F}(y)w_z^{B/F}(z), \tag{6.11}$$

where

$$w_y^{B/F}(y) = \frac{\exp\left[-y^2/2(\ell_{B/F}^{\perp})^2\right]}{\pi^{1/4}(\ell_{B/F}^{\perp})^{1/2}}, \tag{6.12}$$

$$w_z^{B/F}(z) = \frac{\exp\left[-z^2/2(\ell_{B/F}^{\perp})^2\right]}{\pi^{1/4}(\ell_{B/F}^{\perp})^{1/2}}, \tag{6.13}$$

and

$$w_x^{B/F}(x-x_i) = \frac{\exp\left[-(x-x_i)^2/2(\ell_{B/F}^{0})^2\right]}{\pi^{1/4}(\ell_{B/F}^{0})^{1/2}}, \tag{6.14}$$

where

$$\ell_{B/F}^{0} = a/[\pi(V_0/E_{B/F}^{R})^{1/4}], \tag{6.15}$$

is the width of the harmonic oscillator potential wells at each lattice site, with $E_B^R = (\pi\hbar)^2/2a^2m_B$ and $E_F^R = (\pi\hbar)^2/2a^2m_F$ being the Boson and Fermion recoil energies, respectively. In principle, one could even solve the so–called $1-D$ Matthieu equation which results from Eqn. (6.10) in the $x$-direction without the harmonic expansion of the potentials. This is, however, somewhat cumbersome and in the following we will work in the Gaussian approximation. The single–band expansions of the field operators in terms these functions now read:

$$\hat{\Phi}(\mathbf{r}) = \sum_i \hat{a}_i w_x^B(x-x_i)w_y^B(y)w_z^B(z), \tag{6.16}$$

$$\hat{\Psi}(\mathbf{r}) = \sum_i \hat{b}_i w_x^F(x-x_i)w_y^F(y)w_z^F(z), \tag{6.17}$$

where $\hat{a}_i$ and $\hat{b}_i$ are, respectively, the Bosonic and Fermionic annihilation operators of the harmonic ground state at the $i$–th lattice site.

As already mentioned, we will consider the physical situation of very shallow trapping potentials in $x$-direction, such that $\ell_{B/F}^{\parallel} \gg aN_{B/F}$ and consequently local density approximation can be applied in the study of the ground–state properties of the system. Therefore, when exploiting the Wannier function expansions (6.16) and (6.17) to map the full Hamiltonian (4.1) into its lattice version, we discard all terms that are of order $(aN_{B/F}/\ell_{B/F}^{\parallel})^2$ or of higher powers of it, which appear due to the fact that the Wannier functions localized at adjacent lattice are not exactly orthogonal. Otherwise, nonlocal effects caused by the trapping potential, like site–dependent hopping terms, have to be considered.

In this physical setting, the Wannier function expansions (6.16) and (6.17) map the full Hamiltonian (4.1) into the following Hubbard type Hamiltonian:

$$\hat{H} = -\frac{1}{2}\sum_i \left(J_B\hat{a}_{i+1}^{\dagger}\hat{a}_i + J_F\hat{b}_{i+1}^{\dagger}\hat{b}_i + \text{H. c.}\right)$$

$$
\begin{aligned}
&+ \quad \frac{U_{BB}}{2}\sum_i \hat{n}_B^{(i)}(\hat{n}_B^{(i)}-1) + U_{BF}\sum_i \hat{n}_B^{(i)}\hat{n}_F^{(i)} \\
&+ \quad \sum_i V_B^{(i)}\hat{n}_B^{(i)} + \sum_i V_F^{(i)}\hat{n}_F^{(i)} \\
&+ \quad \hbar\left(\lambda\omega_B + \omega_B^0/2\right)\hat{N}_B + \hbar\left(\lambda\omega_F + \omega_F^0/2\right)\hat{N}_F \ . \qquad (6.18)
\end{aligned}
$$

The first line in the above Bose–Fermi Hubbard Hamiltonian describes independent nearest–neighbor hopping of Bosons and Fermions, with amplitudes $J_B$ and $J_F$, respectively. The terms in the second line describe Boson–Boson on site repulsion (with $U_{BB} > 0$) and Boson–Fermion on site interaction. This interaction can be repulsive or attractive, depending on the sign of $U_{BF}$. The third line describes the energy offset at each lattice site due to the $x$ component of the external trapping potentials $V_{B/F}(\mathbf{r})$, and the last line contains the overall constant zero–point energy terms due to the $y$ and $z$ components of $V_{B/F}(\mathbf{r})$ and to the lattice potential $P(x)$. The on site interaction and offset energy terms are simple functions of the on site Boson and Fermion occupation number operators $\hat{n}_B^{(i)} = \hat{a}_i^\dagger\hat{a}_i$ and $\hat{n}_F^{(i)} = \hat{b}_i^\dagger\hat{b}_i$, while the zero–point energy terms are proportional to the total particle number operators $\hat{N}_B = \sum_i \hat{a}_i^\dagger\hat{a}_i$ and $\hat{N}_F = \sum_i \hat{b}_i^\dagger\hat{b}_i$. The frequency

$$
\omega_{B/F}^0 = \hbar/[(\ell_{B/F}^0)^2 m_{B/F}] \qquad (6.19)
$$

fixes the Bosonic and Fermionic harmonic oscillations in each lattice well. The relevant parameters entering in the Hamiltonian are the on site values of the trapping harmonic potential

$$
V_{B/F}^{(i)} \quad = \quad \frac{m_{B/F}}{2}\omega_{B/F}^2 x_i^2 \ , \qquad (6.20)
$$

the nearest–neighbor hopping amplitudes between adjacent sites $x_i$ and $x_{i+1}$ for Bosons and Fermions

$$
\begin{aligned}
J_{B/F} \quad &= \quad \int dx\, w_x^{B/F}(x-x_i)\left[-\frac{\hbar^2}{2m_{B/F}}\frac{d^2}{dx^2}\right. \\
&+ \quad \left. V_0\sin^2\left(\pi\frac{x}{a}\right)\right] w_x^{B/F}(x-x_{i+1}) \ , \qquad (6.21)
\end{aligned}
$$

the strength of the on site repulsion energy between two Bosonic atoms at the same lattice site

$$
\begin{aligned}
U_{BB} \quad &= \quad \frac{4\pi\hbar^2 a_{BB}}{m_B}\int dx\, (w_x^B(x-x_i))^4 \\
&\times \quad \int dy\, (w_y^B(y))^4 \int dz\, (w_z^B(z))^4 \ , \qquad (6.22)
\end{aligned}
$$

and the strength of the on site interaction energy (either repulsive or attractive) between a Bosonic and a Fermionic atom at the same lattice site

$$
\begin{aligned}
U_{BF} \quad &= \quad \frac{2\pi\hbar^2 a_{BF}}{m}\int dx\left[w_x^B(x-x_i)w_x^F(x-x_i)\right]^2 \qquad (6.23) \\
&\times \quad \int dy\left[w_y^B(y)w_y^F(y)\right]^2 \int dz\left[w_z^B(z)w_z^F(z)\right]^2 \ .
\end{aligned}
$$

In typical situations, we may neglect next–to–nearest neighbor hopping amplitudes and nearest–neighbor interaction couplings that are usually some orders of magnitude smaller,

so that the Hamiltonian (6.18) provides a rather accurate model for the dynamics of a Bose–Fermi mixture with three–dimensional scattering in a one–dimensional periodic potential. Terms involving nearest–neighbor interaction strengths and/or next–to–nearest neighbor hopping amplitudes can become relevant and need to be included, e.g., when considering phonon exchange between Fermions, and this would lead to a Bose–Fermi analog of the so–called extended Hubbard models. To evaluate estimates for the parameters entering the Bose–Fermi Hubbard Hamiltonian (6.18) using Eqns. (6.12),(6.13) and (6.14), we will set the Boson recoil energy $E_B^R = \hbar^2\pi^2/(2m_B a^2)$ as the unit of energy. We then introduce the dimensionless quantity $\tilde{V}_0 = V_0/E_B^R$, and, analogously, the dimensionless quantities $\tilde{U}_{BB}$, $\tilde{U}_{BF}$, $\tilde{V}_B^{(i)}$, $\tilde{V}_F^{(i)}$, $\tilde{J}_B$, and $\tilde{J}_F$. We then have

$$\tilde{U}_{BB} = \sqrt{\frac{8}{\pi^3}}\,\frac{a_{BB}\,a}{(\ell_B^\perp)^2}\,\tilde{V}_0^{1/4}\,, \tag{6.24}$$

$$\tilde{U}_{BF} = \sqrt{\frac{8}{\pi^3}}\left(1+\frac{m_B}{m_F}\right)\frac{a_{BF}\,a}{(\ell_B^\perp)^2+(\ell_F^\perp)^2}\tilde{V}_0^{1/4}\,, \tag{6.25}$$

$$\tilde{V}_B^{(i)} = \frac{i^2}{\pi^2(\ell_B^\parallel/a)^4}, \quad \tilde{V}_F^{(i)} = \frac{m_B}{m_F}\,\frac{i^2}{\pi^2(\ell_F^\parallel/a)^4}\,, \tag{6.26}$$

$$\tilde{J}_B = \left(\frac{\pi^2}{4}-1\right)\tilde{V}_0\exp\left[-\frac{\pi^2}{4}\sqrt{\tilde{V}_0}\right], \tag{6.27}$$

$$\tilde{J}_F = \left(\frac{\pi^2}{4}-1\right)\tilde{V}_0\exp\left[-\frac{\pi^2}{4}\sqrt{\frac{m_F}{m_B}\tilde{V}_0}\right]. \tag{6.28}$$

In Fig. 6.1 we show the dependencies of the these parameters on the potential strength $\tilde{V}_0$ (compare also Ref. [125]). For reference we have included as well the overlap integral $\langle w(x-x_i)|w(x-x_{i+1})\rangle$ of adjacent Wannier functions. The overlap is negligible but for very small values of the potential strength, confirming that terms of the order of the overlap integral can be neglected in the Hamiltonian. The Gaussian approximation holds rather well as can be seen by comparing the associated Bosonic hopping amplitude $J_B$ with the one obtained by using the exact 1–$D$ Mathieu equation [117].

Besides the conditions mentioned earlier, all the expressions derived in the present section are justified under the following circumstances: First of all, we must require that the two–body scattering processes are not influenced by the confinements, a condition that is guaranteed if the lengths of the confining and lattice potentials in all directions are much larger than the Boson–Boson and Fermion–Boson scattering lengths. Next, the single–band structure of the lattice Hamiltonian is assured if the lattice spacing $a$ is much greater than the harmonic confinements in each direction at all lattice sites. On the other hand, in this limit the harmonic approximation for the Wannier functions at each lattice well is automatically satisfied. Finally, as mentioned earlier, the assumption of a slowly varying confining potential such that LDA is applicable leads to the condition $\ell_{B/F}^\parallel \gg aN_{B/F}$. We can summarize all the above conditions with the following chain of inequalities:

$$\{|a_{BF}|, a_{BB}\} \ll \{\ell_{B/F}^0, \ell_{B/F}^\perp\} \ll a \ll \ell_{B/F}^\parallel/N_{B/F}\,. \tag{6.29}$$

Our model is for some aspects unrealistic, since in present experimental situations the transverse confinements cannot be made very strong. Therefore a multi–band structure can appear with several radial states being occupied, as reported in a recent experiment by the Florence group on Bose–Fermi mixtures in a 1–$D$ optical lattice [128].

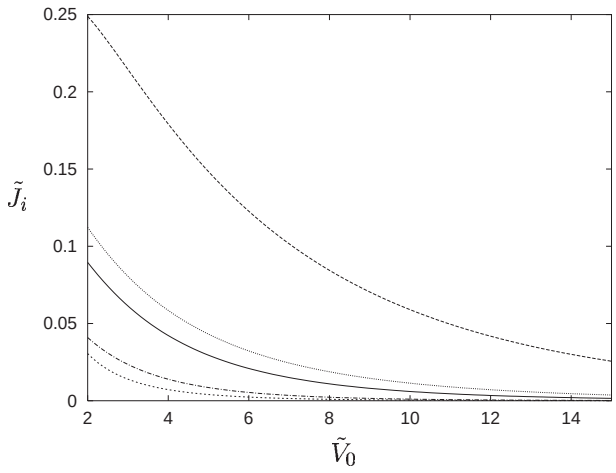


Figure 6.1: Top to bottom: the Fermion hopping amplitude $\tilde{J}_F$ for $m_F/m_B = 0.5$ (dashed line); the Boson hopping amplitude $\tilde{J}_B$ (solid line); the Fermion hopping amplitude for $m_F/m_B = 1.5$ (dotted–dashed line); and, for comparison, the overlap integral $\langle w(x - x_i)|w(x - x_{i+1})\rangle$ of adjacent Wannier functions (dotted line).

## 6.3 Phase stability and the superfluid transition

In this section, we investigate the zero temperature ground state properties of the system in a mean field approximation. For convenience, we will adopt a grand-canonical description through the Hamiltonian

$$\hat{K} = \hat{H} - \mu_B \hat{N}_B - \mu_F \hat{N}_F \,, \tag{6.30}$$

where $\mu_B$ and $\mu_F$ are the Bosonic and Fermionic chemical potentials. According to the Hohenberg–Kohn theorem, the ground state energy

$$E = \langle \Psi_0 | \hat{K} | \Psi_0 \rangle \tag{6.31}$$

is a functional of the on site Bosonic and Fermionic densities $n_B^{(i)} = \langle \hat{a}_i^\dagger \hat{a}_i \rangle$ and $n_F^{(i)} = \langle \hat{b}_i^\dagger \hat{b}_i \rangle$, where the expectation values are taken with respect to the ground state with state vector $|\Psi_0\rangle$. We decompose the functional $E$ according to

$$E = E_B + E_F + E_{BF} - \mu_B \sum_i n_B^{(i)} - \mu_F \sum_i n_F^{(i)} \,, \tag{6.32}$$

where $E_B$ is the energy contribution depending only on the Boson parameters $J_B$, $U_{BB}$, $V_B^{(i)}$; $E_F$ is the energy depending only on the Fermion parameters; and $E_{BF}$ is the term due to the Boson–Fermion interaction. We treat this latter term in mean field approximation: neglecting exchange–correlation effects:

$$E_{BF} = U_{BF} \sum_i n_B^{(i)} n_F^{(i)} \,. \tag{6.33}$$

Exchang–correlation effects have been recently studied for the case of homogeneous mixtures in the continuum (see chapter 3 and Ref. [88]). For the Fermion energy $E_F$, we

take the energy of the noninteracting homogeneous system and exploit LDA on it,

$$E_F = -\frac{2J_F}{\pi}\sum_i \sin(\pi n_F^{(i)}) + \sum_i V_F^{(i)} n_F^{(i)} \ . \tag{6.34}$$

This approximate description of the Fermions is well justified in the presence of a slowly varying trapping potential (so that LDA can be applied), when there are no direct interactions among the Fermions (as in our case), and moreover when one can neglect induced phonon–mediated self–interactions due to the presence of the Bosons. Therefore, in this situation, the nontrivial features of different quantum phases will regard only the Bosonic sector and not the Fermionic one. However, the presence of the Fermions will indirectly contribute to the properties of the different Bosonic phases, and this is the subject that we will study in the following.

In order to find an expression for the Boson energy $E_B$, we will proceed in steps of increasing accuracy. First we perform a very simple mean field analysis in two extreme limits: a completely superfluid Boson ground state and a totally Mott–insulating Boson ground state. In the latter case, we will provide a simple criterion for stability of the mixture against demixing. Next, we will perform a perturbation expansion around the Mott–insulating Boson ground state to recover perturbatively the phase boundary against transition to superfluidity. Finally, in the next section, we will study the ground state properties of the mixture using a Gutzwiller Ansatz for the Bosons capable of describing the intermediate regimes between the insulating and superfluid Bosonic phases.

We first consider the Bosons to be superfluid. In this regime, the chemical potential and the number of particles in a homogeneous system of pure Bosons are related, to lowest order in $U_{BB}$, via [129]:

$$\mu_B = U_{BB} n_0 - 2J_B \ , \tag{6.35}$$

where $n_0$ is the density of condensed Bosons. Additionally, for very weak interaction $n_0 \approx n_B$. Exploiting this result in LDA and using the mean field expression for the Bose–Fermi interaction energy we can then write for the inhomogeneous Bose–Fermi mixture at a given lattice site:

$$U_{BB} n_B^{(i)} = \mu_B + 2J_B - V_B^{(i)} - U_{BF} n_F^{(i)} \ . \tag{6.36}$$

Next, we consider the case of a Mott–insulating Bosonic phase. To lowest order in $J_B$ we neglect the kinetic term altogether. Then it is easily shown that the relation between the Bosonic chemical potential and the Bosonic density for a homogeneous system of pure Bosons is given by

$$\mu_B = U_{BB} n_B - U_{BB}/2 \ . \tag{6.37}$$

By the same strategy as before, we have in the inhomogeneous case at a given lattice site:

$$U_{BB} n_B^{(i)} = \mu_B + U_{BB}/2 - V_B^{(i)} - U_{BF} n_F^{(i)} \ . \tag{6.38}$$

Comparing Eqns. (6.36) and (6.38), we observe the same behavior of the on site density profiles but for a constant correction to the Boson chemical potential depending whether the Bosons are in a superfluid or in a Mott–insulating state. Finally, differentiating the energy functional with respect to the on site populations of the Fermions, we determine the associated density field and the set of coupled equations describing the ground state of the mixture at any lattice site,

$$U_{BB} n_B^{(i)} \quad = \quad \mu_B' - V_B^{(i)} - U_{BF} n_F^{(i)}, \tag{6.39}$$

$$-2J_F \cos(\pi n_F^{(i)}) \quad = \quad \mu_F - V_F^{(i)} - U_{BF} n_B^{(i)}, \tag{6.40}$$

where $\mu'_B$ is the proper expression of the Boson chemical potential according to whether the Bosons are in the Mott–insulating or superfluid regime. These equations are valid at a given lattice site $i$ if $\mu'_B - V_B^{(i)} - U_{BF} n_F^{(i)} > 0$, otherwise one must set $n_B^{(i)} = 0$. On the other hand, if

$$(\mu_F - V_F^{(i)} - U_{BF} n_B^{(i)})/2J_F < 0 \tag{6.41}$$

we must impose $n_F^{(i)} = 0$ at the given lattice site, while $n_F^{(i)} = 1$ must be imposed when $(\mu_F - V_F^{(i)} - U_{BF} n_B^{(i)})/2J_F > 1$. These expressions are the lattice analogs of the Thomas–Fermi description of Boson–Fermion mixtures in the continuum. We remark that in the Mott–insulating regime the Boson on site populations $n_B^{(i)}$ must be rounded off to the integer closest to the solutions of Eqns. (6.39)–(6.40).

In the Mott–insulating regime, we can determine a criterion of linear stability against phase separation of the two species if we expand the energy functional $E$ to second order in the small density variations $\delta n_{B/F}^{(i)}$ around the minimum provided by the solution of Eqns. (6.39)–(6.40):

$$\begin{aligned} \delta^2 E \quad = \quad & \frac{1}{2} \sum_i \begin{pmatrix} \delta n_B^{(i)} \\ \delta n_F^{(i)} \end{pmatrix} \cdot \left[ \begin{pmatrix} U_{BB} & U_{BF} \\ U_{BF} & 2\pi J_F \sin(\pi n_F^{(i)}) \end{pmatrix} \right. \\ & \left. \times \begin{pmatrix} \delta n_B^{(i)} \\ \delta n_F^{(i)} \end{pmatrix} \right] . \end{aligned} \tag{6.42}$$

This quadratic form is positive at a given site $i$ if and only if

$$2\pi J_F \sin(\pi n_F^{(i)}) U_{BB} > U_{BF}^2 \tag{6.43}$$

and $2\pi J_F \sin(\pi n_F^{(i)}) + U_{BB} \geq 0$. This last condition is always satisfied for $U_{BB} > 0$ and identical Fermions. If this is not the case for every site $i$, then the ground state is not stable against demixing. This result is similar to that recently obtained for a mixture of two different Boson species on a lattice [130], which states that the mixture is stable if $U_1 U_2 > U_{12}^2$, where $U_1$ and $U_2$ are the Boson–Boson interaction strengths of species 1 and 2 respectively, and $U_{12}$ is the interspecies coupling. The form of expression (6.43) then suggests that the Pauli on site energy $2\pi J_F \sin(\pi n_F^{(i)})$ has the meaning of a density–dependent interaction strength. A similar correspondence was previously pointed out for homogeneous Bose–Fermi mixtures in the continuum [36].

Introducing a perturbation expansion with respect to $J_B$ around the Mott–insulating ground state we can recover the zero–temperature phase transition to the superfluid phase. The reverse, i.e. to build a perturbative expansion in powers of $U_{BB}$ around the superfluid ground state fails to describe the transition to a Mott insulator, as pointed out in Ref. [129] for the pure Bose case. We follow the procedure adopted in Ref. [130] for the two–component Boson mixture, with the due modifications for the present case of a Boson–Fermion mixture, by treating the Bosonic kinetic (hopping) term as the perturbation with respect to the Bosonic Mott–insulating ground state. This scheme was first introduced for one–component Bose systems in Refs. [129, 131, 132]. We proceed by expanding the ground state energy with respect to the (local) Bosonic superfluid parameter $\psi^{(i)} = \langle \hat{a}_i \rangle$, which we assume to be real. A mean–field prescription of the Bosonic hopping energy in terms of the superfluid parameter reads

$$\hat{T}_B \quad = \quad -\frac{1}{2} J_B \sum_i \hat{a}_{i+1}^\dagger \hat{a}_i + \text{H. c.}$$

$$\approx \quad -\frac{1}{2}J_B\sum_i \psi^{(i+1)}\hat{a}_i + \hat{a}^\dagger_{i+1}\psi^{(i)} - \psi^{(i+1)}\psi^{(i)} + \text{H. c.}. \tag{6.44}$$

This term is regarded as a perturbation to the other terms in Eqn. (6.18). The zeroth order energies $E^0(|m_B^{(i)}\rangle)$ in a Mott-insulting state $|m_B^{(i)}\rangle = \prod_i \frac{(\hat{a}_i^\dagger)^{m_B^{(i)}}}{\sqrt{m_B^{(i)}!}}|0\rangle$ are simply found from Eqn. (6.38). Building up a perturbation series to second order in $J_B$ we have

$$E = E^0(|n_B^{(i)}\rangle) + \langle n_B^{(i)}|\hat{T}_B|n_B^{(i)}\rangle + \sum_{|m_B^{(i)}\rangle\neq|n_B^{(i)}\rangle} \frac{\left|\langle m_B^{(i)}|\hat{T}_B|n_B^{(i)}\rangle\right|^2}{E^0(|n_B^{(i)}\rangle) - E^0(|m_B^{(i)}\rangle)}, \tag{6.45}$$

where $|n_B^{(i)}\rangle$ is the (Mott–insulating) ground state. The first order term only stems from mean-fields in Eqn. (6.44) since the expectation values of the creation and destruction operators appearing in Eqn. (6.44) vanish in the Mott–insulating ground state. The second order term can only couple states to the ground state whose occupation number at a site $i$ differ from the ones of the ground state by one. After some algebra we get the seconder order expansion

$$\begin{aligned} E \quad = \quad & E^0(|n_B^{(i)}\rangle) + J_B\sum_i \psi^{(i+1)}\psi^{(i)} + 2J_B^2\sum_i \psi^{(i+1)}\psi^{(i)} \\ & \times\left[\frac{n_B^{(i)}}{-\mu_B + U_{BB}(n_B^{(i)}-1) + V_B^{(i)} + U_{BF}n_F^{(i)}}\right. \\ & \left.+\frac{n_B^{(i)}+1}{\mu_B - U_{BB}n_B^{(i)} - V_B^{(i)} - U_{BF}n_F^{(i)}}+\right] \end{aligned} \tag{6.46}$$

At the phase boundary between a Mott insulator (MI) and a superfluid (SF) the expansion coefficients of $\psi^{(i+1)}\psi^{(i)}$ must vanish so that the energy functional is differentiable (the phase transition is of second order). This yields the following criterion for the onset of the transition to the (local) SF state:

$$\begin{aligned} & U_{BB}(2n_B^{(i)}-1) - 2J_B \\ & - \left(U_{BB}^2 - 4U_{BB}^2(2n_B^{(i)}+1) + 4J_B^2\right)^{1/2} \\ & < \mu_B - V_B^{(i)} - U_{BF}n_F^{(i)} \\ & < U_{BB}(2n_B^{(i)}-1) - 2J_B \\ & + \left(U_{BB}^2 - 4U_{BB}^2(2n_B^{(i)}+1) + 4J_B^2\right)^{1/2}. \end{aligned} \tag{6.47}$$

The minimum value of $U_{BB}/J_B$, where a MI phase can exist, is given by the condition

$$U_{BB}/J_B = 4n_B^{(i)} + 2 + 2\sqrt{(2n_B^{(i)}+1)^2 - 1}\,, \tag{6.48}$$

and it involves the Fermionic sector indirectly through the dependence of $n_B^{(i)}$ on the Fermionic parameters and density distributions provided by Eqns. (6.39) – (6.40). Apart from this important modification, the phase diagram, at this level of approximation, is analogous to that of a one–component Bose system.

## 6.4 Number–conserving Gutzwiller Ansatz and numerical analysis

The simplest Ansatz for the Boson ground state being capable of describing both the SF and the MI phases is the Gutzwiller Ansatz, which contains the mean field approximations previously discussed as special cases. In contrast to the previous discussion, we assure particle number conservation exactly and not via the chemical potentials. The number–conserving Gutzwiller Ansatz consists of factorizing the amplitudes of superpositions of all possible states of sharp local particle numbers consistent with a fixed total number of Bosons $N_B$, in the following way [133]:

$$|\Psi\rangle_B \quad \longmapsto \quad \sum_{\sum_j n_j = N_B} \prod_i f_{n_i}^{(i)} \frac{(\hat{a}_i^\dagger)^{n_i}}{\sqrt{n_i!}} |0\rangle \ . \tag{6.49}$$

Using the Gutzwiller Ansatz in the determination of the energy functional, while keeping the same approximations previously introduced for the Boson–Fermion interaction and the Fermion energy, the total ground state energy reads

$$E = E_B + E_F + U_{BF} \sum_i n_B^{(i)} n_F^{(i)}, \tag{6.50}$$

where the subsidiary conditions ensuring particle number conservation are

$$\sum_i n_B^{(i)} = \sum_i \langle \hat{a}_i^\dagger \hat{a}_i \rangle = N_B, \tag{6.51}$$

$$\sum_i n_F^{(i)} = \sum_i \langle \hat{b}_i^\dagger \hat{b}_i \rangle = N_F. \tag{6.52}$$

The Boson energy contribution is now

$$\begin{aligned} E_B &= -\frac{1}{2} J_B \left( \sum_i \psi^{(i+1)} \psi^{(i)} + \text{C. c.} \right) \\ &+ \sum_i \left( \frac{U_{BB}}{2} (\sigma_B^{(i)} - n_B^{(i)}) + V_B^{(i)} n_B^{(i)} \right) \ , \end{aligned} \tag{6.53}$$

and the Bosonic observables are related to the Gutzwiller amplitudes by

$$n_B^{(i)} = \sum_{n=0}^{\infty} n (f_n^{(i)})^2, \tag{6.54}$$

$$\sigma_B^{(i)} = \langle \hat{a}_i^\dagger \hat{a}_i \hat{a}_i^\dagger \hat{a}_i \rangle = \sum_{n=0}^{\infty} n^2 (f_n^{(i)})^2, \tag{6.55}$$

$$\psi^{(i)} = \langle \hat{a}_i \rangle = \sum_{n=0}^{\infty} \sqrt{n+1} f_n^{(i)} f_{n+1}^{(i)} \ . \tag{6.56}$$

Moreover, we must impose the natural constraints that

$$\sum_{n=0}^{\infty} (f_n^{(i)})^2 = 1, \tag{6.57}$$

$$0 \leq n_F^{(i)} \leq 1, \tag{6.58}$$

for each lattice site $i$, reflecting the fact that the Gutzwiller amplitudes form a probability distribution for each lattice site, and that the on site Fermion occupation number cannot exceed one.

To identify the ground state amounts to solving a constrained optimization problem: one has to minimize the energy functional (6.53) subject to the constraints given by Eqns. (6.51) and (6.52), together with Eqns. (6.57) and (6.58).

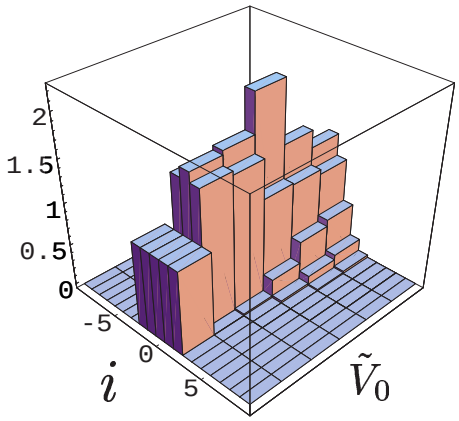


Figure 6.2: On site Bosonic densities for a Bose–Fermi repulsion $a_{BF} = 0.04$, as a function of the lattice potential strength. In this figure – as well as in the following figures – $\tilde{V}_0$ runs from 1 to 8.

We have solved the problem numerically for a small system of ten particles (five Bosons and five Fermions). The first observation is that the optimization problem is not a convex optimization problem. Hence, one has to expect several local, "poorer" extrema in addition to the (not necessarily unique) global one. The numerical solution of this optimization problem has been performed first using a simulated annealing method [134] with an appropriate logarithmic annealing schedule. The quadratic constraints (6.57) and (6.58) have been incorporated in a dynamical penalty formulation (see, e.g., Ref. [135]). Finally, for the local refinement the Nelder–Mead downhill simplex method [136] has been applied.

In Fig. 6.2 we show the change of the on site Bosonic densities with increasing lattice potential strength $\tilde{V}_0$ for a system of five Bosons and five Fermions with moderate repulsive Boson–Fermion interaction. We note from Fig. 6.2 that as the strength of the lattice potential increases the Bosons go in a complete Mott–insulating phase, forming a block crystalline configuration around the center of the trap (which coincides with the origin of the optical lattice) with exactly one Boson per lattice site. The corresponding on site Fermionic densities are plotted in Fig. 6.3. From both figures we can see that, if $U_{BF} > 0$, by increasing the lattice potential strength the system eventually undergoes simultaneously a Boson MI transition and complete phase separation, in accordance with Eqn. (6.43) along with Eqns. (6.24) – (6.28).

The local Bosonic superfluid parameter $\psi^{(i)}$ for the same physical situation is shown in Fig. 6.4. We can see a rather clear signature of the onset of a phase transition to a Mott–insulator regime when the superfluid parameter suddenly drops to very low values at a critical lattice potential strength $\tilde{V}_0^c \simeq 7$.

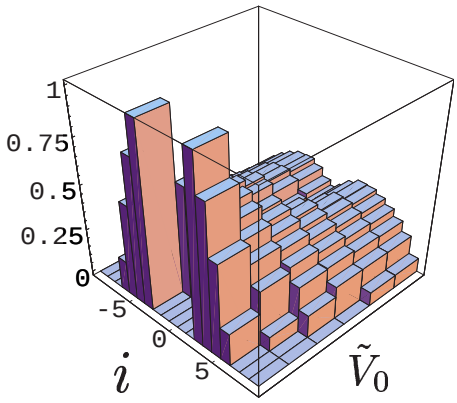


Figure 6.3: On site Fermionic densities for a Bose–Fermi repulsion $a_{BF} = 0.04$, as a function of the lattice potential strength.

We next consider the ground–state properties in the case of an attractive Boson–Fermion interaction. Because of the strong attraction with growing lattice strength, the Fermions follow the Bosons in building a sharp crystalline block around the center of the trap, as can be seen from Figs. 6.5 and 6.6. We cannot expect in this case to observe a simultaneous mean field collapse like the one discussed in previous chapters for continuous systems, as this possibility is forbidden in a single–band approximation. Finally, we consider the behavior of the Bosonic superfluid on site parameter in the case of a Boson–Fermion attractive interaction. Comparing Fig. 6.7 with Fig. 6.4, we see that the transition to a Mott insulating phase for the Bosons takes place at the same lattice potential strength, irrespectively of the repulsive or attractive nature of the Boson–Fermion interaction. This finding confirms the results of the mean field analysis presented in the previous section.

## 6.5 Mirror symmetry breaking and transition to degeneracy

The above optimization problem associated with the constrained minimization of the energy is not convex, hence there can be many local minima in addition to the global one. However, even the ground state may be approximately or exactly degenerate. In fact, this is what happens in the case of Boson–Boson and Boson–Fermion repulsion for large values of the lattice potential strength $\tilde{V}_0$. As $\tilde{V}_0$ grows, it becomes eventually energetically more favorable for the bosons to be arranged in single–particle occupancy of the available sites around the center of the external trap. The Bosonic and Fermionic on–site occupation numbers can only assume the values 0 or 1, and a definite Boson–Fermion symmetry is established in the Bose–Fermi Hubbard Hamiltonian assuming that the on site Fermionic and Bosonic trapping potentials coincide.

A similar transmutation of Bosons into Fermions in strong optical lattices has been pointed out by Paredes and Cirac in a recent paper [115]. They consider a model of pure Bosons in an optical lattice and show that in the limit of very strong Boson–Boson

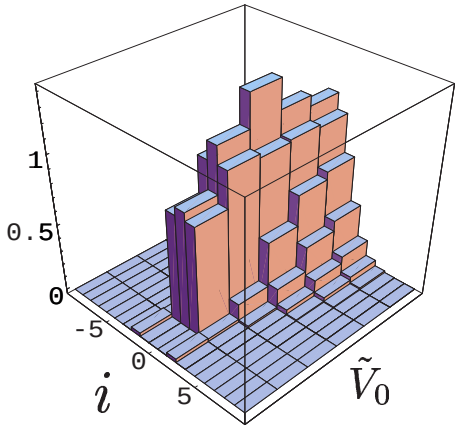


Figure 6.4: The Bosonic superfluid on site order parameter for a Bose-Fermi repulsion $a_{BF} = 0.04$, as a function of the lattice potential strength.

on site interaction, the Bosonic operators can be mapped into Fermionic operators by means of the well known Jordan–Wigner transformation. Let us consider what happens in the case of a Boson–Fermion mixture. As the lattice strength grows, configurations of lowest energy that are mirror–symmetric with respect to the center of the lattice, like e.g. those of Figs. 2 and 3, become approximately energetically equivalent to other symmetric configurations (e.g., a checkerboard of alternating Bosons and Fermions with one particle per lattice site), as well as to nonsymmetric configurations (like a succession of four Fermions followed by five Bosons and then a last Fermion, again with one particle per lattice site), and mirror symmetry breaking takes place. We may thus consider sequences of energy functionals with increasing lattice potential strengths $\tilde{V}_0$. For each value of $\tilde{V}_0$, one may identify a ground state. Then, the difference in energy of this ground state to those states that can be obtained by interchanging the role of Fermions and Bosons will converge to zero as $\tilde{V}_0$ grows. The Boson hopping contribution will become negligible, whereas the behavior of $\tilde{U}_{BB}$ will enforce the mean Bosonic on site occupation number to be at most one. Hence, for each lattice site, the constraints on the Boson and Fermion occupation numbers become identical (at most one Boson or one Fermion per lattice site). Notice that the suppression of the hopping terms is exponential. Moreover, since $\tilde{V}_B^{(i)} = \tilde{V}_F^{(i)}$ for all lattice sites $i$, the larger the value of $\tilde{V}_0$, the more symmetric is the role of Bosons and Fermions. There are then many ground states that are degenerate in energy with respect to any permutation of lattice sites – as long as all particles are located around the minimum of the confining external potential $\tilde{V}_B^{(0)} = \tilde{V}_F^{(0)} = 0$. These degenerate configurations will be given by all possible symmetric and nonsymmetric Fermion and Boson distributions in a region around the center of the lattice, with every site of the region occupied by one and only one particle. Such possible configurations are for example checkerboard alternating patterns of Bosons and Fermions, or Mott Bosonic central configurations with Fermionic wings on the sides, or consecutive block crystalline arrangements of variable length of Bosons and Fermions. In brief, while the Hamiltonian formally retains its mirror symmetry under reflection of the lattice around its center, the degenerate ground states need not, and spontaneous mirror symmetry breaking occurs. At the same time complete Boson–Fermion exchange symmetry sets on. No ground state

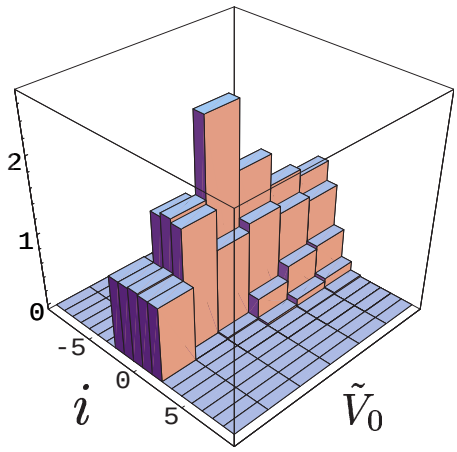


Figure 6.5: On site Bosonic densities for a Bose–Fermi attraction $a_{BF} = -0.04$, as a function of the lattice potential strength.

is *a priori* favored compared to any other: any random pattern of consecutive Bosons and Fermions located around the minimum of the external trapping potential is a legitimate ground state. Fig. 6.8 shows representative on site Bosonic densities in the regime of large values of $\tilde{V}_0$ around $\tilde{V}_0 = 50$ for the case of Boson–Boson and Boson–Fermion repulsion in a system composed of five Bosons and five Fermions: at each value of the lattice potential strength, a particular state is selected from the set of those with same energy. Each vanishing value of the on site Bosonic density means that exactly one Fermion has filled that particular lattice site. The large value chosen for $\tilde{V}_0$ allows to clearly stress the random nature of the configuration patterns even for very small changes of the lattice potential strength, whereas degeneracy and disorder can set in already at lower values of the lattice depth, depending on the tuning of the harmonic oscillator and scattering lengths (see below). The degenerate states are separated by energy barriers. The system is non–ergodic, and hysteresis should be observed: what particular state is chosen, depends on the exact mechanism of preparation of the system and of loading of the mixture into the optical lattice.

The criterion for the onset of degeneracy and non-periodic ground states in the bulk region around the center of the lattice and of the trapping potential is easily identified, by looking at the relative importance of the trapping on site energy with respect to the on site Boson or Fermion interaction energy. For instance, to allow for the Fermionic behavior of the Boson on site occupation numbers (either 0 or 1) one must require that the energy is lower having one Boson at the edge of the bulk central region rather than having it sitting on top of another Boson at the center of the lattice:

$$\tilde{U}_{BB} > \tilde{V}_B \, (i = (N_B + N_F)/2) \ . \tag{6.59}$$

The analogous condition for the Bose–Fermi on site interaction is:

$$\tilde{U}_{BF} > \tilde{V}_{B/F} \, (i = (N_B + N_F)/2) \ . \tag{6.60}$$

For smaller values of $\tilde{V}_0$, the Boson hopping contribution will become more and more important. A representative situation of this intermediate regime is depicted in Figs. 6.2

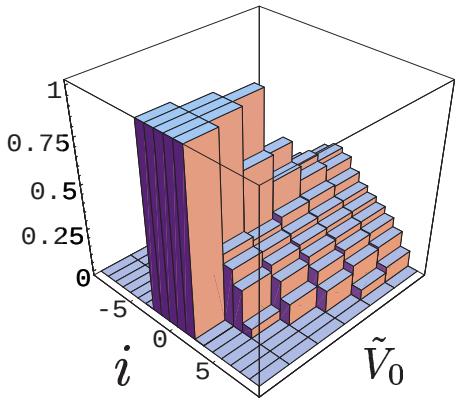


Figure 6.6: On site Fermionic densities for a Bose–Fermi attraction $a_{BF} = -0.04$, as a function of the lattice potential strength.

and 6.3: here, the repulsion between Bosons and Fermions is strong enough to allow for phase separation, while the non–negligible hopping terms still favor configurations where Bosons have Bosons as nearest neighbors. The transition to degeneracy and disorder, exact in the limit of infinite lattice depth, is a novel and peculiar feature of Bose–Fermi mixtures and it should hold in general for any multicomponent Bose and/or Fermi dilute atomic system loaded in a deep optical lattice at zero temperature, provided that inter-component interactions are repulsive and the on site confining potentials coincide for the different components. It clearly cannot take place in a single–component system, say a pure single–component Bose gas, where only a SF–MI transition occurs [112]. The rather complex and rich interplay between ordered and disordered configurations of Bose–Fermi mixtures in very deep optical lattices will be considered in more detail elsewhere.

Certainly a larger number of Bosons and Fermions have to be considered in order to obtain a more realistic description of the system. While our previous analytical findings are applicable to any numbers of atoms, in order to extend the numerical calculations to larger numbers more powerful numerical methods have to be introduced. So far, Monte Carlo simulations with a fairly large number of particles have been carried out only for an inhomogeneous Bose–Hubbard model [137]. The authors have also speculated that the qualitative phase diagram does not depend on the dimensionality of the system.

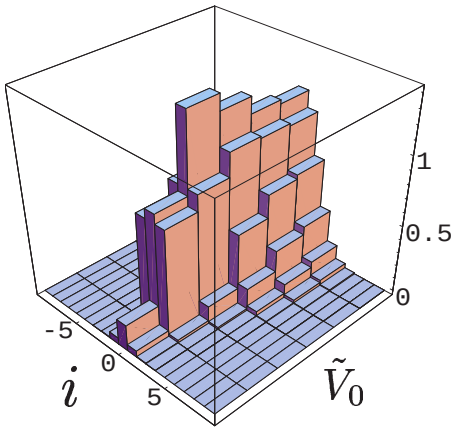


Figure 6.7: The Bosonic superfluid on site order parameter for a Bose–Fermi attraction $a_{BF} = -0.04$, as a function of the lattice potential strength.

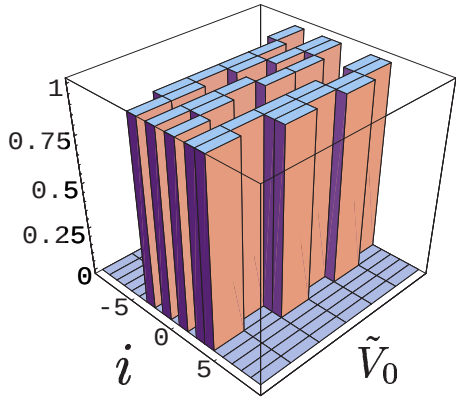


Figure 6.8: The disordered pattern of Bosonic ground–state distributions for repulsive Boson–Boson and Boson–Fermion interactions for large values of $\tilde{V}_0$ around $\tilde{V}_0 = 50$.

# Part IV

# Closing remarks

In this thesis, we have presented results on mixtures of atomic Bosons and Fermions in different spatial settings. Bosonic atoms possess according to the spin-statistics theorem integer Spin. We assumed Spin 0 Bosons throughout this thesis. Fermions have half inter Spin, so in general there are at least two Fermionic components – one with Spin up the other one with Spin down – for Spin one–half Fermions. Due to the Spin-alignment in magnetic traps the Spin degree of freedom is frozen for the Fermions and we could treat the Fermions as one-component particles. In experiments with cold atomic gases the dilute limit provides a very good approximation and thus the particle-particle interactions are dominated by $s$-wave scattering. Fermion-Fermion $s$-wave scattering is prohibited in this setting.

With these assumptions, we started with a homogeneous system, which is an idealized system assuming $N_B$ Bosons and $N_F$ Fermions confined in a volume $V$ with periodic boundary conditions and let $N_B, N_F, V \to \infty$, such that the densities $N_B/V, N_F/V$ are finite. Using the methods of Quantum field theory we derived some physical quantities of interest, the most important of which is the ground state energy beyond a mean-field level. An extension to finite temperature would certainly be advantageous. We expect considerable difficulties near the critical temperature. Well below that temperature, however, we expect no major complications and the calculations will be similar to the present case, except that boson loops will have to be taken into account and frequency integrals will have to be replaced by Matsubara frequency sums.

Within the framework of density functional theory the ground state energy could be incorporated to derive the density field equations beyond a mean-field level for systems of Bose–Fermi mixtures in a trap. More precisely, we have introduced the Kohn-Sham scheme of DFT for inhomogeneous Bose-Fermi systems to determine the ground-state energy and density profiles to second–order in the Boson–Fermion scattering length. We solved these equation numerically for experimentally relevant parameters, compared the theoretical predictions with current experiments, and discussed the importance of the exchange-correlation effects. We have shown that they are substantial for systems, like $^{40}$K-$^{87}$Rb, with a large attractive Boson-Fermion interaction, especially in the critical regime of collapse onset, by comparing the mean–field and the exchange–correlation phase diagrams. We have shown that the phase diagram stability vs. collapse changes considerably due to exchange and correlation effect. The DFT method outlined here can be in principle extended to include higher–order corrections and finite temperature effects (see Ref. [138]).

To learn about the critical temperature of BEC in the presence of Fermions we derived the density field equations on a mean-field level in local density approximation at finite temperature and analytically derived the change in critical temperature in regimes where the Fermions are described by Boltzmann gas or in the quantum degenerate regime, respectively. In the intermediate regime, we gave numerical results. The conclusion of this part was that the shift due to the presence of the Fermions is strongest when they are quantum degenerate, but in general the shift is only up to 5% of the non-interacting

Finally, the system of a Bose–Fermi mixture was considered in the presence of an optical lattice. We have shown that the system can be described by a single–band Hubbard type Hamiltonian for sufficiently strong lattices, found a linear stability criterion against demixing by requiring the energy functional to be positive definite at the minimum, and investigated the MI-SF phases analytically was well as numerically for systems with strong transverse but weak collinear confinement. The optical lattice potential plays a crucial role, allowing to tune the system into regimes of strong Boson–Boson and Boson–Fermion couplings as the lattice depth is increased. According to the possible different combinations of intraspecies and interspecies attractive and repulsive interactions, the system displays a rich phase structure, including the onset of a SF–MI transition in

the Boson sector, and a simultaneous transition to demixing in the Boson–Fermion sector. For very deep lattices the system displays a remarkable transition to a multiply degenerate phase in which all possible permutations of configurations with one Bosonic or Fermionic atom per site are legitimate ground states. The transition is related with breaking of the lattice mirror symmetry for very large values of the lattice depth. This peculiar disordered pattern of degenerate ground–state configurations separated by very large barriers is somehow reminiscent of the behavior of classical disordered systems like glasses and spin glasses, but it takes place in a quantum system at zero temperature. Besides these fundamental theoretical aspects related to the theory of quantum phase transitions Bose-Fermi mixtures in optical lattices are also a promising candidate to observe BCS phase transitions and qualify for potential applications in the physics of quantum information. As with systems involving either Bosons or Fermions that have been studied so far [112, 120, 124, 122, 125], mixtures could be used for the preparation of multi-particle entangled states [125] such as cluster states or certain instances of graph states [139], as well as for the implementation of quantum gates. With Bosons and Fermions serving two different purposes, Bose-Fermi mixtures could in fact allow for new possibilities of quantum information processing in optical lattices. The Fermions would be suitable for storage of quantum information due to their non–interacting behavior, whereas the Bosons could be used to let the systems interact and perform operations.

The complexity of the systems considered in this thesis can be extended in various obvious ways. For example one can consider unpolarized spin-1/2 fermions. Spin unpolarized systems are becoming of more experimental relevance, because one can nowadays also trap by purely optical means. In this case the Fermions are not necessarily spin–aligned. Calculations are very similar to the present situation with the main difference that one has to include the effects of the direct interactions of fermions with different spins. This would correspond to having a third scattering length $a_{FF}$.

As already pointed out quasi one or two dimensional systems are expected to have very special properties. The methods used in this thesis could potentially also be used to those systems if applied with some care.

An interesting perspective would be to investigate how the system behaves not only in the presence of Cooper pairing but also of ordinary molecule formation. Very recently there were even some speculations about the possibility of a atom-molecule Cooper pairing in Bose–Fermi mixtures [140].

# Appendix A

# The ground state energy in terms of Green's functions

Here, we show how the ground state energy can be calculated directly from the Green's functions. First, by using

$$\begin{aligned}\hat{T} &= -\frac{\hbar^2}{2m_B}\int d^3\mathbf{x}\hat{\phi}^\dagger(\mathbf{x})\nabla^2\hat{\phi}(\mathbf{x}) \\ &\quad -\frac{\hbar^2}{2m_F}\int d^3\mathbf{x}\hat{\Psi}^\dagger(\mathbf{x})\nabla^2\hat{\Psi}(\mathbf{x}) \end{aligned} \tag{A.1}$$

and the definitions (2.88) and (2.88) of the Green functions, we can easily see that:

$$\begin{aligned}\langle\mathbf{G}|\hat{T}|\mathbf{G}\rangle &= -i\frac{\hbar^2}{2m_B}\int d^3\mathbf{x}\lim_{\mathbf{x}'\to\mathbf{x}}\nabla^2 G'_B(\mathbf{x},t,\mathbf{x}',t) \\ &\quad +i\frac{\hbar^2}{2m_F}\int d^3\mathbf{x}\lim_{\mathbf{x}'\to\mathbf{x}}\nabla^2 G_F(\mathbf{x},t,\mathbf{x}',t) \end{aligned} \tag{A.2}$$

To determine $\langle\mathbf{G}|\hat{W}|\mathbf{G}\rangle$ in terms of the Green functions is a little more involved. For this purpose, we need the equations of motion of the field operators in the Heisenberg picture:

$$\begin{aligned} &i\hbar\frac{\partial\hat{\phi}_H(\mathbf{x},t)}{\partial t} = \exp(i\hat{K}t/\hbar)[\hat{\phi}(\mathbf{x},t),\hat{K}]\exp(-i\hat{K}t/\hbar) \\ &= \exp(i\hat{K}t/\hbar)\left[\frac{\hbar^2\nabla^2}{2m_B}\hat{\phi}(\mathbf{x}) + \sqrt{n_0}\int d^3\mathbf{x}'\hat{\Psi}^\dagger(\mathbf{x}')U(|\mathbf{x}-\mathbf{x}'|)\hat{\Psi}(\mathbf{x}')\right. \\ &\quad \left. + \sqrt{n_0}\int d^3\mathbf{x}'\hat{\Psi}^\dagger(\mathbf{x}')U(|\mathbf{x}-\mathbf{x}'|)\hat{\Psi}(\mathbf{x}')\hat{\phi}(\mathbf{x}) - \mu\hat{\phi}(\mathbf{x})\right]\exp(-i\hat{K}t/\hbar) \\ &= \frac{\hbar^2\nabla^2}{2m_B}\hat{\phi}_H(\mathbf{x},t) + \sqrt{n_0}\int d^3\mathbf{x}'\hat{\Psi}^\dagger_H(\mathbf{x}',t)U(|\mathbf{x}-\mathbf{x}'|)\hat{\Psi}_H(\mathbf{x}',t) \\ &\quad +\sqrt{n_0}\int d^3\mathbf{x}'\hat{\Psi}^\dagger_H(\mathbf{x}',t)U(|\mathbf{x}-\mathbf{x}'|)\hat{\Psi}_H(\mathbf{x}',t)\hat{\phi}_H(\mathbf{x},t) - \mu\hat{\phi}(\mathbf{x},t) \end{aligned} \tag{A.3}$$

and

$$i\hbar\frac{\partial\hat{\Psi}_H(\mathbf{x},t)}{\partial t} = \exp(i\hat{K}t/\hbar)[\hat{\Psi}(\mathbf{x},t),\hat{K}]\exp(-i\hat{K}t/\hbar)$$

$$
\begin{aligned}
&= \exp(i\hat{K}t/\hbar)\left[\frac{\hbar^2\nabla^2}{2m_F}\hat{\Psi}(\mathbf{x}) + n_0\int d^3\mathbf{x}' U(|\mathbf{x}-\mathbf{x}'|)\hat{\Psi}(\mathbf{x})\right.\\
&\quad +\sqrt{n_0}\int d^3\mathbf{x}' U(|\mathbf{x}-\mathbf{x}'|)\hat{\phi}^\dagger(\mathbf{x})\hat{\Psi}(\mathbf{x}) + \sqrt{n_0}\int d^3\mathbf{x}' U(|\mathbf{x}-\mathbf{x}'|)\hat{\phi}^\dagger(\mathbf{x})\hat{\Psi}(\mathbf{x})\\
&\quad \left.+\int d^3\mathbf{x}'\hat{\phi}^\dagger(\mathbf{x}')U(|\mathbf{x}-\mathbf{x}'|)\hat{\phi}(\mathbf{x}')\hat{\Psi}(\mathbf{x})\right]\exp(-i\hat{K}t/\hbar)\\
&= \frac{\hbar^2\nabla^2}{2m_F}\hat{\Psi}_H(\mathbf{x},t) + n_0\int d^3\mathbf{x}' U(|\mathbf{x}-\mathbf{x}'|)\hat{\Psi}_H(\mathbf{x},t)\\
&\quad +\sqrt{n_0}\int d^3\mathbf{x}' U(|\mathbf{x}-\mathbf{x}'|)\hat{\phi}^\dagger_H(\mathbf{x},t)\hat{\Psi}_H(\mathbf{x},t) +\\
&\sqrt{n_0}\int d^3\mathbf{x}' U(|\mathbf{x}-\mathbf{x}'|)\hat{\phi}^\dagger_H(\mathbf{x},t)\hat{\Psi}_H(\mathbf{x},t)\\
&\quad +\int d^3\mathbf{x}'\hat{\phi}^\dagger_H(\mathbf{x}',t)U(|\mathbf{x}-\mathbf{x}'|)\hat{\phi}_H(\mathbf{x}',t)\hat{\Psi}_H(\mathbf{x},t), \qquad (A.4)
\end{aligned}
$$

where we have used $[\hat{O},\hat{P}\hat{Q}] = [\hat{O},\hat{P}]\hat{Q} - \hat{P}[\hat{Q},\hat{O}]$ for the Boson operators and $[\hat{O},\hat{P}\hat{Q}] = \{\hat{O},\hat{P}\}\hat{Q} - \hat{P}\{\hat{Q},\hat{O}\}$ for the Fermion operators. Adding the equations in the following way $\frac{1}{2}\hat{\phi}^\dagger_H(\mathbf{x},t)\cdot(A.3) + \frac{1}{2}(A.3)^\dagger\cdot\hat{\phi}_H(\mathbf{x},t) + \hat{\Psi}^\dagger_H(\mathbf{x},t)\cdot(A.4)$, rearranging terms and integrating over $\mathbf{x}$ gives:

$$
\begin{aligned}
&\int d^3\mathbf{x}\frac{1}{2}\hat{\phi}^\dagger_H(\mathbf{x},t)\left(i\hbar\frac{\partial}{\partial t} + \frac{\hbar^2\nabla^2}{2m_B} + \mu\right)\hat{\phi}_H(\mathbf{x},t)\\
&+\frac{1}{2}\left[\left(-i\hbar\frac{\partial}{\partial t} + \frac{\hbar^2\nabla^2}{2m_B} + \mu\right)\hat{\phi}^\dagger_H(\mathbf{x},t)\right]\hat{\phi}_H(\mathbf{x},t)\\
&+\hat{\Psi}^\dagger_H(\mathbf{x},t)\left(i\hbar\frac{\partial}{\partial t} + \frac{\hbar^2\nabla^2}{2m_F}\right)\hat{\Psi}_H(\mathbf{x},t)\\
&= \hat{V}_{1,H}(t) + \frac{3}{2}\hat{V}_{2,H}(t) + \frac{3}{2}\hat{V}_{3,H}(t) + 2\hat{V}_{4,H}(t)
\end{aligned}
$$

Taking the ground state average of this we get:

$$
\begin{aligned}
&\int d^3\mathbf{x}\lim_{\mathbf{x}'\to\mathbf{x}}\left(i\hbar\frac{\partial}{\partial t} - i\hbar\frac{\partial}{\partial t'}|_{t'\to t^+}\right.\\
&\left.-\frac{\hbar^2\nabla^2}{2m_B} - \frac{\hbar^2\nabla'^2}{2m_B} + 2\mu\right)\langle\mathbf{G}|\hat{\phi}^\dagger_H(\mathbf{x}',t')\hat{\phi}_H(\mathbf{x},t)|\mathbf{G}\rangle\\
&+\left(i\hbar\frac{\partial}{\partial t} - \frac{\hbar^2\nabla^2}{2m_F}\right)\langle\mathbf{G}|\hat{\Psi}^\dagger_H(\mathbf{x}',t^+)\hat{\Psi}_H(\mathbf{x},t)|\mathbf{G}\rangle\\
&= 2\langle\mathbf{G}|\hat{V}_H(t)|\mathbf{G}\rangle - n_0\langle\mathbf{G}|\frac{d\hat{V}_H(t)}{dn_0}|\mathbf{G}\rangle
\end{aligned}
$$

now we use $\mu V = \langle\mathbf{G}|\frac{d\hat{V}}{dn_0}|\mathbf{G}\rangle$ (see Ref. [81]),

$$
n_0 V = N_B - \int d^3\mathbf{x}\langle\mathbf{G}|\hat{\phi}^\dagger_H(\mathbf{x},t)\hat{\phi}_H(\mathbf{x},t)|\mathbf{G}\rangle
$$

and the definition of the Green's functions:

$$
2\langle\mathbf{G}|\hat{V}_H(t)|\mathbf{G}\rangle = \mu N_B - \int d^3\mathbf{x}\lim_{\mathbf{x}'\to\mathbf{x}}[\mu i G'_B(\mathbf{x},t,\mathbf{x}',t)
$$

$$+\frac{1}{2}\left(i\hbar\frac{\partial}{\partial t}-i\hbar\frac{\partial}{\partial t'}|_{t'\to t^+}-\frac{\hbar^2\nabla^2}{2m_B}-\frac{\hbar^2\nabla'^2}{2m_B}+2\mu\right)iG'_B(\mathbf{x},t,\mathbf{x}',t')$$
$$-\left(i\hbar\frac{\partial}{\partial t}-\frac{\hbar^2\nabla^2}{2m_F}\right)iG_F(\mathbf{x},t,\mathbf{x}',t^+)$$

From this, we finally get:

$$\begin{aligned}E_0 &= \langle\mathbf{G}|\hat{T}_H(t)+\hat{V}_H(t)|\mathbf{G}\rangle\\ &= \frac{1}{2}\mu N_B+\frac{1}{2}\int d^3\mathbf{x}\lim_{\mathbf{x}'\to\mathbf{x}}\left[\left(i\hbar\frac{\partial}{\partial t}-\frac{\hbar^2\nabla^2}{2m_B}\right)iG'_B(\mathbf{x},t,\mathbf{x}',t^+)\right.\\ &- \left.\left(i\hbar\frac{\partial}{\partial t}-\frac{\hbar^2\nabla^2}{2m_F}\right)\right]iG_F(\mathbf{x},t,\mathbf{x}',t^+),\end{aligned}\tag{A.5}$$

where we have used $\nabla^2 G'_B(\mathbf{x},t,\mathbf{x}',t')=\nabla'^2 G'_B(\mathbf{x},t,\mathbf{x}',t')$ and $\frac{\partial}{\partial t}G'_B(\mathbf{x},t,\mathbf{x}',t')=-\frac{\partial}{\partial t'}G'_B(\mathbf{x},t,\mathbf{x}',t')$ (since in space and time homogeneous systems the Green functions can only depend on $\mathbf{x}-\mathbf{x}'$ and $t-t'$).
If we use the Fourier transforms for the Green functions and pass to the limit $V\to\infty$ where $\sum_{\mathbf{k}}\ldots\to\frac{V}{(2\pi)^3}\int d^3\mathbf{k}\ldots$:

$$\begin{aligned}\frac{E_0}{V}=\frac{1}{2}\mu n_B &+ \frac{1}{2(2\pi)^4}\int\int d^3\mathbf{k}d\omega\left[\left(\hbar\omega+\frac{\hbar^2\mathbf{k}^2}{2m_B}\right)iG_B(\mathbf{k},\omega)\right.\\ &- \left.\left(\hbar\omega+\frac{\hbar^2\mathbf{k}^2}{2m_F}\right)iG_F(\mathbf{k},\omega)\right]\end{aligned}\tag{A.6}$$

# Appendix B

# Evaluation of the integrals in the $T$- Matrix

## B.1 Evaluation of the $T$-Matrix and coupling constant renormalization

### B.1.1 The first integral $\mathcal{I}$

We define

$$\mathcal{I} = \int d^3\mathbf{k} \frac{\theta(|\mathbf{P}/2 - \mathbf{k}| - k_F)}{\hbar P^0 - \hbar^2(\mathbf{P}/2 + \mathbf{k})^2/2m_B - \hbar^2(\mathbf{P}/2 - \mathbf{k})^2/2m_F + \mu + i\nu}. \tag{B.1}$$

Transforming the integration variables to $\mathbf{P}/2 - \mathbf{k}$ gives:

$$\mathcal{I} = \int d^3\mathbf{k} \frac{\theta(|\mathbf{k}| - k_F)}{\hbar^2\mathbf{k}^2/2m - \hbar^2\mathbf{P}\cdot\mathbf{k}/m_B - \hbar P^0 + \hbar^2\mathbf{P}^2/2m_B - \mu - i\nu}. \tag{B.2}$$

Setting $a = \hbar^2/2m$, $b = \hbar^2 P/m_B$ and $E = -\hbar P^0 + \hbar^2 P^2/2m_B - \mu$ and transforming to spherical coordinates we get:

$$\begin{aligned} \mathcal{I} &= 2\pi \int_{k_F}^{k_c} dk k^2 \int_0^\pi d\phi \sin\phi \frac{1}{ak^2 - bk\cos\phi + E - i\nu} \\ &= \frac{2\pi}{b} \int_{k_F}^{k_c} dk k \ln \frac{ak^2 - bk + E - i\nu}{ak^2 + bk + E - i\nu}, \end{aligned} \tag{B.3}$$

where we will ultimately consider the limit $k_c \to \infty$. Using $D = (b/2a)^2 - E/a = -\frac{m}{m_B+m_F}P^2 + \frac{2mP^0}{\hbar} + \frac{2m\mu}{\hbar^2}$ we can approximate for small $\nu$ (if $D \neq 0$; the case $D = 0$ can be treated similarly and gives the same answer as taking the limit $D \to 0$ at the very end):

$$ak^2 - bk + E - i\nu = a\left(k - \frac{mP}{m_B} - \sqrt{D} - \frac{i\nu}{2a\sqrt{D}}\right)\left(k - \frac{mP}{m_B} + \sqrt{D} + \frac{i\nu}{2a\sqrt{D}}\right)$$

and

$$ak^2 + bk + E - i\nu = a\left(k + \frac{mP}{m_B} - \sqrt{D} - \frac{i\nu}{2a\sqrt{D}}\right)\left(k + \frac{mP}{m_B} + \sqrt{D} + \frac{i\nu}{2a\sqrt{D}}\right)$$

and integrate the logarithms of these factors separately to get:

$$\begin{aligned}\mathcal{I} &= -\frac{2\pi m_B}{\hbar^2 P}\int_{k_F}^{k_c} dk k \\ &\times\Bigg(\ln\frac{k+mP/m_B+\sqrt{D}+i\nu/2a\sqrt{D}}{k-mP/m_B-\sqrt{D}-i\nu/2a\sqrt{D}} \\ &+\ln\frac{k+mP/m_B-\sqrt{D}-i\nu/2a\sqrt{D}}{k-mP/m_B+\sqrt{D}+i\nu/2a\sqrt{D}}\Bigg).\end{aligned} \tag{B.4}$$

The integral can be solved [141] to give

$$\begin{aligned}\lim_{k_c\to\infty}\mathcal{I} &= -\frac{8\pi m k_c}{\hbar^2}+\frac{4\pi m k_F}{\hbar^2} \\ &+\frac{\pi}{\hbar^2}\left(\frac{m_B k_F^2}{P}-\frac{m^2 P}{m_B}-2m\sqrt{D}-\frac{m_B D}{P}\right) \\ &\times\ln\frac{k_F+mP/m_B+\sqrt{D}+i\nu/2a\sqrt{D}}{k_F-mP/m_B-\sqrt{D}-i\nu/2a\sqrt{D}} \\ &-\frac{\pi}{\hbar^2}\left(\frac{m_B k_F^2}{P}-\frac{m^2 P}{m_B}+2m\sqrt{D}-\frac{m_B D}{P}\right) \\ &\times\ln\frac{k_F-mP/m_B+\sqrt{D}+i\nu/2a\sqrt{D}}{k_F+mP/m_B-\sqrt{D}-i\nu/2a\sqrt{D}},\end{aligned} \tag{B.5}$$

where outside the logarithms we have taken the limit $\nu\to 0$ (simply setting $\nu=0$), and we have made use of the identity

$$\lim_{x\to\infty} x^2\ln\frac{1+\alpha/x}{1-\alpha/x}=2\alpha x, \tag{B.6}$$

for the limit $k_c\to\infty$. There remains an ultraviolet divergent term; the Boson-Fermion $T$-matrix [Eqn. (3.7)] is however ultimately renormalized by the second integral.

The real part of $\mathcal{I}$ is readily evaluated in the limit $\nu\to 0$ by setting $\nu=0$ and using the absolute values inside the logarithms:

$$\begin{aligned}\lim_{\nu\to 0}\mathrm{Re}\mathcal{I} &= -\frac{8\pi m k_c}{\hbar^2}+\frac{4\pi m k_F}{\hbar^2} \\ &+\frac{\pi}{\hbar^2}\left(\frac{m_B k_F^2}{P}-\frac{m^2 P}{m_B}-\frac{m_B D}{P}\right) \\ &\times\ln\left|\frac{(k_F+mP/m_B)^2-D}{(k_F-mP/m_B)^2-D}\right| \\ &-\frac{2\pi m}{\hbar^2}\sqrt{D}\ln\left|\frac{(k_F+\sqrt{D})^2-(mP/m_B)^2}{(k_F-\sqrt{D})^2-(mP/m_B)^2}\right|.\end{aligned} \tag{B.7}$$

Using the identity (easily evaluated by polar decomposition)

$$\lim_{\nu\to 0^+}\mathrm{Im}\ln\frac{a+i\nu}{b-i\nu}=\begin{cases}0 & : \ \mathrm{sgn}(a)=\mathrm{sgn}(b)\\ \pi & : \ \mathrm{sgn}(a)\neq\mathrm{sgn}(b)\end{cases}, \tag{B.8}$$

the imaginary part of $\mathcal{I}$ in the limit $\nu \to 0$ can be evaluated to be:

$$\lim_{\nu\to 0} \mathrm{Im}\mathcal{I} = \frac{\pi^2}{\hbar^2}\left(\frac{m_B k_F^2}{P} - \frac{m^2 P}{m_B} - 2m\sqrt{D} - \frac{m_B D}{P}\right), \tag{B.9}$$

if $D > 0$ and $k_F < |mP/m_B - \sqrt{D}|$;

$$\lim_{\nu\to 0} \mathrm{Im}\mathcal{I} = -\frac{4\pi^2 m\sqrt{D}}{\hbar^2}, \tag{B.10}$$

if $D > 0$ and $|mP/m_B - \sqrt{D}| < k_F < mP/m_B + \sqrt{D}$; and

$$\lim_{\nu\to 0} \mathrm{Im}\mathcal{I} = 0, \tag{B.11}$$

if $D \leq 0$ or $k_F > mP/m_B + \sqrt{D}$.

### B.1.2 The second integral $\mathcal{J}$

We define

$$\begin{aligned} \mathcal{J} &= -\int d^3\mathbf{k} \frac{1}{\hbar^2\mathbf{k}_1^2/2m - \hbar^2\mathbf{k}^2/2m + i\nu} \\ &= \frac{4\pi}{a}\int_0^{k_c} dk \left(1 - \frac{k_1^2 + i\nu/a}{k^2 - k_1^2 - i\nu/a}\right), \end{aligned} \tag{B.12}$$

where as before $a = \hbar^2/2m$, and we have transformed to polar coordinates and integrated over the angle variables. The integral can be evaluated [141] to give

$$\begin{aligned} \mathcal{J} &= \frac{4\pi k_c}{a} - \frac{2\pi}{a}\sqrt{k_1^2 - i\nu/a}\ln\frac{k_c + \sqrt{k_1^2 - i\nu/a}}{k_c - \sqrt{k_1^2 - i\nu/a}} \\ &\quad + \frac{2\pi}{a}\sqrt{k_1^2 - i\nu/a}\ln\frac{\sqrt{k_1^2 - i\nu/a}}{-\sqrt{k_1^2 - i\nu/a}}. \end{aligned} \tag{B.13}$$

We then use

$$\lim_{k_c\to\infty} \ln\frac{k_c + \sqrt{k_1^2 - i\nu/a}}{k_c - \sqrt{k_1^2 - i\nu/a}} = 0 \tag{B.14}$$

to get

$$\lim_{\nu\to 0} \mathcal{J} = \frac{8\pi m k_c}{\hbar^2} + i\frac{4\pi^2 m k_1}{\hbar^2}. \tag{B.15}$$

If we now take the sum of Eqns. (B.5) and (B.15), the ultraviolet divergent terms cancel exactly. The resulting expression for $\mathcal{I} + \mathcal{J}$ can then be substituted into Eqn. (3.7) to get Eqn. (3.8) for the renormalized Boson-Fermion $T$-matrix.

# Appendix C

# Evaluation of the ground state energy with Green's functions

We start with the Fermionic contribution to the ground state energy given in Eqn. (A.6):

$$\frac{E^F}{V} = -\frac{1}{2(2\pi)^4}\int\int d^3\mathbf{p}dp^0\left(\hbar p^0 + \frac{\hbar^2\mathbf{p}^2}{2m_F}\right)iG_F(p^\mu) \tag{C.1}$$

In order to perform the time integration, we have to close the contour in the upper half plane. As we have seem from the solution to the pole equation (3.29), there is no pole in the upper half plane if $p > k_F$. So there is no contribution to the integral for $p > k_F$. For $p < k_F$, we have a pole above the real axis at the value given by (3.28). If we use the residue theorem we get:

$$\begin{aligned}\frac{E^F}{V} &= \frac{1}{(2\pi)^2}\int_0^{k_F} dpp^2\left(\frac{\hbar^2p^2}{m_F}\right.\\ &+\frac{2\pi\hbar^2}{m}an_B + \frac{2a^2\hbar^2k_Fn_B}{m} + \frac{a^2\hbar^2n_0m_B}{2m^2p}\left(k_F^2-p^2\right)\ln\frac{k_F+p+\frac{i\nu}{2a\sqrt{D}}}{k_F-p-\frac{i\nu}{2a\sqrt{D}}}\\ &\left.-\frac{a^2\hbar^2n_Bm_B}{2m^2p}\left(k_F^2-(\delta)^2p^2\right)\ln\frac{k_F-\delta p+\frac{i\nu}{2a\sqrt{D}}}{k_F+\delta p-\frac{i\nu}{2a\sqrt{D}}}\right),\end{aligned} \tag{C.2}$$

which is up to prefactors exactly the same expression a the one for $\Sigma_B(0)$ found from Eqn. (3.11).

So we can use this result to obtain:

$$\frac{E^F}{V} = \frac{3}{5}\frac{\hbar^2k_F^2}{2m_F}n_F + \frac{\pi\hbar^2a_{BF}n_Bn_F}{m}\left(1+\frac{a_{BF}k_F}{\pi}f(\delta)\right)., \tag{C.3}$$

with $f(\delta)$ defined as in Eqn. (3.14).

We can also calculate the Boson contribution to Eqn. (A.6), which is:

$$\frac{E^B}{V} = \frac{1}{2}\mu n_B + \frac{1}{2(2\pi)^4}\int\int d^4p^\mu\left(\hbar p^0 + \frac{\hbar^2\mathbf{p}^2}{2m_B}\right)iG_B(p^\mu) \tag{C.4}$$

We now use first-order $G_B(p^\mu)$ from (3.18) to get[58]:

$$\frac{1}{2(2\pi)^4}\int\int d^4p^\mu\left(\hbar p^0 + \frac{\hbar^2\mathbf{p}^2}{2m_B}\right)iG_B(p^\mu) = -\frac{64\sqrt{\pi}(n_Ba_B)^{\frac{5}{2}}\hbar^2}{15m_B}.$$

Using also (3.16) we get:

$$\frac{E^B}{V} = \frac{2\pi a_B \hbar^2}{m_B} n_B^2 + \frac{\pi \hbar^2 a_{BF} n_B n_F}{m} \left(1 + \frac{a_{BF} k_F}{\pi} f(\delta)\right), \tag{C.5}$$

where we have neglected terms of the order of the Bose gas parameter. Adding (C.3) and (C.5) gives the same result as Eqn. (3.35).

# Bibliography


[1] M. H. Anderson, J. R. Ensher, M. R. Matthews, C. E. Wieman, and E. A. Cornell, *Observation of Bose-Einstein condensation in a dilute atomic vapor*, Science **269**, 198 (1995).

[2] K. B. Davis, M. O. Mewes, M. R. Andrews, N. J. van Druten, D. S. Durfee, D. M. Kurn, and W. Ketterle, *Bose-Einstein Condensation in a Gas of Sodium Atoms*, Phys. Rev. Lett. **75**, 3969 (1995).

[3] S. N. Bose, *Planck's Law and the Hypothesis of Light Quanta*, Z. Phys. **26**, 178 (1924).

[4] A. Einstein, *Quantentheorie des einatomigen idealen Gases*, Sitzungsber. Kgl. Preuss. Akad. Wiss. 261 (1924).

[5] A. Einstein, *Quantentheorie des einatomigen idealen Gases, 2. Abhandlung*, Sitzungsber. Kgl. Preuss. Akad. Wiss. 3 (1925).

[6] A. Einstein, *Quantentheorie des idealen Gases*, Sitzungsber. Kgl. Preuss. Akad. Wiss. 18 (1925).

[7] A. Griffin, D. W. Snoke, and S. Stringari, *Bose-Einstein condensation* (Cambrigde University Press, Cambridge, 1995).

[8] Z. Idziaszek and K. Rzazewski, *Two characteristic temperatures for a Bose-Einstein condensate of a finite number of particles*, cond-mat/0304361 (2003).

[9] in *Proceedings of the International School of Physics 'Enrico Fermi': Course CXL*, edited by M. Inguscio, S. Stringari, and C. E. Wieman (IOS Press, Amsterdam, 1998).

[10] E. Fermi, *Sulla quantitetione del gas perfetto monoatomico*, Rend. Lincei **3**, 145 (1926), reprinted in: Collected Papers, vol. I Italy 1921-1938, E. Fermi (ed. E. Amaldi *et. al.*, University of Chcago Press, 1962).

[11] E. Fermi, *Zur Quantelung des einatomigen Gases*, Z. Phys. **36**, 902 (1926), reprinted in: Collected Papers, vol. I Italy 1921-1938, E. Fermi (ed. E. Amaldi *et. al.*, University of Chcago Press, 1962).

[12] P. A. M. Dirac, *On the Theory of Quantum Mechanics*, Proc. Roy. Soc. A **112**, 661 (1926).

[13] W. Pauli, *Über den Zusammenhang des Abschlusses der Elektronengruppen im Atom mit der Komplexstruktur der Spektren*, Z. Phys. **31**, 765 (1925).

[14] J. Bardeen, L. N. Cooper, and J. R. Schrieffer, *Theory of superconductivity*, Phys. Rev. **108**, 1175 (1957).

[15] Y. Ohashi and A. Griffin, *The BCS-BEC Crossover in a Gas of Fermi Atoms with a Feshbach Resonance*, Phys. Rev. A **67**, 033603 (2003).

[16] R. Micnas, J. Ranninger, and S. Robaszkiewicz, *Superconductivity in narrow-band systems with local nonretarded attractive interactions*, Rev. Mod. Phys. **62**, 113 (1990).

[17] M. Letz, *Crossover from BCS superconductivity to BEC of pairs: The role of the lifetime of the pairs*, Mol. Phys. Rep. **24**, 44 (1999).

[18] K. M. O'Hara, S. L. Hemmer, M. E. Gehm, S. R. Granade, and J. E. Thomas, *Observation of a stronlgy-interacting degenersat Fermi gas of atoms*, Science **298**, 2179 (2002).

[19] B. DeMarco and D. S. Jin, *Onset of Fermi Degeneracy in a Trapped Atomic Gas*, Science **285**, 1703 (1999).

[20] A. G. Trusscott, K. E. Strecker, M. W. I, G. B. Partridge, and R. G. Hulet, *Observation of Fermi Pressure in a Gas of Trapped Atoms*, Science **291**, 2570 (2001).

[21] F. Schreck, L. Khaykovich, K. L. Corwin, G. Ferrari, T. Bourdel, J. Cubizolles, and C. Salomon, *Quasipure Bose-Einstein Condensate Immersed in a Fermi Sea*, Phys. Rev. Lett. **87**, 080403 (2001).

[22] Z. Hadzibabic, C. A. Stan, K. Dieckmann, S. Gupta, M. W. Zwierlein, A. Görlitz, and W. Ketterle, *Two species mixture of quantum degenerate Bose and Fermi gases*, Phys. Rev. Lett. **88**, 160401 (2002).

[23] G. Roati, F. Riboli, G. Modugno, and M. Inguscio, *Fermi-Bose quantum degenerate $^{40}K$-$^{87}Rb$ mixture with attractive interaction*, Phys. Rev. Lett. **89**, 150403 (2002).

[24] J. T. D. M. Wouters, J. Tempere, *Three-Fluid Description of the Sympathetic Cooling of a Boson-Fermion Mixture*, Phys. Rev. A **66**, 043414 (2002).

[25] C. Presilla and R. Onofrio, *Cooling dynamics of ultracold two-species Fermi-Bose mixtures*, Phys. Rev. Lett. **90**, 030404 (2003).

[26] P. Hohenberg and W. Kohn, *Inhomogeneous Electron Gas*, Phys. Rev. **136**, B864 (1964).

[27] A. J. Moerdijk, B. J. Verhaar, and A. Axelsson, *Resonances in ultracold collisions of $^6Li$, $^7Li$ and $^{23}Na$*, Phys. Rev. A **51**, 4852 (1995).

[28] K. Mølmer, *Bose Condensates and Fermi Gases at Zero Temperature*, Phys. Rev. Lett. **80**, 1804 (1998).

[29] M. Amoruso, A. Minguzzi, S. Stringari, M. P. Tosi, and L. Vichi, *Temperature-dependent Density Profiles of Trapped Boson-Fermion Mixtures*, Eur. Phys. J. D **4**, 261 (1998).

[30] T. Miyakawa, K. Oda, T. Suzuki, and H. Yabu, *Static properties of the Bose-Fermi mixed Condensate of Alkali atoms*, J. Phys. Soc. Jpn. **69**, 2779 (2000).

[31] N. Nygaard and K. Mølmer, *Component separation in harmonically trapped boson-fermion mixtures*, Phys. Rev. A **59**, 2974 (1999).

[32] R. Roth and H. Feldmeier, *Mean-field instability of trapped dilute boson-fermion mixtures*, Phys. Rev. A **65**, 021603 (2002).

[33] R. Roth, *Structure and stability of trapped atomic boson-fermion mixtures*, Phys. Rev. A **66**, 013614 (2002).

[34] Z. Akdeniz, A. Minguzzi, P. Vignolo, and M. P. Tosi, *Demixing in mesoscopic boson-fermion clouds inside cylindrical harmonic traps: Quantum phase diagram and the role of temperature*, Phys. Rev. A **66**, 0136209 (2002).

[35] X. X. Yi and C. P. Sun, *Phase separation of a trapped Bose-Fermi gas mixture: Beyond the Thomas-Fermi approximation*, Phys. Rev. A **64**, 023609 (2001).

[36] L. Viverit, C. J. Pethick, and H. Smith, *Zero-temperature phase diagram of binary boson-fermion mixtures*, Phys. Rev. A **61**, 053605 (2000).

[37] M. J. Bijlsma, B. A. Heringa, and H. T. C. Stoof, *Phonon exchange in dilute Fermi-Bose mixtures: Tailoring the Fermi-Fermi interaction*, Phys. Rev. A **61**, 053601 (2000).

[38] H. Heiselberg, C. J. Pethick, H. Smith, and L. Viverit, *Influence of Induced Interactions on the Superfluid Transition in Dilute Fermi Gases*, Phys. Rev. Lett. **85**, 2418 (2000).

[39] I. Al-Hayek and B. Tanatar, *Model boson-fermion mixture within the self-consistent-field approximation*, Phys. Rev. B **60**, 10388 (1999).

[40] F. Mazzanti, A. Polls, and J. Boronat, *High-momentum dynamic structure function of liquid $^3$He-$^4$He mixtures: a microscopic approach*, cond-mat/0010361 (2000).

[41] J. Ranninger and S. Robaszkiewicz, *Superconductivity of locally paired electrons*, Physica B **135**, 464 (1985).

[42] T. Kostyrko and J. Ranninger, *Spectral properties of the boson-fermion model in the superconducting state*, Phys. Rev. B **54**, 13105 (1995).

[43] P. Capuzzi and E. S. Hernández, *Zero sound density oscillations in Fermi-Bose mixtures*, Phys. Rev. A **64**, 043607 (2001).

[44] T. Miyakawa, T. Suzuki, and H. Yabu, *Sum-rule approach to collective oscillations of a boson-fermi mixed condensate of alkali-metal atoms*, Phys. Rev. A **62**, 063613 (2000).

[45] H. Hu, X.-J. Liu, and M. Modugno, *Expansion of a quantum degenerate boson-fermion mixture*, cond-mat/0301182 (2003).

[46] M. Wouters, J. Tempere, and J. T. Devreese, *Resonant dynamics in boson-fermion mixtures*, cond-mat/0303220 (2003).

[47] T. Maruyama, H. Yabu, and T. Suzuki, *Time-dependent dynamics of the Bose-Fermi Mixed condensed system*, cond-mat/0303216 (2003).

[48] A. Minguzzi and M. P. Tosi, *Schematic phase diagram and collective excitations in the collisional regime for trapped boson-fermion mixtures at zero temperature*, Phys. Lett. A **268**, 142 (2000).

[49] P. Capuzzi, A. Minguzzi, and M. P. Tosi, *Collective excitations of a trapped boson-fermion mixture across demixing*, cond-mat/0301522 (2003).

[50] S. K. Yip, *Collective modes in a dilute Bose-Fermi mixture*, Phys. Rev. A **64**, 023609 (2001).

[51] T. Sogo, T. Miyakawa, T. Suzuki, and H. Yabu, *Random-phase approximation study of collective excitations in the Bose-Fermi mixed condensate of alkali-metal gases*, Phys. Rev. A **66**, 013618 (2002).

[52] C. P. Search, H. Pu, W. Zhang, and P. Meystre, *Quasiparticle spectrum and dynamical stability of an atomic Bose-Einstein condensate coupled to a degenerate Fermi gas*, Phys. Rev. A **65**, 063615 (2002).

[53] B. H. Valtan, M. Nishida, and S. Kurihara, *Collective excitations of dilute Bose-Fermi superfluid mixtures*, Laser Phys. **12**, 217 (2001).

[54] W. Zhang, H. Pu, C. P. Search, P. Meystre, and E. M. Wright, *Two-fermion bound state in a Bose-Einstein condensate*, Phys. Rev. A **67**, 021601 (2003).

[55] M. Y. Kagan, D. V. Efremov, and A. V. Klaptsov, *Composite fermions in the Fermi-Bose mixture with attractive interaction between fermions and bosons*, cond-mat/0209481 (2002).

[56] L. Viverit, *Boson induced s-wave pairing in dilute boson-fermion mixtures*, Phys. Rev. A **66**, 023605 (2002).

[57] D. V. Efremov and L. Viverit, *p-wave Cooper pairing of Fermions in mixtures of dilute Fermi and Bose gases*, Phys. Rev. B **65**, 134519 (2002).

[58] A. L. Fetter and J. D. Walecka, *Quantum theory of many-particle systems* (McGraw-Hill, Inc, New York, 1971).

[59] M. D. Lee, S. A. Morgan, M. J. Davis, and K. Burnett, *Energy-dependent scattering and the Gross-Pitaevskii equation in two-dimensional Bose-Einstein condensates*, Phys. Rev. A **65**, 043617 (2002).

[60] T. Busch, B.-G. Englert, K. Rzażewski, and M. Wilkens, *Two cold atoms in a harmonic trap*, Found. Phys. **28**, 549 (1998).

[61] *Handbook of mathematical functions*, tenth ed., edited by M. Abramowitz and I. A. Stegun (National Bureau of Standards, Washington, 1972).

[62] A. Görlitz *et al.*, *Realization of Bose-Einstein Condensates in Lower Dimensions*, Phys. Rev. Lett. **87**, 130402 (2002).

[63] H. Ott, J. Fortagh, G. Schlotterbeck, A. Grossmann, C. Z. M. Brack, and M. V. N. Murthy, *Bose-Einstein Condensation in a Surface Microtrap*, Phys. Rev. Lett. **87**, 230401 (2001).

[64] A. E. Leanhardt, A. P. Chikkatur, D. Kielpinski, Y. Shin, T. L. Gustavson, W. Ketterle, and D. E. Pritchard, *Propagation of Bose-Einstein Condensates in a Magnetic Waveguide*, Phys. Rev. Lett. **89**, 040401 (2002).

[65] K. K. Das, *Bose-Fermi mixtures in one dimension*, Phys. Rev. Lett. **90**, 170403 (2002).

[66] F. Gleisberg, W. Wonneberger, U. Schlöder, and C. Zimmermann, *Non-interacting Fermions in a one-dimensional harmonic atom trap: exact one-particle properties at zero temperature*, Phys. Rev. A **62**, 063602 (2000).

[67] P. Bloom, *Two-dimensional Fermi gas*, Phys. Rev. B **12**, 125 (1974).

[68] M. D. Girardeau, *Relationship between systems of impenetrable bosons and fermions in one dimension*, J. Math. Phys. **1**, 516 (1960).

[69] E. H. Lieb and W. Lininger, *Exact analysis of an interacting Bose gas. I. The general solution and the ground state*, Phys. Rev. **130**, 1605 (1963).

[70] V. Dunjko, V. Lorent, and M. Olshanii, *Bosons in cigar-shape traps: Thomes-Fermi regime, Tonks-Girardeau regime, and between*, Phys. Rev. Lett. **86**, 5413 (2001).

[71] M. Schick, *Two-dimensional system of hard-core bosons*, Phys. Rev. A **3**, 1067 (1970).

[72] D. F. Hines and N. E. Frankel, *Hard-disc Bose gas*, Phys. Lett. **68A**, 12 (1978).

[73] D. S. Petrov, M. Holzmann, and G. V. Shlyapnikov, *Bose-Einstein condensation in quasi-2d trapped gases*, Phys. Rev. Lett. **84**, 2551 (2000).

[74] J. O. Andersen and H. Haugerud, *Ground state of a trapped Bose-Einstein condensate in two dimensions: Beyond the mean-field approximation*, Phys. Rev. A **65**, 033615 (2002).

[75] M. Olshanii, *Atomic scattering in the presence of an external confinement and a gas of impenetrable bosons*, Phys. Rev. Lett. **81**, 938 (1998).

[76] D. S. Petrov and G. V. Shlyapnikov, *Interatomic collisions in a tightly confined Bose gas*, Phys. Rev. A **64**, 012706 (2001).

[77] N. Bogolubov, *On the theory of superfluidity*, J. Phys. **11**, 23 (1947).

[78] C. W. Gardiner, *Particle-number-conserving Bogoliubov method which demonstrates the validity of the time-dependent Gross-Pitaevskii equation for a highly condensed Bose gas*, Phys. Rev. A **56**, 1414 (1997).

[79] M. D. Girardeau, *Comment on Particle-number-conserving Bogoliubov method which demonstrates the validity of the time-dependent Gross-Pitaevskii equation for a highly condensed Bose gas*, Phys. Rev. A **58**, 775 (1997).

[80] Y. Castin and D. R, *Low-temperature Bose-Einstein condensates in time-dependent traps: Beyond the U(1) symmetry-breaking approach*, Phys. Rev. A **57**, 3008 (1998).

[81] N. M. Hugenholtz and D. Pines, *Ground-State Energy and Excitation Spectrum of a System of Interacting Bosons*, Phys. Rev. **116**, 489 (1959).

[82] A. A. Abrikosov, L. P. Gorkov, and I. E. Dzyaloshinsk, *Methods of Quantum Field Theory in Statistical Physics* (Dover Publications, New York, 1963).

[83] S. T. Beliaev, *Energy-spectrum of a non-ideal Bose gas*, Sov. Phys. JETP **34**, 299 (1958).

[84] V. M. Galitskii and A. B. Migdal, *Application of quantum field theory methods to the many body problem*, Sov. Phys. JETP **34(7)**, 96 (1958).

[85] F. Matera, *Fermion pairing in Bose-Fermi mixtures*, cond-mat/0305609 (2003).

[86] C. Menotti, M. Krämer, L. Pitaevskii, and S. Stringari, *Dynamic structure factor of a Bose Einstein condensate in a 1D optical lattice*, cond-mat/0212299 (2003).

[87] W. Hofstetter, J. I. Cirac, P. Zoller, E. Demler, and M. D. Lukin, *High-Temperature Superfluidity of Fermionic Atoms in Optical Lattices*, Phys. Rev. Lett. **89**, 220407 (2002).

[88] L. Viverit and S. Giorgini, *Ground-state properties of a dilute Bose-Fermi mixture*, Phys. Rev. A **66**, 063604 (2002).

[89] C. C. Bradley, C. A. Sackett, and R. G. Hulet, *Bose-Einstein Condensation of Lithium: Observation of Limited Condensate Number*, Phys. Rev. Lett. **78**, 985 (1997).

[90] Y. Kagan, A. E. Muryshev, and G. V. Shlyapnikov, *Collapse and Bose-Einstein Condensation in a Trapped Bose Gas with Negative Scattering Length*, Phys. Rev. Lett. **81**, 933 (1998).

[91] S.-T. Chui and V. N. Ryzhov, *Collapse transition in mixtures of Bosons and Fermions*, cond-mat/0211411 (2002).

[92] G. Modugno, G. Roati, F. Riboli, F. Ferlaino, R. J. Brecha, and M. Inguscio, *Collapse of a Degenerate Fermi Gas*, Science **297**, 2240 (2002).

[93] R. Roth and H. Feldmeier, *Phase diagram of trapped degenerate Fermi gases including effective s- and p-wave interactions*, J. Phys. B **34**, 4629 (2001).

[94] R. M. Dreizler and E. K. U. Gross, *Density Functional Theory* (Springer-Verlag, Berlin, 1990).

[95] W. Kohn and L. J. Sham, *Self-Consistent Equations Including Exchange and Correlation Effects*, Phys. Rev. **140**, A1133 (1965).

[96] R. Roth and S. Feldmeier, *Effective s- and p-wave contact interactions in trapped degenerate Fermi gases*, Phys. Rev. A **64**, 464 (2001).

[97] M. Modugno, private communication, 2003.

[98] H. Shi and A. Griffin, *Finite-temperature excitations in a dilute Bose-condensed gas*, Phys. Rep. **304**, 1 (1998).

[99] G. Baym, J.-P. Blaizot, M. Holzmann, F. Lalo, and D. Vautherin, *Bose-Einstein transition in a dilute interacting gas*, J. Phys. B **24**, 107 (2001).

[100] K. Huang, *Statistical mechanics* (John Wiley & Sons, New York, 1963).

[101] D. A. Butts and D. S. Rokhsar, *Trapped Fermi gases*, Phys. Rev. A **55**, 4346 (1997).

[102] H. Hu and X.-J. Liu, *Thermodynamics of a trapped Bose-Fermi mixture*, cond-mat/0302570 (2003).

[103] V. Bagnato, D. E. Pritchard, and D. Kleppner, *Bose-Einstein condensation in an external potential*, Phys. Rev. A **35**, 4354 (1987).

[104] S. Grossmann and M. Holthaus, *On Bose-Einstein condensation in harmonic traps*, Phys. Lett. **A208**, 188 (1995).

[105] S. Giorgini, L. P. Pitaevskii, and S. Stringari, *Condensate fraction and critical temperature of a trapped interacting Bose gas*, Phys. Rev. A **54**, R4633 (1996).

[106] M. Greiner, I. Bloch, O. Mandel, T. W. Hänsch, and I. Bloch, *Exploring Phase Coherence in a 2D Lattice of Bose-Einstein condensates*, Phys. Rev. Lett. **87**, 160405 (2001).

[107] M. Greiner, O. Mandel, T. Esslinger, T. W. Hänsch, and I. Bloch, *Quantum phase transition from a superfluid to a Mott insulator in a gas of ultracold atoms*, Nature **415**, 39 (2002).

[108] C. Orzel, A. K. Tuchman, M. L. Fenslau, M. Yasuda, and M. A. Kasevich, *Squeezed States in a Bose-Einstein Condensate*, Science **291**, 2386 (2001).

[109] J. R. Anglin and W. Ketterle, *Bose-Einstein condensation of atomic gases*, Nature **416**, 211 (2002).

[110] P. S. Jessen and I. H. Deutsch, , Adv. At. Mol. Opt. Phys. **37**, 95 (1996).

[111] S. Sachdev, *Quantum phase transitions* (Cambridge University Press, Cambridge, 1999).

[112] D. Jaksch, C. Bruder, J. I. Cirac, C. W. Gardiner, and P. Zoller, *Cold Bosonic Atoms in Optical Lattices*, Phys. Rev. Lett. **81**, 3108 (1998).

[113] D. van Oosten, P. van der Straten, and H. T. C. Stoof, *Quantum phases in an optical lattice*, Phys. Rev. A **63**, 053601 (2001).

[114] J. Ruostekoski, G. V. Dunne, and J. Javanainen, *Particle number fractionization of an atomic Fermi-Dirac gas in an optical lattice*, Phys. Rev. Lett. **88**, 180401 (2002).

[115] B. Paredes and J. I. Cirac, *From Cooper Pairs to Luttinger Liquids with Bosonic Atoms in Optical Lattices*, Phys. Rev. Lett. **90**, 150402 (2002).

[116] A. Recati, P. O. Fedichev, W. Zwerger, and P. Zoller, *Spin-Charge Separation in Ultracold Quantum Gases*, Phys. Rev. Lett. **90**, 020401 (2003).

[117] H. P. Büchler, G. Blatter, and W. Zwerger, *Commensurate-Incommensurate Transition of Cold Atoms in an Optical Lattice*, Phys. Rev. Lett. **90**, 130401 (2003).

[118] A. J. Kerman, V. Vuletic, C. Chin, and S. Chu, *Beyond Optical Molasses: 3D Raman Sideband Cooling of Atomic Cesium to High Phase-Space Density*, Phys. Rev. Lett. **84**, 439 (2000).

[119] P. S. Jessen, D. L. Haycock, G. Klose, G. A. Smith, I. H. Deutsch, and G. K. Brennen, , Quant. Inf. Comp. **1**, 20 (2001).

[120] I. H. Deutsch, G. K. Brennen, and P. S. Jessen, , Fortschr. d. Phys. **48**, 925 (2000).

[121] D. Jaksch, H.-J. Briegel, J. I. Cirac, C. W. Gardiner, and P. Zoller, *Entanglement of Atoms via Cold Controlled Collisions*, Phys. Rev. Lett. **82**, 1975 (1999).

[122] J. J. Garcia-Ripoll and J. I. Cirac, *Quantum Computation with Unknown Parameters*, Phys. Rev. Lett. **90**, 127902 (2003).

[123] U. Dorner, P. Fedichev, D. Jaksch, M. Lewenstein, and P. Zoller, *Entangling strings of neutral atoms in 1D atomic pipeline structures*, quant-ph/0212039 (2002).

[124] J. Pachos and P. L. Knight, *Quantum Computation with a One-Dimensional Optical Lattice*, quant-ph/0301084 (2003).

[125] L.-M. Duan, E. Demler, and M. D. Lukin, *Controlling Spin Exchange Interactions of Ultracold Atoms in Optical Lattices*, cond-mat/0210564 (2002).

[126] M. P. A. Fisher, P. B. Weichmann, G. Grinstein, and D. S. Fisher, *Boson localization and the superfluid-insulator transition*, Phys. Rev. B **40**, 546 (1989).

[127] E. H. Lieb and F. Y. Wu, *Absence of Mott Transition in an Exact Solution of the Short-Range, One-Band Model in One Dimension*, Phys. Rev. Lett. **20**, 1445 (1968), erratum: Phys. Rev. Lett.**21**, 192 (1968).

[128] G. Modugno, private communication, 2003.

[129] D. van Oosten, P. van der Straten, and H. T. C. Stoof, *Mott insulators in an optical lattice with hight filling factors*, cond-mat/0205066 (2002).

[130] G.-H. Chen and Y. S. Wu, *Quantum phase transition in a multicomponent Bose-Einstein condensate in optical lattices*, Phys. Rev. A **67**, 013606 (2003).

[131] J. K. Freericks and H. Monien, *Phase diagram of the Bose Hubbard model*, Europhys. Lett. **26**, 545 (1994).

[132] K. Sheshadri, H. R. Krishnamurthy, R. Pandit, and T. V. Ramarishnan, *Superfluid and insulating phases in an interacting-Boson model: Mean-field theory and the RPA*, Europhys. Lett. **22**, 257 (1993).

[133] W. Krauth, M. Caffarel, and J.-P. Bouchaud, *Gutzwiller wave function for a model of strongly interacting bosons*, Phys. Rev. B **45**, 3137 (1991).

[134] S. Kirkpatrick, C. D. Gelatt, and M. P. Vecchi, , Science **220**, 621 (1983).

[135] B. W. Wah and T. Wang, in *Proc. Principles and Practice of Constrained Programming* (Springer, Heidelberg, 1999).

[136] J. A. Nelder and R. Mead, , Comp. Journal **7**, 308 (1965).

[137] G. G. Batrouni, V. Rousseau, R. T. Scalettar, M. Rigol, A. Muramatsu, P. J. H. Denteneer, and M. Troyer, *Mott Domains of Bosons Confined on Optical Lattices*, Phys. Rev. Lett. **89**, 117203 (2002).

[138] N. D. Mermin, *Thermal Properties of the Inhomogeneous Electron Gas*, Phys. Rev. **137**, A1441 (1965).

[139] W. Dür and H.-J-Briegel, *Entanglement Purification for Quantum Computation*, Phys. Rev. Lett. **90**, 067901 (2003).

[140] M. Mackie, O. Dannenberg, J. Piilo, and J. J. K.-A. Suominen, *High-Temperature Cooper pairing Between Different Chemical Species*, physics/0305057 (2003).

[141] A. P. Prudnikov, Y. A. Brychov, and O. I. Marichev, *Integrals and series*, fourth ed. (Gordon and Breach Science Publishers, Amsterdam, 1998), Vol. 1.

# Index